Insights from a metabolic chimera:

Pyruvate Kinase and Aspartate-Glutamate Carrier distributions reveal key metabolic links between Neurons and Glia in the retina.

Ken James Lindsay

A dissertation

submitted in partial fulfillment of the

requirements for the degree of

Doctor of Philosophy

University of Washington

2014

Reading Committee:

James B. Hurley, Chair

Stephen D. Hauschka

Dana L. Miller

Ian R. Sweet

Program Authorized to Offer Degree:

Biochemistry

University of Washington

Abstract

Insights from a metabolic chimera:

Pyruvate Kinase and Aspartate-Glutamate Carrier distributions reveal key metabolic links between Neurons and Glia in the retina.

Ken James Lindsay

Chair of the Supervisory Committee:

Professor James B. Hurley

Biochemistry

The development of ophthalmology and vision research has established an abundance of knowledge on the process of vision. The study of the retina has contributed information about neuronal and biochemical signaling mechanisms that convert the detection of light to a neuronal signal. However, what fuels the process of photo-transduction remains unknown. Perhaps this is what makes the observation that so many metabolic diseases have the unusual distinction of leading to retinal degeneration so intriguing. The goal of my research has been to understand the unique metabolic regulation of the photoreceptor to establish what implications this has for the basal health of the retina.

Aerobic glycolysis is a metabolic phenomenon typically associated with tumor cells which has also been observed within the retina. This metabolic process has been attributed to expression of a unique isoform of pyruvate kinase, PKM2. In order to determine how aerobic glycolysis influences overall retina metabolism, we sought to determine the localization of PKM2 within the retina and thereby which cells within the retina are reliant on aerobic glycolysis. Our work revealed a unique localization

of PKM2 to photoreceptor cells and exclusion of pyruvate kinase in Müller glia of the retina. Combined with the complimentary expression of a glutamate aspartate transporter in the photoreceptor and absence from the Müller glia, the distribution of these enzymes are well positioned to shuttle lactate from glycolytic photoreceptors and drive glutamate turnover in the Müller glia. We established through studies of retina metabolic flux that the demand for aerobic glycolysis in the photoreceptor cell is used to fuel the neuronal glutamate/glutamine cycle that is essential to neuronal signaling within the retina.

In the course of our studies of retina metabolism, we sought to optimally culture isolated photoreceptor cells and resolve what is required for outer-segment retention and preservation of photoreceptor cell function. Following up on previous observations that Dark Adaptation improves outer segment retention, we tested the effects of light adaptation on isolated outer-segments. Our experiments indicated that outer segment morphology was unaffected by light adaptation, but could be modified by culture conditions. Preliminary experiments with optical tweezers revealed a previously unobserved tether on photoreceptor outer segments that may introduce a tension component necessary for maintenance of outer segment morphology and photoreceptor cell synthesis of outer segment discs. We believe that refinement of these techniques for cultivation of primary intact photoreceptor cells will allow us to delve further into the unique metabolism of the individual cell types of the retina and how the individual demands of cells in the retina may impact the overall effects of metabolic catastrophe on retina degeneration.

TABLE OF CONTENTS

LIST OF FIGURES

ACKNOWLEDGEMENTS

The work in this thesis represents not just my own efforts, but also that of many who have taught me valuable techniques and journeyed with me on the road of academic research. James B. Hurley, my advisor, mentor, and principle investigator, provided me with not only the time, but space and resources with which to grow in his lab. I have learned much from both our conversations as well as the environment which he has cultivated in the lab. I can attest to the continued comradery of the lab alumni which frequent lab functions and never fail to stay in contact. Previous graduate student Jason Chen and Post-doctoral researcher Vishy Ramamurthy are still close collaborators and good friends.

I would also like to thank my thesis committee: Stephan Hauschka for sticking with us long after our initial work in the study of Creatine Kinase, Dana Miller for providing her take on metabolism through the perspective of *C. elegans*, Ian Sweet for our continued collaboration in the study of cellular respiration, Kevin Conley for insight into metabolism and always answering the tough questions that get a project moving, and Jack Saari for providing a wealth of knowledge from his experience in the field of vision science.

The lab is also a key component to success in graduate school, I owe a great deal of technical assistance to Jonathan Linton who has become not only a good friend, but a trusted source on the methods of biochemistry, genotyping, and beer brewing. All of which aided my acquisition of technical knowledge. When it came to the actual experiments which culminated in this work, my assistant Stephanie Sloat, provided much needed aid in a time of research struggle. I can honestly say that I

have learned much from her (as the quality of my lab note-book can attest to) as I've seen her progress from undergraduate to research scientist. I wish her well in her Post-Baccalaureate studies. She will always be a great student and I look forward to seeing what she will do next.

Others in the lab provided not only company, but also a much needed ear to listen to my questions, and more importantly, a voice to answer them. Lars Holzhausen gave me the first glimpses of what graduate school was like and aided me with his wit throughout my first years. Andrei Chertov was an excellent colleague with whom to field-test ideas and discuss the nuances of lab work and videogames beyond just sharing methods and lab space. While the old-guard will always be respected, the new graduate students Michelle Giamarco, with her colorful stories, and Mark Kanow, for his comic relief, have been an immeasurable asset to the lab. They have given me much needed hope for future graduate students and the world beyond graduate school.

Throughout my graduate studies, the Brockerhoff lab has always worked in close collaboration with the Hurley lab. Fellow graduate student, Ashley George helped me develop the skills for immunohistochemistry which culminated in the work you are reading. She has also provided further assistance through much needed questions of my own work throughout the joint lab meetings between our two labs. I pretty much owe everything I know about zebrafish to her. Post Docs in the lab also provided interesting questions, but also a glimpse into what a post-doc is like. Sara Hayden taught me a lot about confocal imaging through her own experience. Whitney Cleghorn also provided good advice for the road ahead while also showing

me the versatility of metabolism in her work on zebrafish. Jianhai Du taught me a lot about collaboration as we developed the experiments that resulted in our published work in PNAS. His efforts contributed a significant part to the research composing Chapter 2 of this dissertation.

However, lab space and comradery are not enough to complete a PhD. I owe my sincere gratitude to the Department of Biochemistry at the University of Washington for taking a chance on me and allowing me to be a part of an excellent team and with such a diverse range of faculty. Outside of my department, Martin Sadilek of the Department of Chemistry was indispensable in his knowledge of Mass Spectrometry and assistance. I would never have learned these methods without his knowledge and patience. The Vision Science department has become huge part of my studies as the Hurley lab moved to the South Lake Union campus of the University of Washington. Dan Possin and Jing Huang have provided a wealth of knowledge on both the history of the department, but also in learning to appreciate the important details behind immunohistochemistry. In addition, the conversations with the Neitz and Chao labs have proven to be both entertaining and enlightening. The move to South Lake Union also opened up new avenues of research thanks to Brian Johnson and Kim Collins at the HIC for making a lot of our live cell imaging possible and to Michelle Black for introducing us to FACS.

The journey from start to finish in graduate school can take you in a variety of directions I really owe a lot to my friends, family, and these fine people for making any of this possible.

DEDICATION

To my friends and family, without whom I would have finished up a long time ago, but I wouldn't have learned nearly as much. Thanks for being there and teaching me so much along the way. I owe a special dedication to my father, James A. Lindsay, who taught me to keep breathing and was an inspiration for me to become "a damn good biochemist".

Chapter 1: Introduction

The Interaction of Metabolic Regulation between Various cell Types in the Retina.

The first attempts to observe high speed motion through film in 1887 with Eadweard Muybride's photographic sequence of a race horse galloping revealed the speed of visual perception and gave clues to how fast neurons in the visual cortex are capable of processing images perceived by the eye. On a physiological level, the retina is an easily accessible tissue for studying neuronal connections (1). Biochemically, the photoreceptor has a prodigious concentration of Rhodopsin(2), a membrane bound G-protein essential to the visual process. The high concentration of this protein in the retina allowed for the first studies and structure of a purified membrane G-protein coupled receptor(3) and has served as a model system for studying G-protein mediated signal transduction. As a result of its function, the specialized morphology of this tissue has provided indispensable insights into research from chemistry to physiology.

Beyond the scientific advances made in the study of the retina, one cannot overlook the fact that the retina is the main organ enabling us to see the world around us. Blindness has a profound impact in the life of an individual. Research into the cause and treatment of retina degeneration is lauded for its capacity to dramatically improve an individual's quality of life. Yet despite the close tie between blindness and metabolic disorders, research into the basic metabolism of the retina has generated more questions than answers. In recent years it has become clear that photoreceptors and Müller glia of the retina have complementary demands for consumption and production of glutamine, respectively. As this molecule sits at a nexus between signaling molecule and metabolite, this raises the question as to whether this commensal difference in

photoreceptor and Müller glia glutamine production also has implications for the metabolic profile of these different cell types. Therefore, in order to understand the metabolism of the retina, we must go deeper into the metabolic needs of individual cell types.

To answer this question, I investigated the unique metabolic demands of the photoreceptor from energy expenditure to anabolic processes. To understand what fuels these demands I researched the extent of glycolysis and oxidative phosphorylation not only within the photoreceptor, but between the various cells in the retina. In the process, this revealed an important link between glycolysis and oxidative phosphorylation through maintenance of cellular redox potential, which plays an important role in not only photoreceptor cell function, but also survival. The result of these studies has not only shed light on photoreceptor cell metabolism, but also how we might create better tools for studying the isolated cell and understanding the link between retina metabolism and degeneration.

The Retina and the Photo-transduction Cascade

The Retina is the neuronal conduit by which we see the world around us. It is composed of several cell types that transduce the light evoked signals from the photoreceptor to the inner retinal neurons in an electrochemical message; transmitting the colorful images of the world around us to the gray matter within. Between the various cell layers of the retina there is a complex interchange of signals between neighboring cells which are integrated between each layer into a single electrical signal through the optic nerve. Each cell type provides a different function in this cellular network, each with its own metabolic needs to fulfill its distinct role. The energy demands of the retina, as a whole, have been studied extensively and have yielded much information on how the metabolic needs of the retina are met and what implications this has on retinal function. However, the needs of the individual cell are less characterized. The layout of the retina provides a schematic for the distribution of energy and will help elucidate the sites of highest energy demand and their impact on retina function.

Figure 1: The Eye and the Retina

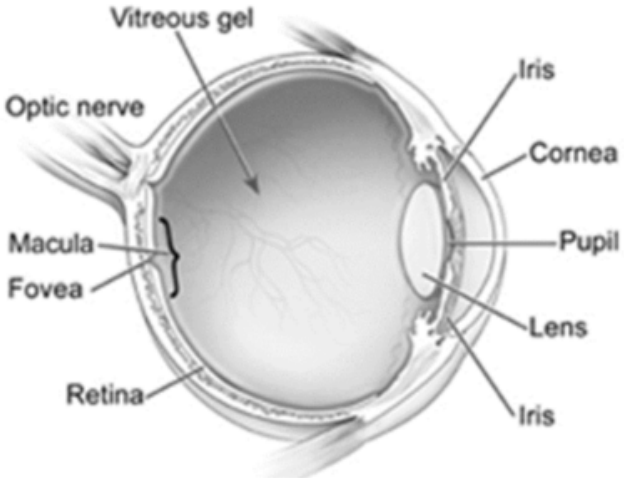

The retina is the light sensitive tissue lining the back of the eye. It lies between the vitreous gel of the interior and the oxygen rich vasculature lining the back of the eye, known as the choroid. The retina is composed of several neuronal cell types and relies on Müller glia and astrocytes to support overall retina function.

Image courtesy of www.nei.nih.gov

Figure 2. The layout of the Retina

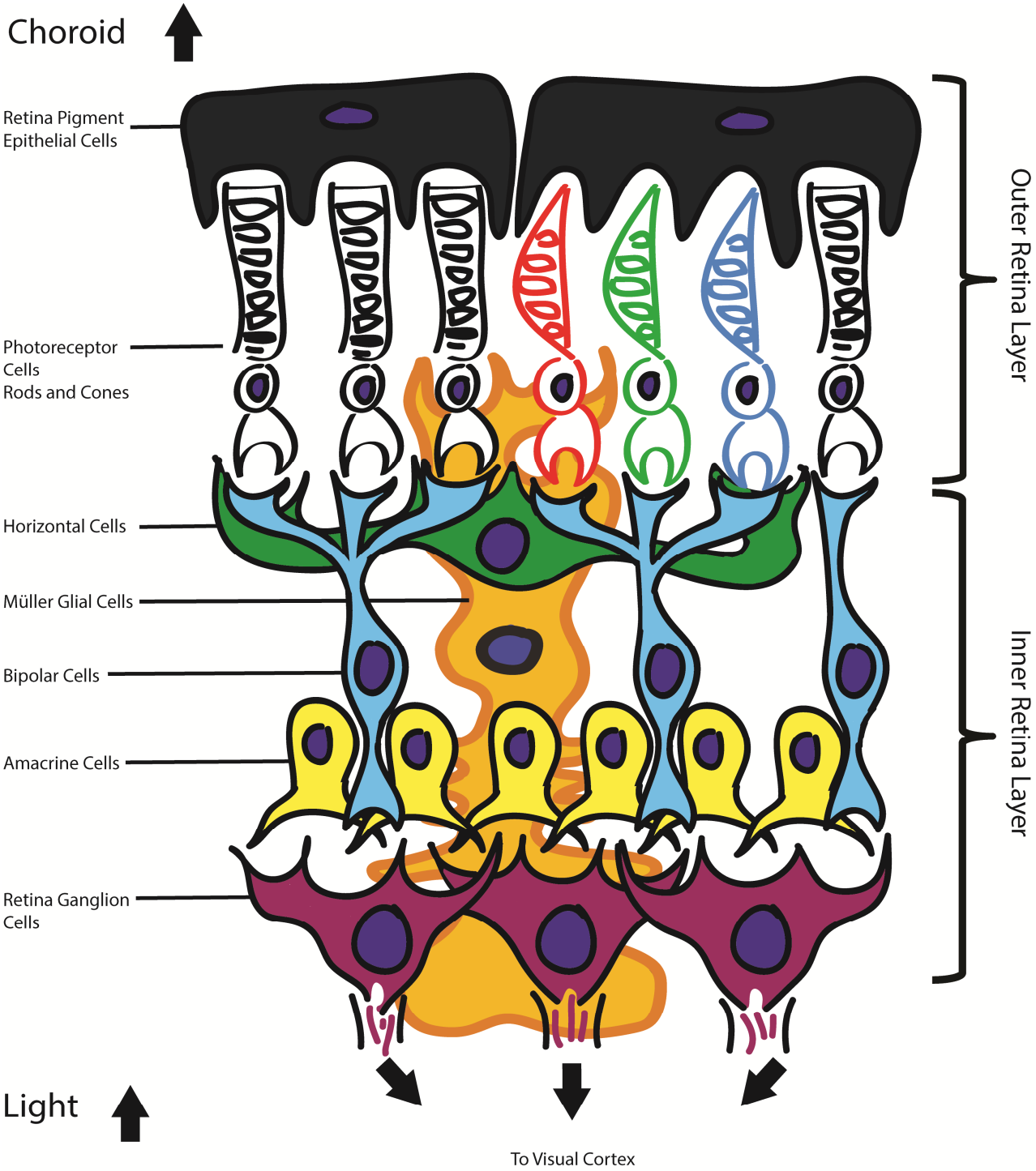

The retina is oriented with the photoreceptor outer-segments oriented towards the back of the eye. Light must pass through inner retina neurons, before reaching the light-sensitive photoreceptors.

The choroid, the vascularized tissue lining the back of the eye, is the main blood supply to the retina, providing it with oxygen and metabolic substrates such as glucose. At the interface of choroid and the retina is a dark pigmented cell layer known as the retinal pigment epithelium (RPE). The RPE is a single cell layer of heavily pigmented cells which line the choroid and which engulf the tips of photoreceptor outer segments. In this position, they have a highly polarized morphology as they serve to mediate nutrient transport from the choroid to the retina and serve to turn-over photoreceptor outer segment discs. This enables the retina to recycle 11-cis-retinal, the chromophore of rhodopsin that is critical to the photo-transduction cascade. Separation of the RPE from photoreceptors, or inhibition of phagocytosis can result in retina degeneration.

Figure 3: The Photoreceptor Cell

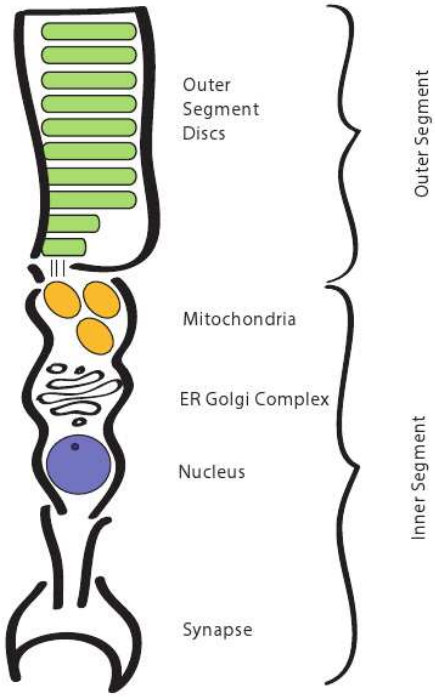

The photoreceptor cell is characterized by a distinct polarized morphology with the light detecting outer segment at one end and the synapse at the other. The outer segment is composed of stacks of membranous outer segment discs. Mitochondria are localized to an ellipsoid complex with the ER-Golgi at the base of the outer segment. In between the ellipsoid and the outer segment is a thin connecting cilium which facilitates transport of vesicles to the outer segment.

Photoreceptors, the light detecting cells of the retina, have a distinct polarized morphology with an outer-segment containing stacks of disc membranes at one end and an inner segment at the other, which synapses to downstream neurons. There are two types of photoreceptors, rods, which are sensitive to low levels of light and are responsible for night vision and cones, which specialize in color vision in daylight. In humans, cones typically come in three varieties Red, Green, and Blue based on the wavelengths of light they can detect. The outer-segments of rods are comprised of a stack of membranous discs, distinct from the cell membrane and contain the proteins and pigments responsible for the photo-transduction cascade. The inner segment of the photoreceptor contains the ellipsoid, the bulk of mitochondria and Golgi-ER complexes, as well as the nucleus. At the end of the inner segment is the synapse where synaptic glutamate is released to signal downstream neurons.

Deeper into the retina are several neuronal cells that integrate the light activated signal of the photoreceptors: the bipolar, horizontal, and amacrine cells. These cells comprise the inner retinal layer. Bipolar cells accept signals from photoreceptors and neighboring bipolar cells to produce a graded synaptic signal to the retina ganglion cells. Rod and cone bipolar cells connect to photoreceptor synapses and relay the signal, along with amacrine cells, to the retina ganglion cells. In between these cells are the horizontal cells which integrate signals from multiple photoreceptor cells.(4)

During photoreceptor synaptic signaling, Horizontal cells respond to photoreceptor cell glutamate release and depolarize. This causes the horizontal cells to release GABA into the synaptic space, which inhibits photoreceptor glutamate release(5) and resets the photoreceptor cell. Horizontal cells and amacrine cells provide similar roles in providing lateral integration of signals from bipolar cells to the retinal ganglion cells. This modulation of bipolar signals is responsible for the ability of the retina to respond to a broad range of light intensities and is critical for visualizing contrast and motion detection. Ganglion cells integrate the combined signal of amacrine and horizontal cells and are the final cell layer connecting the retina to the visual cortex.

In addition to neurons, there is an additional cell type that provides trophic support to the neuronal cells of the retina: the Müller glia. Müller glia are a unique cell type which intercalate between neurons from the inner retina to the outer limiting membrane. They support processes necessary for maintenance of cell function: potassium ion (K^+) and water homeostasis, turnover of transmitter molecules such as glutamate and GABA, quenching of reactive oxygen species through glutathione production, and release of growth factors to surrounding cells. (6)The metabolic relationship between photoreceptors and Müller glia have been used as a model for similar interactions between astrocytes and neurons.(7)

The Photo-Transduction Cascade

The photo-transduction cascade is a complex biochemical process whereby light is detected and this signal is propagated by a series of signaling events to downstream neurons. Integration of these electrochemical impulses to downstream neurons will carry the signal to the brain(8). This photo-transduction cascade is located in the photoreceptor and is initiated in the outer-segment discs that contain the light sensitive chromophore 11-cis-retinal.

Figure 4: The Photo-transduction Cascade

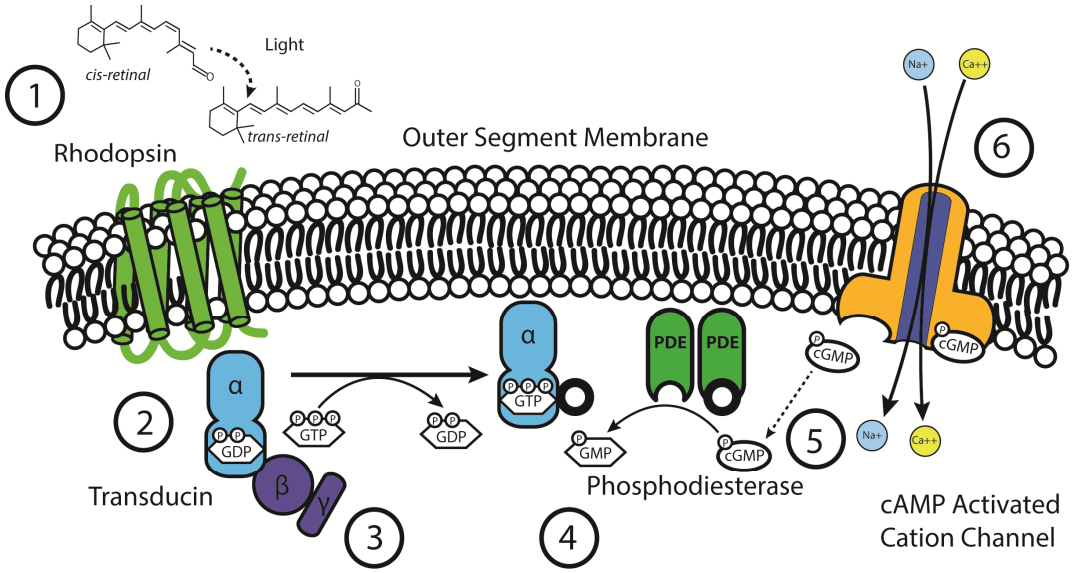

In its inactive state, 11-cis-retinal is covalently bound to the membrane protein Rhodopsin. When light strikes the photoreceptor, it excites 11-cis-retinal causing a photo-isomerization to all-trans-retinal [1]. The isomerization of 11-cis retinal dissociates it from Rhodopsin, activating Rhodopsin in the process. The all-trans retinal released from the photoreceptor cell is re-isomerized to 11-cis-retinal in the adjacent retina pigment epithelium. Activated Rhodopsin binds to the hetero-trimeric G-protein, Transducin [2]. This causes exchange of GDP for GTP in the α-subunit of Transducin, which dissociates the α-subunit from the β and γ subunit complex [3].(9) The free alpha subunit binds to and activates phosphodiesterase (PDE)[4]. Active PDE breaks down cytosolic cGMP to GMP(10)[5]. The decrease in cGMP closes cGMP gated ion channels in the outer-segment, halting the flow of Sodium ($Na^{+)}$ and Calcium ($Ca^{2+)}$ into the photoreceptor outer-segment(11) [6]. Each step in this pathway activates a cascade of numerous simultaneous downstream events resulting in a rapid quenching of the signal following the initial photo-excitation.

At rest, the photoreceptor is depolarized at roughly -40mV due to a combination of an outward K^+ current and in inward Sodium (Na^+) Current. The change in ion flow following PDE activation and closing of cGMP gated cation channels hyperpolarizes the cell due to the continuous action of the Na^+/K^+ ATPase which pumps Na^+ out of the cell. Hyperpolarization closes voltage gated Calcium (Ca^{2+}) channels in the inner segment and synapse. As Ca^{2+} is necessary for synaptic vesicle release(12), this halts the release of synaptic glutamate and stops the signal to downstream bipolar cells, signaling light adaptation.

In order to detect the next photon of light, the cell must reset. This is coordinated by an internal mechanism that deactivates each of the steps of phototransduction. As Ca^{2+} levels fall due to the action of the $Na^+/ Ca^{2+} / K^+$ exchanger, Ca^{2+} dissociates from guanylate cyclase activating protein (GCAP)(13), resulting in an activation of guanylate cyclase. Guanylate cyclase converts GTP into cGMP, raising cGMP levels and reopening cGMP gated cation channels. In addition to rising cGMP levels, upstream activated processes are reset as free Rhodopsin is deactivated through phosphorylation by rhodopsin kinase(14). Phosphorylated Rhodopsin has a high affinity for the protein arrestin, which inactivates Rhodopsin. Meanwhile GTPase Activating Protein (GAP) stimulates hydrolysis of GTP bound to α-Transducin to GDP, inactivating Transducin to restore the complex to its heterotrimeric state. These combined actions, eliminate the upstream activation of the photo-transduction cascade, inactivating PDE and causing a further elevation in cGMP levels. The binding of cGMP to cGMP gated ion channels results in an influx of Na^+ and Ca^{2+} into the cell, known as the Dark Current. This influx of cations depolarizes the photoreceptor membrane. The depolarization of the inner

segment, opens voltage gated Ca^{2+}channels in the synapse. This rise in synaptic Ca^{2+} stimulates the release of synaptic glutamate and signals the dark adapted state(15).

Figure 5: Light vs. Dark Adaptation downstream of Photo-transduction

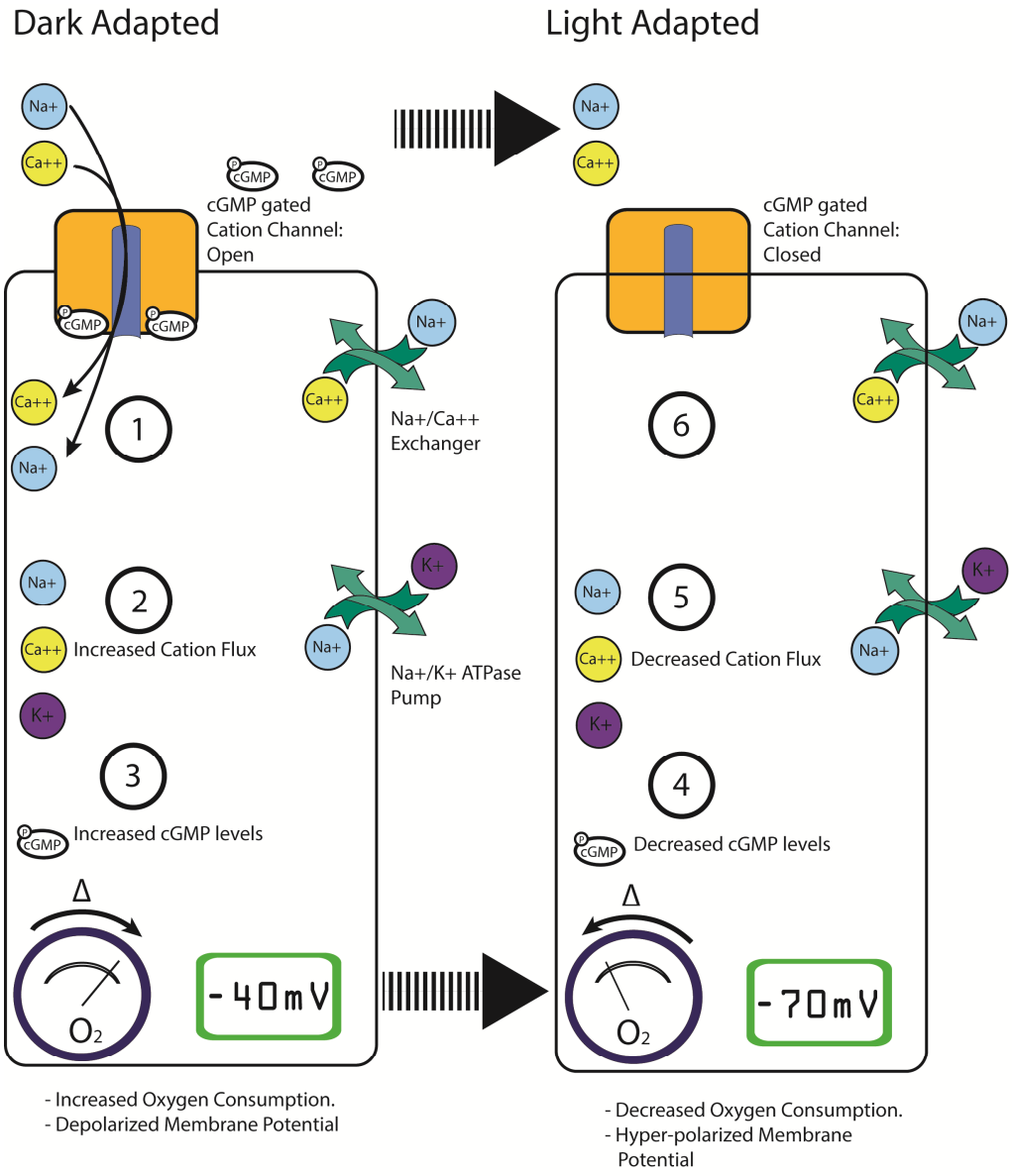

During Dark Adaptation, there is an influx of cations (1) through cGMP gated cation channels, resulting in an increase in overall cation flux (2). The decrease in cGMP is due to inhibited guanylate cyclase (3). The increase in cation flux results in a depolarized membrane potential and increased energy expenditure by the Na+/K+ ATPase to maintain membrane potential. During light adaptation, guanylate cyclase is activated, resulting in decreased cGMP levels (4). This closes cGMP gated ion channels and results in decreased cation flux. (5), (6). The result is a hyperpolarized membrane with decreased energy demands to maintain membrane potential.

Metabolic changes in the retina during Light and Dark Adaptation

An interesting aspect of this entire mechanism is that photoreceptors signal the absence of light and are, counter-intuitively, far more energetically active in the dark adapted state than the light adapted state. During dark adaptation, non-gated K+ channels bring K+ into the cell, resulting in a hyperpolarized current of -70mV. Meanwhile, cGMP gated Na+ channels allow sodium to flow into the cell, depolarizing the membrane potential to -40mV. Na+/K+ ATPase pumps maintain the ion gradient across the plasma membrane, resulting in an increase in ATP consumption during dark adaptation(16,17). This increase in energy consumption has been observed in the measurement of retina oxygen consumption, which increases within the photoreceptor layer of the retina during the light to dark transition(18).

Photoreceptors are the main energy consuming cells within the retina, comprising up to 50% of the total mass of the retina(17). While rod cells are capable of detecting a broad range of detectable light, cone photoreceptor cells are insensitive to lower light levels. In cones, due to their moderate light sensitivity, the synaptic activity and the ion channel energy expenditure is in an intermediate state between light and dark adaptation. This intermediate energy demand results in a persistently higher average energy expenditure to maintain their membrane potential than rods. As a result, the layout of rods and cones in the retina between species localizes a small number of cone cells towards the center of the retina (or fovea) to limit the number of high energy consuming cells to the most effective region. Humans tend to be cone dominant and have a higher degree of color vision than mice which have rod dominant vision. Mice have rod dominated vision, so studies of retina energy metabolism could be extended to

model predominantly rod mediated metabolism. While there are several animal models with predominantly color vision, such as zebrafish(19) and ground squirrels (20), mice represent a well-characterized, yet simplified model organism of mammalian retina metabolism.

Source of Energy: Retina Metabolism is predominantly Glycolytic

Adenosine Triphosphate (ATP) is the main energy currency of the cell. Harnessing the energy of dephosphorylation of ATP to ADP, numerous cellular functions are fueled through the breakdown of ATP. As an energy source, mitochondrial oxidative phosphorylation of glucose provides the highest amount of Adenosine Triphosphate (ATP) per unit substrate compared to glycolysis.

- Glycolysis: 2 ATP per molecule of glucose
- Oxidative Phosphorylation : 36 ATP per molecule of glucose

Purely in terms of ATP production, glycolysis is not the most efficient method of energy production. However, glycolysis also serves as a means of producing metabolic building blocks for the cell. At several steps in glycolysis, substrates may be drawn off to synthesize precursor molecules. Glucose-6-Phosphate may be shunted into the Pentose Phosphate Pathway, dihydroxyacetone phosphate may be used to synthesis glycerol backbones, and 3-phosphoglycerate may be used to synthesize serine. In tumors, glycolysis is used to increase cellular mass, by shifting cellular metabolism to the glycolytic pathway even in the presence of high oxygen concentrations, a phenomenon known as aerobic glycolysis, which has been observed not only in cancer cells, but also in the retina.

Figure 6: Metabolic energy sources in the Retina: Glycolysis

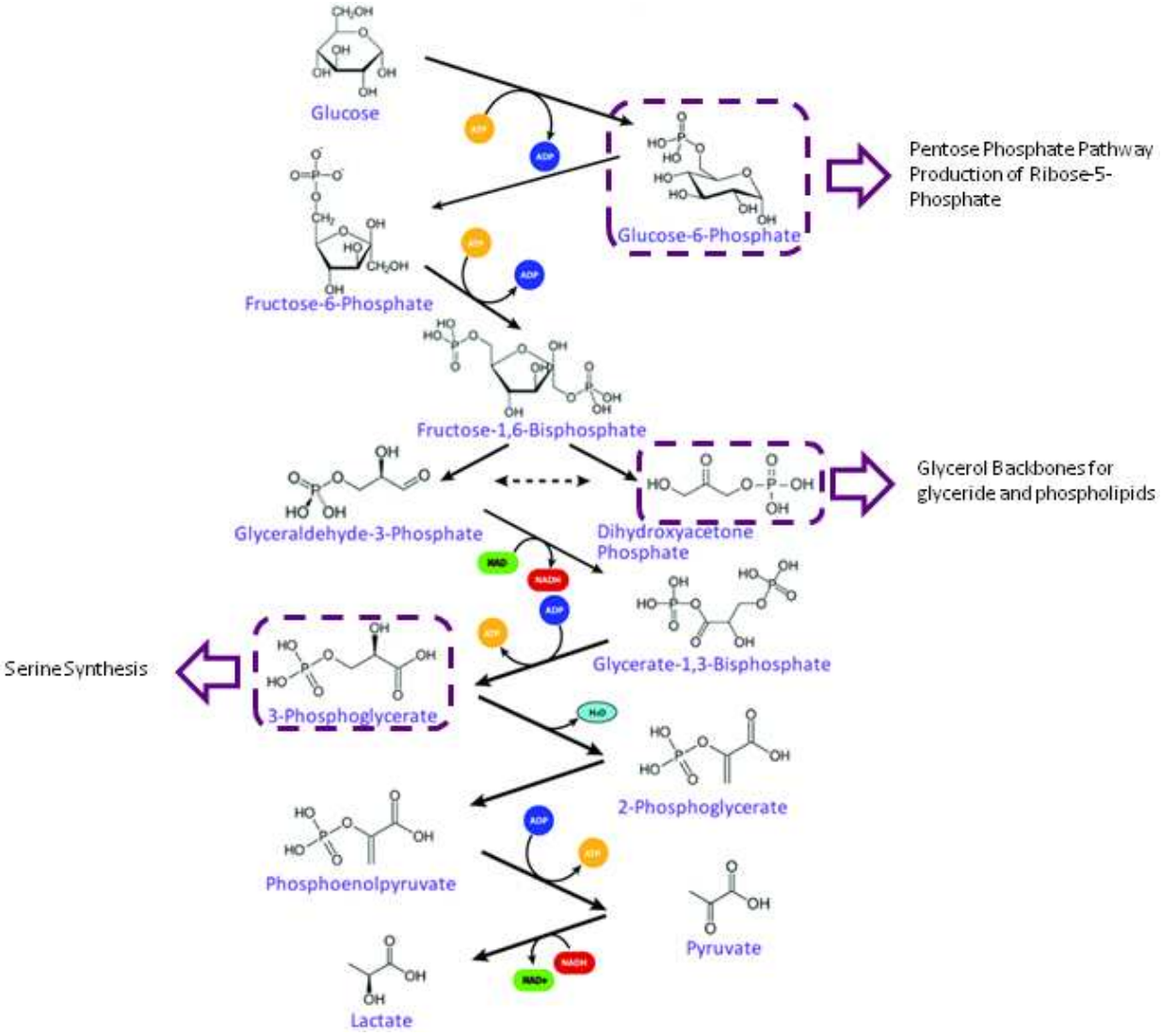

Glycolysis, the enzymatic break-down of glucose, is capable of not only rapidly generating ATP, but also NAD+ through the formation of lactate. NAD+ is a necessary precursor to maintain the rate of glycolysis in a cell. In Intermediates of the glycolytic pathway can be used to generate metabolic precursors, such as Ribose-5-Phosphate, Glycerol, Serine, and other amino acids.

The Warburg Effect in the Retina

Within minutes of oxygen deprivation, retina function is severely impaired (21), thus highlighting the need for aerobic metabolism in the retina. However, the metabolism of the retina has also long been associated with aerobic glycolysis, a process in which glycolytic breakdown of glucose to lactate occurs in the presence of oxygen, despite the capacity of cells to use pyruvate in oxidative metabolism (22,23). This effect was first noticed by Otto Van Warburg in 1927, during his initial studies of cellular metabolism(24) in which he compared the metabolism of various tissues with tumors, namely through oxygen consumption and generation of lactate. While aerobic glycolysis was first observed in cancerous tissue, it also occurs in many other rapidly dividing cell types, such as T cells and embryonic tissues(25,26). In general, this effect is associated with a rapid intake of glucose and reduction of pyruvate to lactate rather than oxidation of pyruvate for mitochondrial respiration.

However, why the retina behaves in this manner is not entirely clear. More importantly, which cells in the retina may rely on aerobic glycolysis to function was not known. In attempting to determine which cells exhibit the greatest reliance on aerobic glycolysis, we hypothesized that photoreceptor cells may have qualities matching that of a rapidly dividing cell. The reason for this metabolic behavior may be explained by the need for metabolic precursors for the turnover of photoreceptor outer segments and the need for cellular reducing equivalents(27).

Turnover of Rod Outer Segments: A Demand for Aerobic Glycolysis

The outer-segment is a unique extension of the photoreceptor cilium and the site of the photo-transduction cascade. A thin connecting cilium connects the stack of rod outer segment discs to the inner segment of the photoreceptor, bridging the gap between sensor and neuron(28). Each day, upon initial light adaptation, the photoreceptor sheds roughly 10% of its apical rod outer segments(29). Shed discs are phagocytized by the adjoining retinal pigment epithelium and broken down to protein and lipid components(30). This process of outer segment shedding and renewal while differing in stimulus or circadian regulation, is conserved amongst vertebrates.

Figure 7: Turnover of Rod Outer Segment Discs

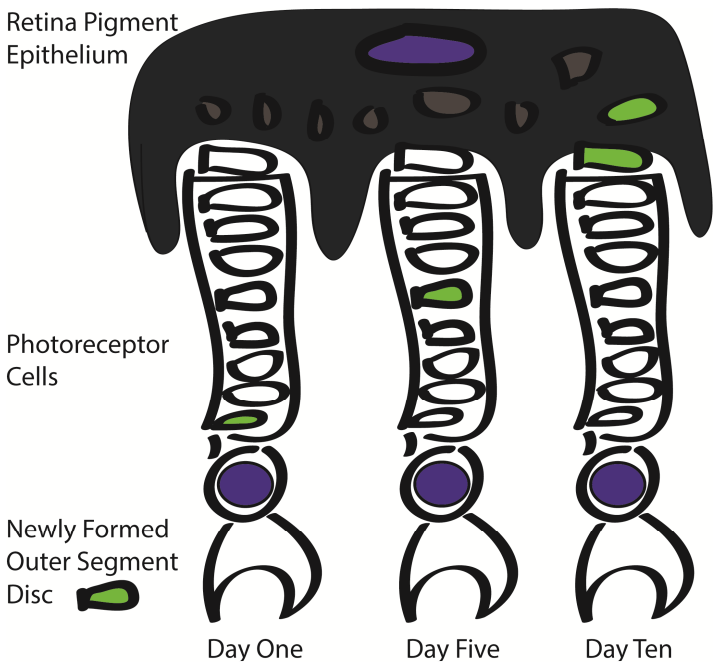

In experiments conducted by Richard Young in 1971, Radio-labeled amino acids were injected into mouse retinas and retinas were harvested at various time points for EM imaging. The distribution of amino acids started out as diffuse, but by the end of 24 hours, concentrated into a disc region at the base of the outer segment. This was found to be the result of Rhodopsin biosynthesis, the most predominantly expressed protein in the photoreceptor and concentrated in outer segment disc membranes. By sampling at different time points, it was shown that the disc containing radio labeled amino acids would progress towards the tip of the outer segment. By day ten, the disc was phagocytized by the RPE and amino acid labeling was dispersed due to breakdown of the outer segment disc.

Daily renewal of rod outer segments requires synthesis of an equal quantity of discs each day to maintain outer-segment length and photoreceptor function. Calculations of the overall lipid membrane turnover estimate that the renewal of outer-segments discs represents roughly 100X the dimensions of the photoreceptor cell membrane. While the photoreceptor cell is highly differentiated and post-mitotic (31), this high demand for membrane and protein synthesis may explain why aerobic glycolysis is localized to the photoreceptor and is a metabolic process necessary for cell function.

The maintenance of this organelle places a high demand on the photoreceptor for biosynthesis of new phospholipids and Rhodopsin. Rather than an unnecessary expense, it is hypothesized that daily turnover of these discs is an alternative pathway to dispose of misfolded or oxidized proteins(32). The shedding of outer segment discs and phagocytosis by the RPE limits the potential build-up of damaged cellular components in the photoreceptor and defers the energy demands of disposal to the RPE. Synthesis of outer-segment membranes and proteins requires the necessary building blocks associated with aerobic glycolysis. However, the result of sustained glycolysis is the build-up of lactic acid, which must be removed from the cell.

In vertebrates, a system known as the Cori Cycle serves to balance demands from glycolysis and oxidative phosphorylation. During strenuous exercise, lactic acid will build up in muscles as the demand for ATP from Glycolysis exceeds that of the ability of the cell to undergo oxidative phosphorylation, either due to short-term ATP demand or lack of oxygen. This lactic acid may be released into the blood stream where it is used by the liver to generate more glucose through gluconeogenesis, or by the heart, a highly

aerobic tissue which oxidizes lactate to fuel cellular processes(33). A similar mechanism exists in the brain between neurons and glia and this is known as the Astrocyte-Neuronal Lactate Shuttle (ANLS).

The Astrocyte Neuronal Lactate Shuttle in the Retina

Figure 8: The Astrocyte Neuronal Lactate Shuttle

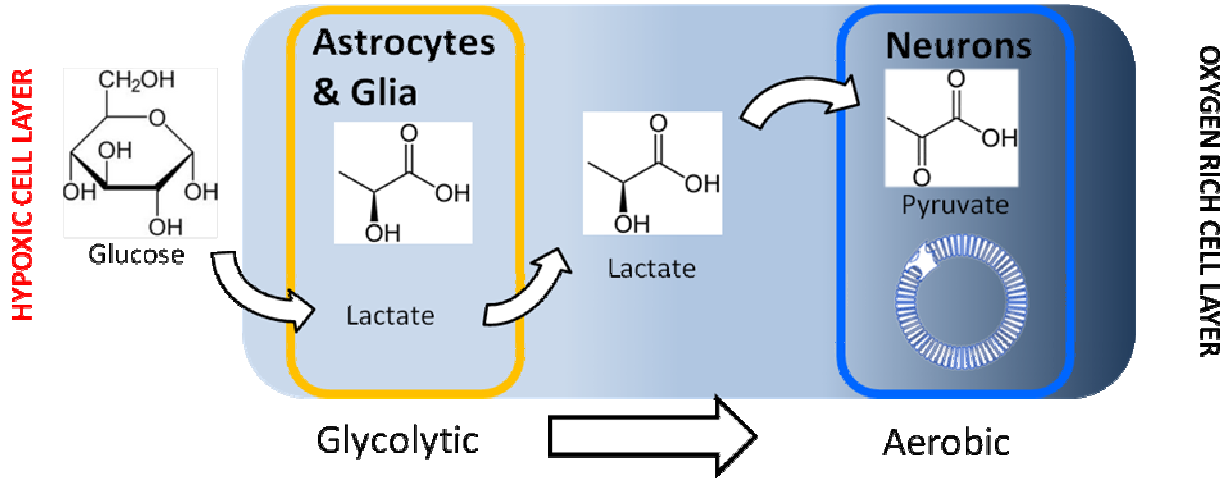

Originally put forward by to explain the metabolic connection between neurons and their supporting glia cells(34), the hypothesis has long been held that cells which are hypoxic utilize glycolysis to sustain metabolic activity, producing lactate. Lactate, a highly reduced molecule may then be oxidized into pyruvate and utilized by nearby cells capable of aerobic metabolism. A similar mechanism is proposed to work in tumors, where the interior of the cancerous cell mass becomes increasingly hypoxic due to the high rate of glycolytic flux and cells on the periphery that are exposed to more oxygen may use aerobic metabolism to metabolize lactate.

In the typical model of ANLS, astrocytes and glia are heavily glycolytic, whereas neurons, and by extension to the retina, photoreceptors, are primarily aerobic. In the brain, where glia represent a large percentage of the overall cell number, this method reserves oxygen for neuronal energy function and allows the neurons to continue functioning in the face of metabolic insults such as hypoglycemia and hypoxia.(35) In order to understand the validity of the hypothesis and how this meshes with overall glycolytic activity in the retina, we must understand the link between glycolysis and oxidative phosphorylation, which is linked not only through intracellular redox potential, but also the first enzyme of glycolysis: Hexokinase.

Mitochondrial Oxidative Phosphorylation is used to fuel Glycolysis.

During light adaptation of the retina, insulin receptors located on the photoreceptor cell are auto-activated and hexokinase II translocates to the Voltage Dependent Anion Channel (VDAC) of the mitochondria in the inner segment(36).This association to mitochondria alters the utilization of mitochondria generated ATP from general ATP production towards phosphorylation of glucose(37). This suggests that there is an increase in glycolysis during light adaptation, utilizing ATP from oxidative phosphorylation to fuel glycolysis. In studies of lactate generation in the retina, it was shown that lactate production does increase slightly during dark adaptation. However, if the photoreceptor, relies primarily on glycolysis (similar to a neuron), it is unclear how this theory can integrate with the canonical ANLS. To understand the role of glycolysis in the retina and this change in energy demand between light and dark will require an understanding of oxidative phosphorylation within the retina.

Figure 9: Oxidative Phosphorylation: The Citric Acid Cycle

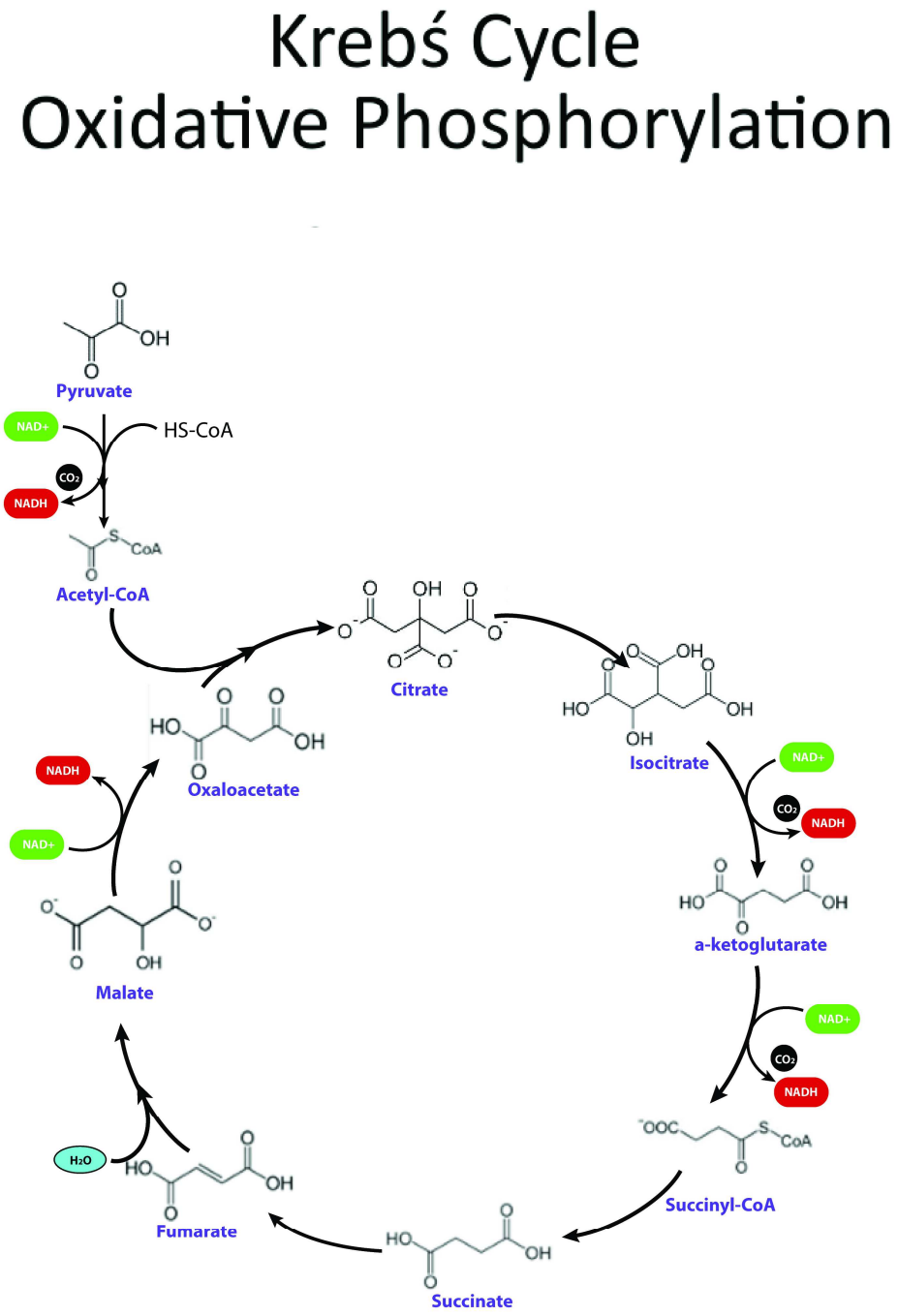

Pyruvate, whether taken up exogenously or as a by-product of glycolysis, enters the mitochondria through the mitochondrial pyruvate carrier, where it is immediately decarboxylated to Acetyl-Coa. These carbons are incorporated into the Citric acid cycle, where each Acetyl-CoA is capable of generating roughly 4 NADH per turn of the TCA cycle which can be shunted into the electron transport chain to generate ATP. For 2 Pyruvate molecules generated from Glucose, this can yield up to 36 molecules of ATP, making this a much more efficient means of ATP synthesis.

Mitochondria are predominantly localized in the photoreceptor layer of the retina. While glycolysis does play a large role in overall retina metabolism aerobic metabolism and oxidative phosphorylation also play and important role in the retina's ability to fuel its high energy demands. Studies of mitochondrial localization within the vertebrate retina have revealed that mitochondria are localized in two distinct layers, one layer in the inner retina and one in the outer retina. In species with avascular retinas, those lacking inner-retina vasculature, such as guinea pigs and larval salamanders, the outer retina layer is the only layer with functioning intact mitochondria(38)**.** In species with vascularized retinas, such as mice and humans, photoreceptors contain the bulk of mitochondria in an ellipsoid region abutting the outer-segment(39). Regardless of the retina vasculature, while the retina is highly glycolytic, it would appear that photoreceptors rely heavily on mitochondria and oxidative phosphorylation to fuel the processes of vision. This also suggests that glycolysis may play a larger role in fueling inner retina metabolism, even in cells with inner retina vasculature.

Ca^{2+} regulates the overall flux of glutamate into oxidative phosphorylation.

Studies of isolated brain mitochondria have revealed that mitochondrial metabolism of glutamate is significantly altered by intracellular Ca^{2+} levels through regulation of aspartate-glutamate carrier AGC1. Increases in intracellular Ca^{2+}concentration favored the respiration of the mitochondria on glutamate and malate (40), with pyruvate respiration unaltered. Similar changes in intracellular Ca^{2+} concentration are observed in depolarization of the photoreceptor during light to dark adaptation, suggesting that this same process may occur in photoreceptor

mitochondria. The result of increased glutamate uptake by photoreceptor mitochondria is the production of NAD+ necessary to increase glycolytic flux through the Malate Aspartate Shuttle.

The Malate Aspartate Shuttle in the Retina.

While pyruvate metabolism is typically the main fuel for mitochondrial oxidative phosphorylation, glutamate based respiration is also a critical component to photoreceptor cell survival, as demonstrated in previous studies of retina metabolism(41). AGC1 provides a bridge between the cytosol and the inner mitochondrial matrix in fueling oxidative phosphorylation allowing reducing equivalents to be exchanged between the mitochondrial matrix and the cytosol.

Figure 10: The Malate-Aspartate Shuttle

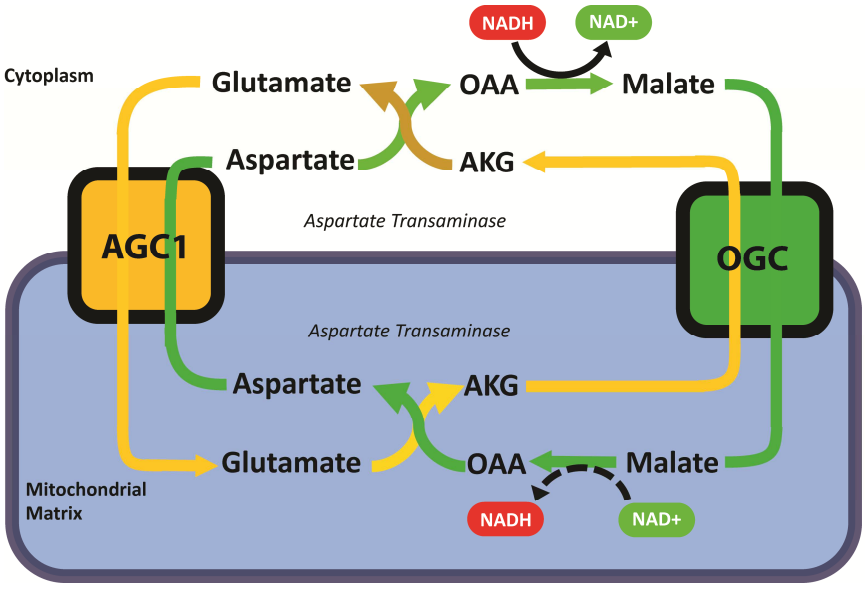

The Malate Aspartate Shuttle provides a means of balancing NADH levels between the cytosol and the mitochondrial matrix. This process relies on Glutamate from the cytosol being exchanged for Aspartate by AGC1. Aspartate is then transaminated to Oxaloacetate by Aspartate transaminase and the resulting Oxaloacetate reduced to Malate by malate dehydrogenase. This Malate can then be exchanged for a-KG by the Oxoglutarate carrier OGC. The transport of Malate allows for NADH to be brought into the Mitochondrial Matrix, allowing for more NAD+ to be formed in the cytosol. As a result, reducing equivalents may be exchanged between the cytosol and the mitochondria.

In the retina, AGC1 is excluded from the Müller cells of the outer retina (42), suggesting that aerobic metabolism, and by extension, the intracellular redox potential between the various neurons and glia, may be significantly altered due to the abrogated Malate-Aspartate Shuttle of Müller glia.

Redox Potential ties Cellular Metabolism to Response to Oxidative Stress.

The cellular redox potential, or balance between oxidized and reduced forms of NAD and NADP, plays an important role in how the cell responds to oxidative damage. Glutathione is an anti-oxidant present in high concentrations in neurons. It is composed of two tri-peptides composed of glutamate, cysteine, and lysine, which possess a disulfide bond between two molecules of glutathione, which can then be reduced by NADPH to dissociate the tri-peptides. Due to its reliance on NADPH to reduce its oxidized form, glutathione is closely tied to intracellular redox potential and therefore predominantly associated with mitochondria(43), which are the primary source of NADPH in the photoreceptor inner segment(44).

Previous studies on glutathione in the retina demonstrated that it was highly enriched in Müller glia and inner retina neurons while low in photoreceptor cell outer segments(45). Glutamate is a necessary precursor for glutathione production and previous studies by Marc and Cameron demonstrated that immuno-localization of reduced glutathione had an inverse relationship between these two metabolic components with Müller glia uptake of glutamate being used to synthesize not only glutamine, but also glutathione(46). Studies of the effect of hypoxic damage on cellular redox potential, have shown that glutathione is depleted in Müller glia(47) during

ischemic damage suggesting that Müller glia may be a sink for antioxidants which may be transferred to nearby neurons in response to oxidation insult. As mitochondria are an essential source of NADPH in the retina (44), disruption of the supply of NADPH through either glycolysis or oxidative phosphorylation would prevent formation of this antioxidant, placing the cell at risk for oxidative damage and degeneration.

Impaired Retina Metabolism Leads to Degeneration.

As there are several unique genes and morphological features attributed to photoreceptor cells, it is not surprising that defects in photo-transduction genes, turnover of outer segment discs, or separation of photoreceptor cells from adjoining RPE and Müller glia can ultimately lead to photoreceptor cell death and retina degeneration(48)**.** Tracing through the pathway of photo-transduction, it has been shown that defects in Rhodopsin Kinase(49,50), Phosphodiesterase(51), and Guanylate Cyclase(52) result in retina degeneration. However, defects in Transducin do not induce retinal degeneration, suggesting that there is more to this process than just a lack of photo-transduction. Our understanding of how metabolism fuels photoreceptor cell processes may help to differentiate light and dark adapted responses from defects in photo-transduction that lead to cell death.

In addition to defects in genes involved in photo-transduction or specific to photoreceptor cells, there are also several mutations in metabolically related genes, which result in blindness or retina degeneration. Leber's Hereditary Optic Neuropathy (LHON) and Dominant Optic Atrophy (DOA) are two of the earliest known optic neuropathies(53), in which mitochondrial dysfunction is shown to result in degeneration

of retina ganglion cells(54). In addition, defects in Pyruvate Dehydrogenase(55) and Isocitrate Dehydrogenase(56) can contribute to retina degeneration. Aside from genetic mutations, the basic nature of the retina appears to be extremely sensitive to metabolic disruption. Hypoxia or loss of blood supply can result in vision loss within minutes with long-term hypoglycemia leading to retina degeneration(57). Therefore, understanding the metabolic pathways involved in photoreceptor cell function may allow for restoration of vision through metabolic intervention, as observed with ketogenic diet treatments of glaucoma(58).

The study of retina metabolism will reveal new insights to the causes of retina degeneration by answering how defects in photo-transduction machinery differ from basal metabolic activity, thereby allowing a means of counter-acting metabolic deficiencies caused by these mutations. While the retina's high glycolytic activity has been known for some time, little is known regarding the source of aerobic glycolysis in the retina. Our work has focused on the localization of aerobic glycolysis to the photoreceptor cell and on understanding the impact of this process on overall retina metabolism. The work presented in this thesis has revealed novel differences between previous models of retina metabolism as a model of neuronal metabolism. In our studies of the unique energy demands of individual cell types in the retina, we have also made gains in culturing the isolated photoreceptors. This information and development of culturing techniques will allow for the study of isolated photoreceptors and contribute to our basic knowledge and treatment of retina degeneration.

Chapter 2: Pyruvate Kinase and aspartate-glutamate carrier distributions reveal key metabolic links between neurons and glia in the retina.

Introduction

Aerobic glycolysis is a metabolic adaptation proliferating cells use to meet anabolic demands (59,60). In tumors it is called the "Warburg effect. Tumors convert ~90% of the glucose (Glc) they consume to lactate (Lac) whereas the brain converts only 25% of the glucose it uses to lactate (61). In retinas of vertebrate animals, energy is produced in a way that resembles tumor metabolism more than brain metabolism. Aerobic Glycolysis accounts for 80-96% of glucose used by retinas(16,62–64). Retinas are made up of neurons and glia (4). The outermost layer of the retina is occupied by photoreceptor cells. The inner layers contain a diverse collection of signal processing neurons. Müller glia span the retina from the base of the photoreceptor outer segment to the end of the inner retina. Despite knowledge of the overall layout of cells and metabolism of the retina, the site of retina aerobic glycolysis has not been established.

Exchange of fuels and in the trade-off of lactate in the Astrocyte Neuronal Lactate Shuttle is an important part of the relationship between neurons and glia(65–68). Transfer of metabolites between intracellular compartments, such as transfer of reducing equivalents through the mitochondria Malate Aspartate Shuttle also is important. Glycolysis is supported by re-oxidation of cytosolic NADH, which can be catalyzed by cytosolic lactate dehydrogenase (LDH) or by the mitochondrial Malate Aspartate Shuttle (MAS). Photoreceptors and other neurons in the retina express aspartate/glutamate carrier 1 (AGC1)(42), a mitochondrial Aspartate-Glutamate Carrier

that has a key role in the MAS. However, Müller cells (MCs) are AGC1 deficient (42). The significance of the distribution of AGC1 has been enigmatic.

Aerobic metabolism in tumors is linked to expression of a specific isoform of Pyruvate Kinase, PKM2 (69,70). Pyruvate Kinase (PK) catalyzes the final step in glycolysis, synthesis of pyruvate (71). Liver (PKL) and erythrocyte (PKR) isoforms are splice variants from the PKLR gene and PKM1 and PKM2 are splice variants of the PKM gene. A unique feature of PKM2 is that it is responsive to allosteric and posttranslational regulators (71). PKM2 expression in cancer cells correlates with reduced yield of ATP from glucose and accumulation of glycolytic intermediates. PKM2 also favors synthesis of serine and Pentose Phosphate Pathway intermediates that support anabolic activity (72). Association of PKM2 with aerobic glycolysis in tumors motivated us to explore the relationship between PKM2 and aerobic glycolysis in retina. We found that PKM2 is abundant and located only in the outer retina, implicating photoreceptors as a primary site of aerobic glycolysis. Unexpectedly, we also found that Müller glia are deficient for all isoforms of PK. What make this interesting is that while Hexokinase and Phosphofructokinase, two upstream glycolytic enzymes which control glucose entry into the cell may have higher exothermic control, slowing down these enzymes would only slow down the overall rate of glycolysis. At the step of Pyruvate Kinase, the cell controls whether glycolysis will continue on to pyruvate and potentially oxidative phosphorylation, or continue to shunt glycolytic intermediates into synthesis of cellular building blocks.

The exclusion of AGC1 and PK from Müller glia led us to investigate metabolic relationships between photoreceptors and Müller Cells. We found that cultured Müller

Cells have an impaired ability to metabolize glucose, but they metabolize aspartate (Asp) effectively. Our findings reveal that the metabolic benefits of down-regulating PK and AGC1 in Müller Cells correlates with specific metabolic adaptations in the retina. Rather than using glucose to fuel their mitochondria, Müller Cells use lactate and aspartate from neurons to direct their cell metabolism towards their overall cellular function, while allow Photoreceptors to use glucose to fuel their intense metabolic demands.

Results

Glycolytic enzyme activity in retina compared to other tissues.

Our experiments sought to determine the overall level of glycolytic activity in the retina compared to other tissues and continue on to analyzing the distribution of activity and enzyme expression in the retina. We compared maximum specific activities (V_{max}) of glycolytic enzymes in homogenates of retina, muscle, brain, liver, a SV40 transformed Müller Cell Line (RMC-1) (73) and HeLa cells. (Fig 1) The activities of these glycolytic enzymes generally increased from the first to final step of glycolysis. Pyruvate Kinase was found to have the highest enzymatic activity in all tissues except liver. Therefore, it would appear that glycolysis was active in the retina, but which isoforms were responsible for pyruvate kinase activity would determine the distribution of this activity in the retina.

Figure 2.1 Glycolytic enzyme activities in the retina.

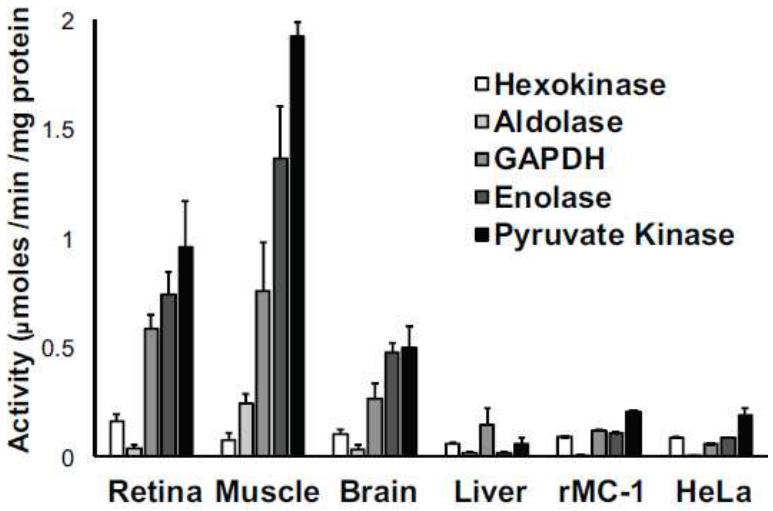

Activities of glycolytic enzymes in homogenates of retina, muscle, liver, brain and in 2 control cell lines. rMC-1 (rat müller cell) cells are an SV-40 immortalized cell line with Müller Cell characteristics. HeLa cells served as a tissue culture model of rapidly dividing cells. Activities were measured at substrate concentrations above the reported Km for each enzyme.

The M2 isoform of pyruvate kinase is the predominant isoform in the retina.

We evaluated PK expression in brain, liver, muscle and retina with antibodies specific for PKLR, PKM1 and PKM2. PKLR was present in homogenates of liver, but not retina (Fig. 2). Consistent with this observation, no PKLR was found in a proteomic analysis of rat retina (74). PKM1 is expressed in several tissues, such as brain, muscle and retina, but not in liver whereas PKM2 is most abundant in retina and in either Müller cell like cell line (rMC-1) or HeLa cells compared to other tissues studied. (Fig. 2).

Figure 2.2 Pyruvate Kinase Isoform Expression varies between tissue types.

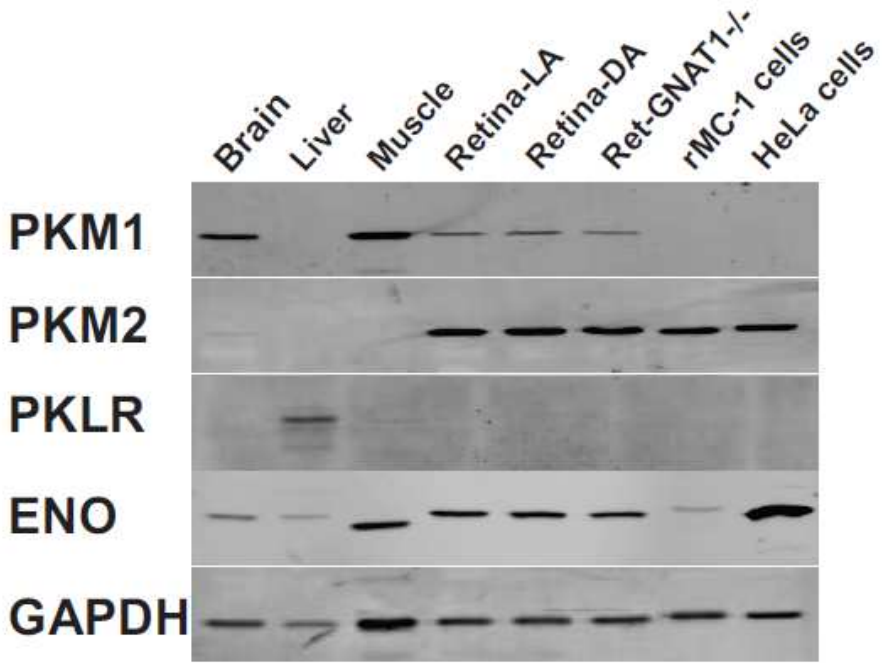

Immunoblot analysis of PK isoforms in homogenates of whole brain, liver, and muscle and retina ("LA": light-adapted and "DA": dark-adapted), GNAT1-/- retinas were included because they are unresponsive to light. rMC-1 is an SV-40 transformed MC line (18) and HeLa is a cancer cell line which served as a model for rapidly dividing cells. Each lane is loaded with 5 µg protein.

We quantified PKM1 and PKM2 in mouse retina by calibration with pure recombinant PKM1 and PKM2 (concentration determined by amino acid analysis) (Fig. 3). Our analysis showed there are ~150 pmol PKM2 and ~26 pmol PKM1 per mouse retina. This was surprising, since PKM2 is calculated to be present at 25% of the amount of rhodopsin, the most abundant protein in photoreceptors (600 pmol per retina) (75,76) Such a high concentration suggests a unique reliance demand of retina tissue for PKM2 expression.

Figure 2.3 PKM2 expression is higher than M1 expression in the retina.

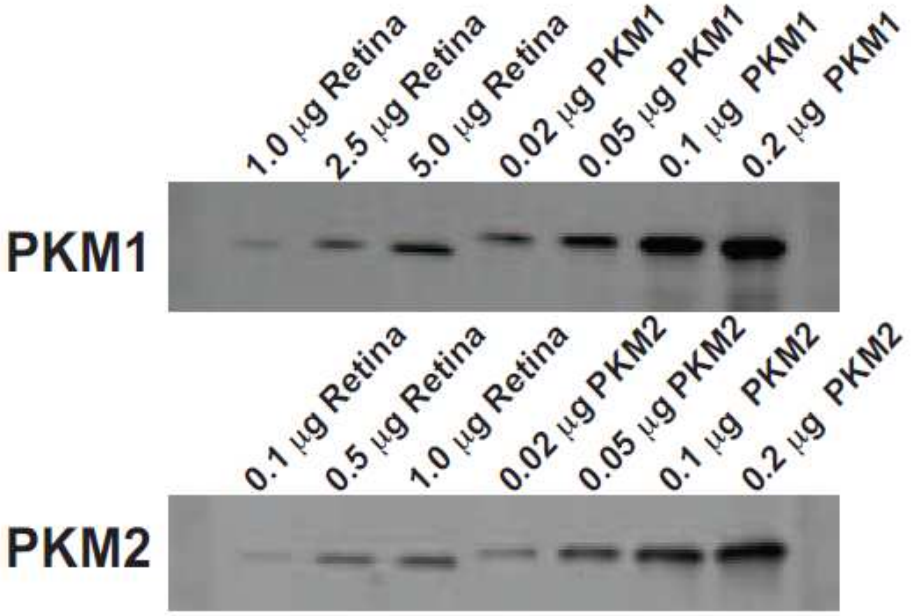

Quantitative immunoblot analysis comparing retina homogenate with known amounts of purified PKM1 and PKM2. Per mg of tissue, PKM2 is the predominant isoform expressed in the retina.

PKM2 in the retina is only expressed in photoreceptor cells.

We evaluated the distribution of PK in light-adapted retinas by assaying PK activity in serial sections of frozen unfixed rat retinas (Fig. 4A)(77,78). We noted two distinct peaks of activity. Rhodopsin and synaptotagmin marked outer segments and synaptic terminals of PRs. Immunoblot analysis (top panel Fig. 4A) detected PKM2 only in the outer retina. Immunohistochemical analysis showed that PKM2 is confined to cell bodies and synaptic terminals of photoreceptors (left panel Fig. 4B) whereas PKM1 is in photoreceptors and inner retinal neurons (left panel Fig. 4C). This result was surprising, in that little is known of the dynamics of PKM1 and PKM2 expressed within the same cell type and it is heretofore unknown of primary cells to down regulate all forms of pyruvate kinase.

Figure 2.4. Distribution of Pyruvate Kinase Isoforms in the retina.

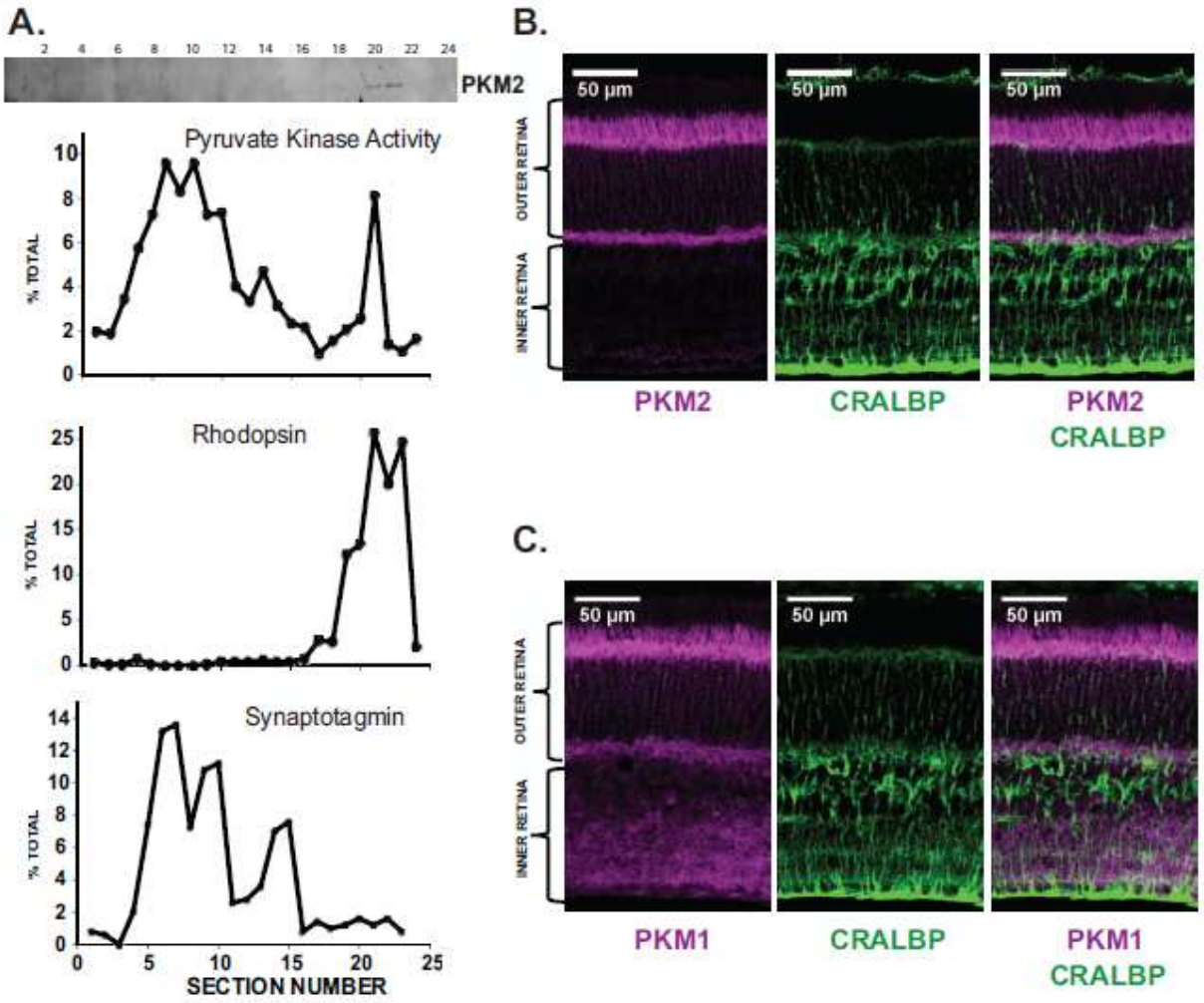

A. Distribution of PK activity (top panel) in serial sections of rat retina. Rhodopsin (middle panel) shows the location of PR outer segments. Synaptotagmin (lower panel) shows locations of synapses. Immunoblot shows PKM2 immunoreactivity. B. Immunohistological localization of PKM2 (left) and CRALBP, a Müller glia specific cell marker (middle) and their overlap (right) in mouse retina. C. Immunohistological localization of PKM1 (left) CRALBP (middle) and their overlap (right) in mouse retina.

PKM2 is regulated allosterically, but not influenced by light.

In addition to its unique form of regulation, PKM2 is also sensitive to multiple types of allosteric regulation (71). Build-up of upstream glycolytic intermediates, such as Fructose 1,6 – Bisphosphate is induces activation of PKM2 pyruvate kinase activity. In addition, growth hormones, such as Triiodo thyronine and amino acids such as Phenylalanine will induce dissociation of the active enzyme, halting glycolysis at the step of pyruvate kinase and favoring the build-up of upstream glycolytic intermediates. We found that in a retina tissue lysate, phenylalanine (5 mM) inhibits PK whereas Fructose 1,6-Bisphosphate (1 mM) stimulates enzyme activity by 15% and is effective at reversing inhibition of PK activity caused by phenylalanine (Fig. 5). This suggests that these regulatory mechanisms to control PKM2 enzyme activity are still in place in the retina, and by extension photoreceptors, despite the expression of PKM1. In similar experiments, we were unable to find differences between PK activities in homogenates prepared from light vs. dark-adapted retinas. Immunoblotting did not reveal any light vs. dark effects on Y105 phosphorylation (79) or on PKM1 or PKM2 expression. Therefore if glycolysis is regulated in the retina during light to dark adaptation, it would not appear to be through the Pyruvate Kinase enzyme.

Since, PKM2 in cancer cells diverts glycolytic intermediates to serine and glycine (80), this metabolic possibility was investigated in retinas. We incubated retinas with U-C^{13} glucose and compared incorporation of C^{13} into lactate vs. into serine. In 5 minutes 44±2% of C^{12} lactate is replaced by C^{13} lactate in light vs. 52±5% in darkness. In previous experiments, cancer cells were found to label serine from C^{13} glucose within 10 minutes (72), however, we found no labeling of serine from C^{13} glucose in retinas

even after 6 hours of incubation with U- C^{13} glucose. We conclude that PKM2 in retina does not divert carbons from glycolysis into serine to the extent that it does in cancer cells. Aside from direct effects on metabolic activity, PKM2 is also known to be a regulator of gene transcription (71). However, in our immunohistochemical experiments, PKM2 was excluded from nuclei in retinas, so it also is unlikely to influence transcription (71).

Figure 2.5. Allosteric regulation of Retina Pyruvate Kinase activity is retained in tissues expressing both PKM1 and PKM2.

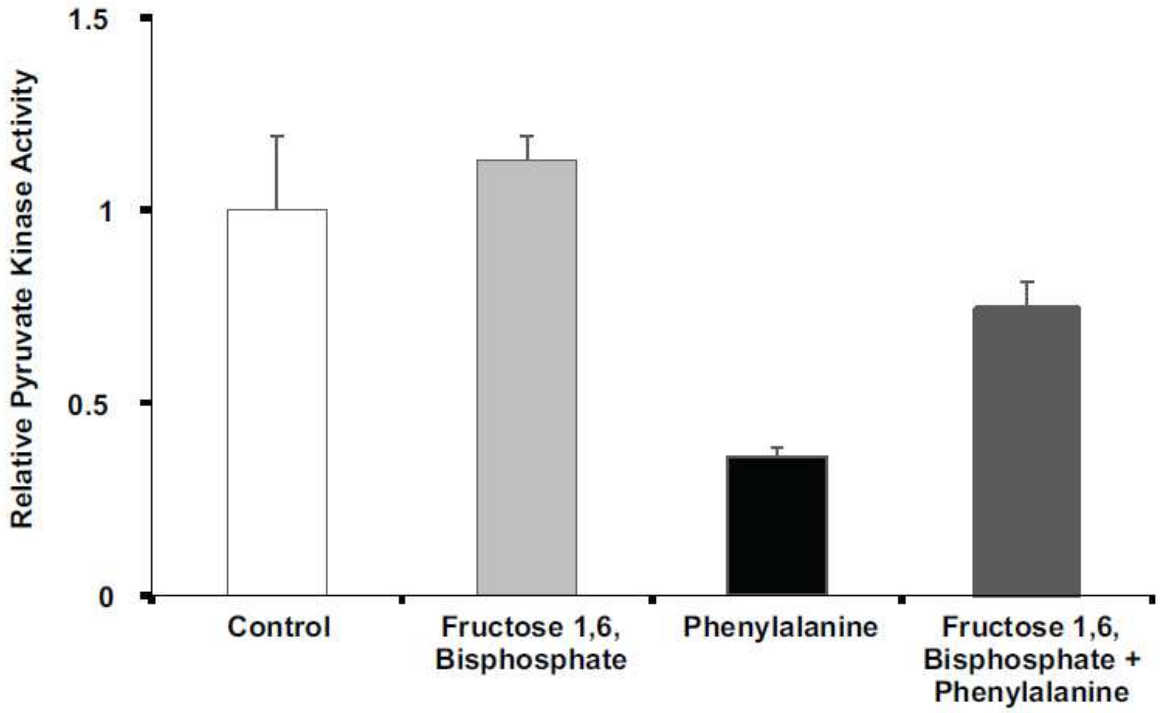

The Y-axis represents PK activity relative to the control. 5 µg of retinal homogenate was assayed at 0.57 mM PEP with 1 mM F1,6BP or 5 mM phenylalanine. Fructose 1,6-Bisphosphate was shown to increase pyruvate kinase activity and Phenylalanine dramatically inhibited enzyme activity, suggesting that these allosteric regulators may play a significant role in dynamically controlling pyruvate kinase activity of the cell. In addition, it was shown that comparable levels of Fructose 1,6-Bisphosphate would reverse inhibition by Phenylalanine.

Müller cells are deficient for all PK isoforms.

We evaluated PKM1 and PKM2 in MCs in retinas by co-labeling retinas with a Müller cell specific marker, CRALBP (middle panels in Fig. 4B, C). Neither co-localized with CRALBP (right panels Fig. 4B,C). To confirm that our method detects glycolytic proteins in Müller cells we also probed CRALBP-labeled sections with antibodies to Enolase and GAPDH. Both co-localize with CRALBP (Fig. 6). In agreement with previous observation, AGC1-/- was excluded from Müller glia Cells.

Figure 2.6. Immunohistochemical localization of Glycolytic enzymes and Aspartate Glutamate Carrier in Retina sections.

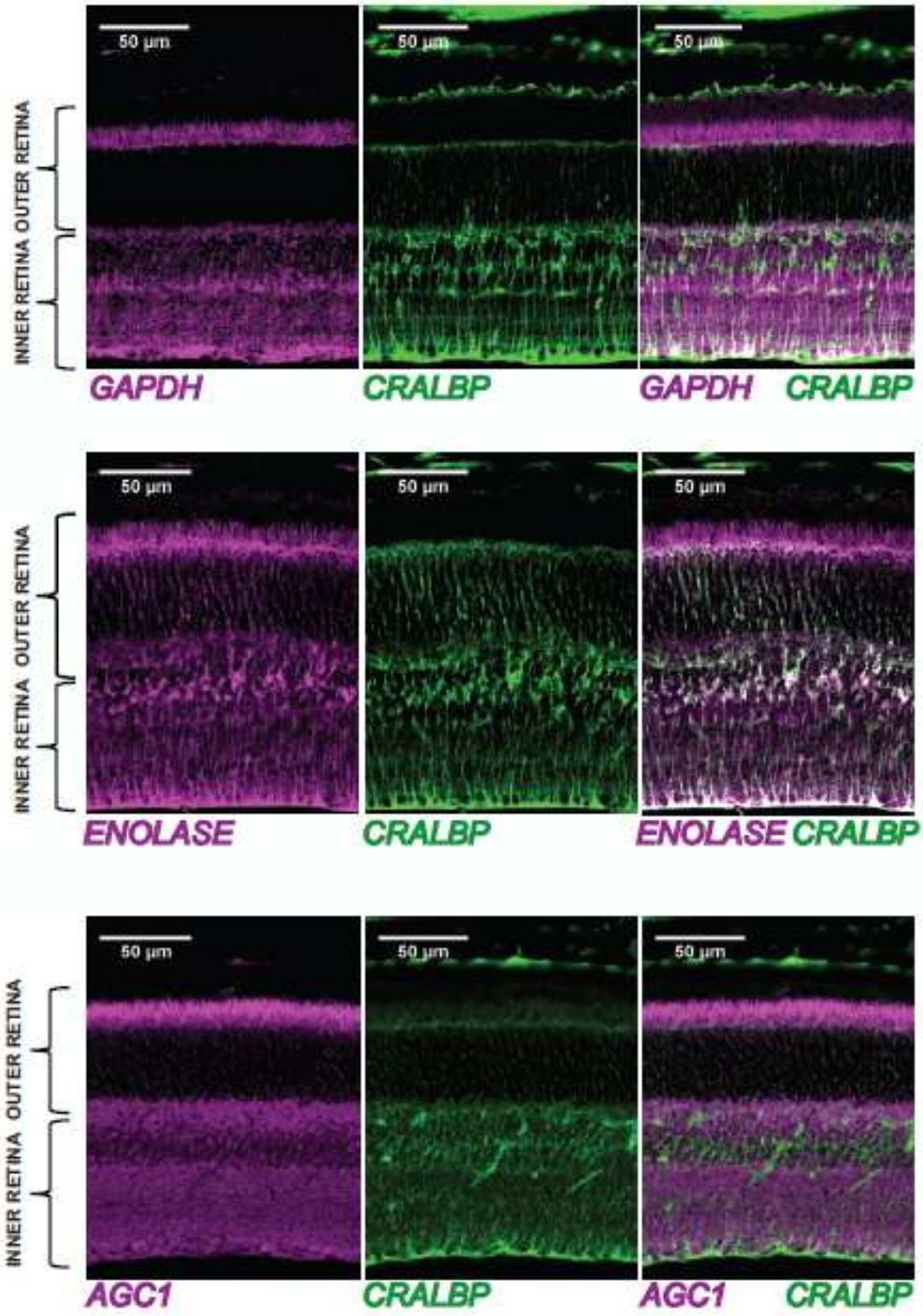

Localization of GAPDH, Enolase and AGC1 (magenta) and the Müller cell marker, CRALBP (green) in mouse retina. While GAPDH and Enolase demonstrate some colocalization (white), much like pyruvate kinase isoforms, AGC1, is also absent from Müller Glia.

To confirm our observations from IHC, we corroborated our data with that of a published gene expression database derived from Müller cells isolated from mouse retinas (81). To evaluate how well this database reflects native Müller cell expression we examined genes expressed only in photoreceptors, such as GNAT1 or Transducin a component of the photo-transduction cascade and IRBP of Interstitial Retinoid Binding Protein which is involved in chromophore turnover in the photoreceptor, or only in Müller cells, such as GLUL or Glutamine Synthetase and CRALBP or cellular retinaldehyde Binding Protein. Our analysis confirmed the accuracy of the database. GNAT1 and IRBP occur more frequently in photoreceptors than in Müller cells and GLUL and CRALBP occur more frequently in Müller cells than in photoreceptors (Fig. 7). We also analyzed PKM and PKLR. PKM sequences are enriched in photoreceptors whereas they are 12 fold less abundant in Müller cells. PKLR is 50-100 fold less abundant than PKM in both photoreceptors and Müller cells (Fig. 7).

Figure 2.7 Gene Transcript Analysis of Adult Photoreceptor and Müller Cells

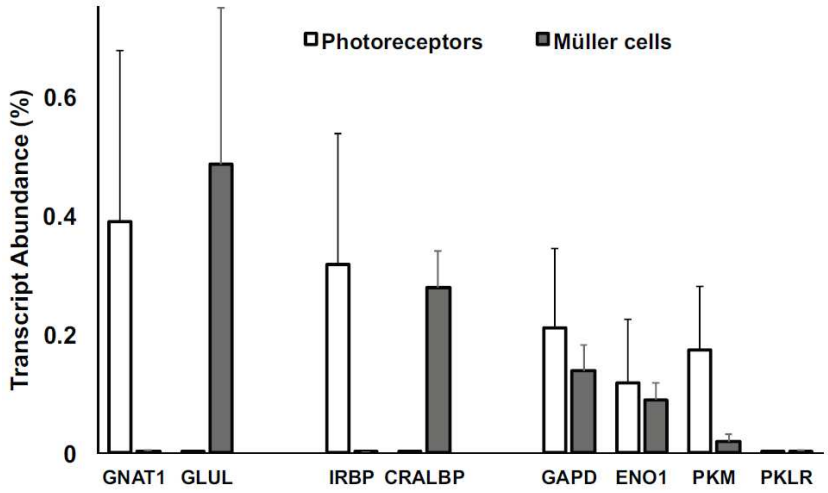

Analysis of transcript abundance vs. total transcript reads in microarray data (81) derived from freshly isolated individual Müller cells and Photoreceptors. "PKM" represents PKM1 and PKM2 transcripts from the PKM gene. Genes associated with photoreceptors (GNAT1 and IRBP) are highly expressed in those cell types, where genes associated with Müller Glia (GLUL and CRALBP) are expressed in that cell types, lending validity to the data from this transcript analysis.

Photoreceptors are the main source of lactate production in the retina.

Our findings that Müller cells do not express PK and that photoreceptors express abundant PKM2 suggested that photoreceptors, not Müller cells, are the primary source of lactate. Overall, retinas are known to convert glucose to lactate at a very fast rate(16,42,62–64). To determine if photoreceptors are the major source of lactate, we compared retinas with photoreceptors to retinas without photoreceptors. Adult AIPL1-/- (Aryl Hydrocarbon Interacting Protein Like 1) mouse retinas have no photoreceptors because AIPL1 deficiency causes photoreceptor degeneration(51). We extracted metabolites from mutant and control retinas and quantified them by GC-MS (**Fig. 8)**. Taurine and docosahexaenoic acid (DHA), photoreceptor-specific metabolites, are reduced 90% and 83% in AIPL1-/- retinas. Lactate decreases by 74%, with the intermediate pyruvate increasing, consistent with photoreceptors being the major site of lactate production. Glutamine accumulates, indicating that photoreceptors are a major site for glutamine utilization.

Figure 2.8 Examination of photoreceptor linked metabolites. WT vs. AIPL1-/- mouse retinas.

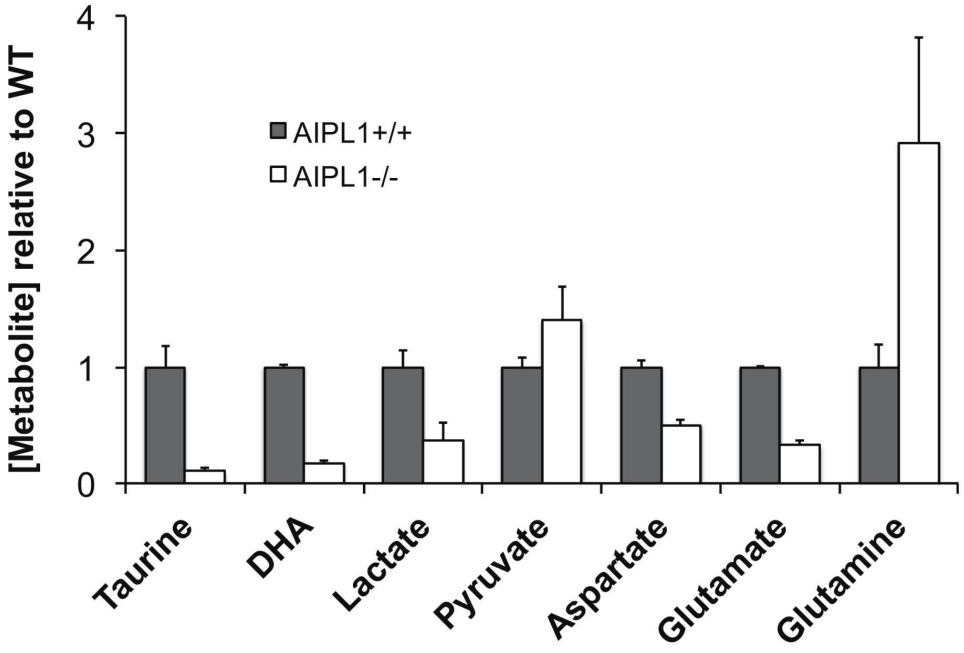

Comparison of metabolites in adult retinas from WT vs. AIPL1-/- mice. Retinas were isolated from light-adapted 2 month old WT and AIPL1-/- mice, extracted and metabolites were quantified by GC-MS. N = 2 for WT retinas and 3 for AIPL1-/- retinas. Values are presented as concentrations of metabolite per retina and normalized to the WT controls.

Cultured Müller Cells are less effective than intact retinas at converting Glucose to Lactate.

To evaluate contributions of Müller cells to lactate production we used Müller cells isolated from young mouse retinas and cultured for 10-14 days. During that time, Müller cells grow to confluence while neurons degenerate(82). We incubated cultured Müller cells with C^{13} glucose and used Gas Chromatography Mass Spectrometry (GC-MS) to measure appearance of m3 isotopomers of lactate and pyruvate (**Fig. 9).** An isotopomer is an isotopic isomer of a compound. Each compound has incorporated C^{13} isotopes from the intended metabolites, but the number and position of these isotopes

in the compound may vary. Using a C^{13} isotopically labeled substrate one can trace how this substrate is metabolized by measuring the isotope incorporation into various downstream metabolites. The time course of incorporation of C^{13} from glucose into whole mouse retina metabolites is shown for comparison. C^{13} from glucose is incorporated into Lac ~60X faster in whole retinas than in cultured Müller cells. This indicates neurons, not Müller cells, are the primary site of lactate produced in the retina.

Figure 2.9

Cultured Muller cells use Aspartate more effectively than Glucose, Lactate, and Glutamine

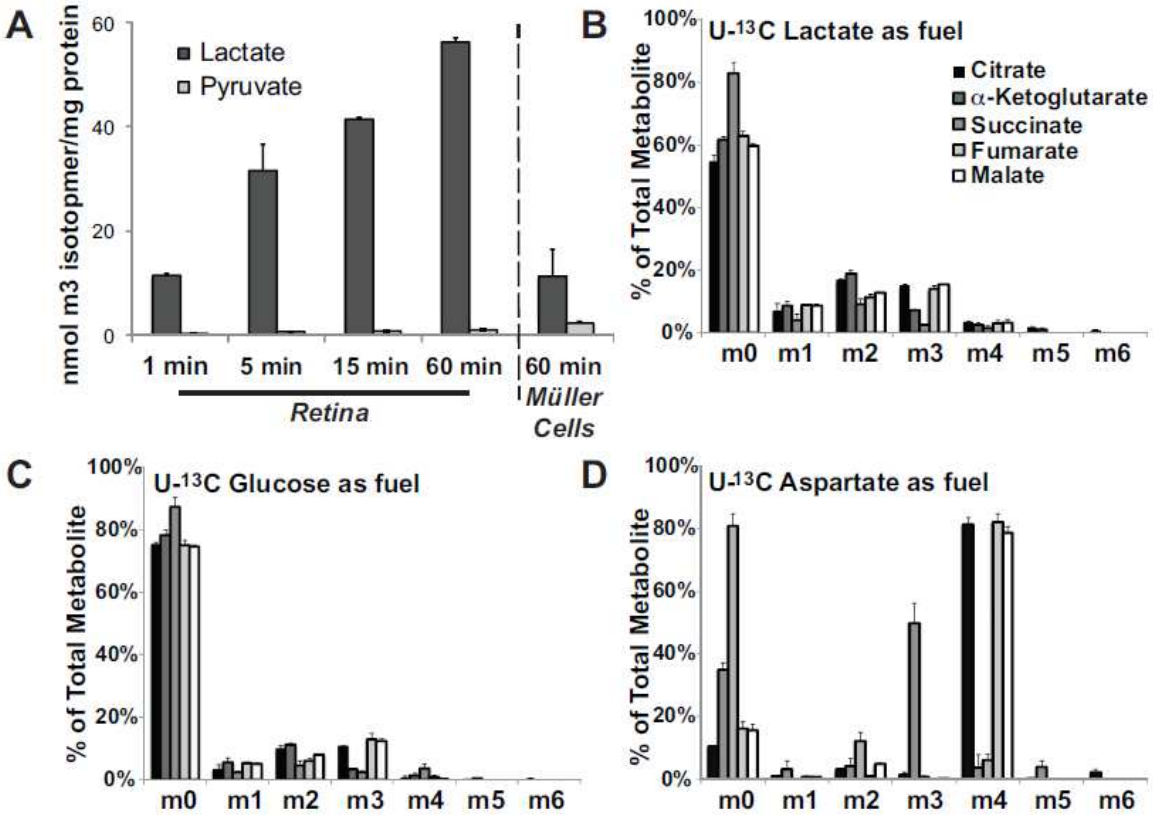

A. Accumulation of m3 lactate and pyruvate from C^{13} glucose in retinas and in cultured Müller cells. Cultured Müller cells do not make lactate fast enough for Müller glia to be the primary source of lactate from retinas. B-D. Cultured Müller cells were incubated 1 hour with (B) 5 mM U-C^{13} lactate, (C) 5 mM U- C^{13} glucose, (D) 5 mM U- C^{13} aspartate. The C^{13} enrichment is expressed as percent of total ion intensity of all isotopomers for each metabolite. (n = 3). C^{13} aspartate is incorporated more effectively than any other fuel.

Aspartate is the preferred fuel for cultured Müller Cells.

To quantify fuel preferences of cultured Müller cells, we incubated them 1 hr with either U-C^{13} lactate or U-C^{13} glucose and measured incorporation of C^{13} into TCA intermediates (Fig. 9B,C). Neither lactate, nor glucose contributed significant C^{13} (Fig. 9B,C). We also tested U- C^{13} aspartate because Pardo et al. (83) found that other types of glial cells use aspartate as a carbon source. We found aspartate is the fuel used most effectively by cultured MCs to contribute carbons to TCA intermediates (Fig. 9D). An isotopomer analysis (**Fig. 10)** shows how cultured MCs convert U-C^{13} aspartate into citrate, α-ketoglutarate, glutamate and glutamine. MCs also use carbons from aspartate to make malate and fumarate by reverse malate dehydrogenase and fumarase reactions. Due to the bypass provided by the MAS, very little succinate is labeled in the TCA cycle from these experiments. Rapid exchange of cytosolic malate for mitochondrial α-ketoglutarate limits the extent to which intermediates are recycled through the TCA cycle.

Figure 2.10 Pathways in cultured Müller cells by which carbons from aspartate incorporate into TCA intermediates and amino acids.

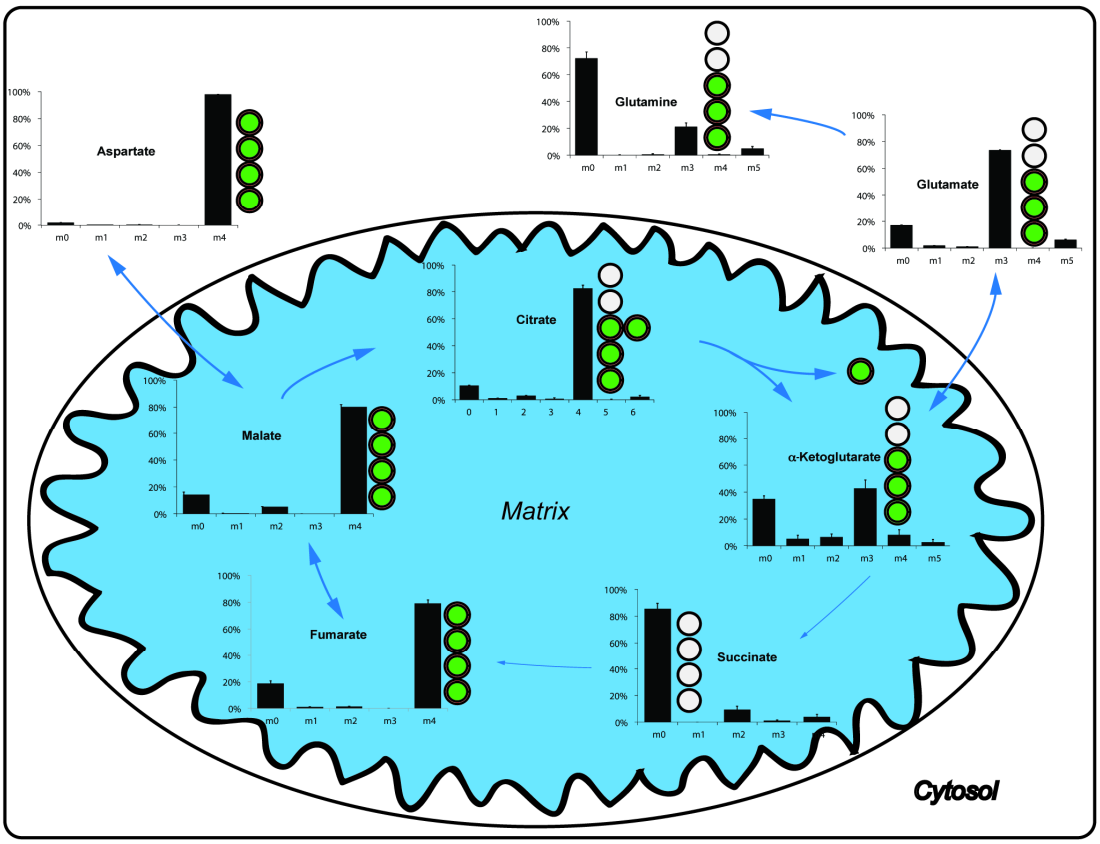

Isolated Müller cells were incubated with 5 mM U-C^{13} aspartate for 1 hour. C^{13} labeled carbons are highlighted as red circles and unlabeled carbons are black circles. Blue arrows represents predominant directions, line weight reflects rates of reaction (n = 3). Aspartate effectively incorporates into malate, citrate, α-ketoglutarate and glutamate as well as into fumarate via dehydration of malate. Succinate incorporates label very slowly from aspartate.

Aspartate enhances glycolysis in cultured Müller Cells.

We reasoned that supplementation of aspartate might stimulate oxidation of glucose by enhancing regeneration of cytosolic NAD+. Aspartate entering Müller cells can be transaminated to oxaloacetate, which then oxidizes NADH. We tested this by incubating cultured Müller cells with U-C^{13} glucose in the presence or absence of

aspartate and found that aspartate enhances incorporation of C^{13} into pyruvate and lactate (Fig. 11A).

Aspartate enhances incorporation of carbons from glucose and lactate into mitochondrial intermediates.

Aspartate also enhances incorporation into citrate of two C^{13}'s from either U-C^{13} glucose or U-C^{13} lactate (Fig. 11B). We also noted evidence of pyruvate carboxylase activity. In the presence of U-C^{13} glucose or U-C^{13} lactate, ~*10*% of malate and citrate in retina incorporates three C^{13}'s. (Fig. 11C) m3 isotopomers are formed when m3 pyruvate is incorporated into mitochondrial intermediates by Pyruvate carboxylase. The contribution of Pyruvate carboxylase becomes minor when unlabeled aspartate is present (Fig. 11C).

Aspartate and lactate enhance glutamine synthesis in cultured Müller Cells and in retina.

Müller cells can synthesize glutamine. However, when we provide glucose as the only fuel, neither cultured Müller cells (Fig. 11D), nor intact retinas(64) release significant glutamine into the culture medium. We found 6 fold more glutamine in the medium when glucose is supplemented with aspartate. However, when aspartate is provided with lactate instead of glucose, glutamine rose 42 fold compared to glucose alone (Fig. 11D).

To confirm that MCs use Lac and Asp in a more physiological context we incubated whole intact retinas with C^{13} Lac for 2 hours with *vs.* without Asp. We

measured glutamine in the retinas instead of in the medium because glutamine release is undetectable from light-adapted retinas(64). Asp caused a 144 fold increase in labeling of glutamine, which is made only in Müller cells (**Fig. 11E**). Labeling of TCA intermediates, which occurs in all retinal cells, was stimulated 1.5-7 fold by Asp (right side of **Fig. 11E**). We also incubated retinas with 5 mM Lac together with 5 mM of either Asp, dimethyl α-ketoglutarate (DMK), dimethyl succinate (DMS), dimethyl fumarate (DMF), asparagine or proline. Aspartate and Asparagine were the most effective at raising levels of glutamine (**Fig. 11F**). However, the use of methylated TCA cycle intermediates demonstrated that carbons from the TCA cycle were used to generate glutamate, with the actual preferred substrates of the cell being Aspartate.

Figure 2.11 Aspartate stimulates Glucose oxidation

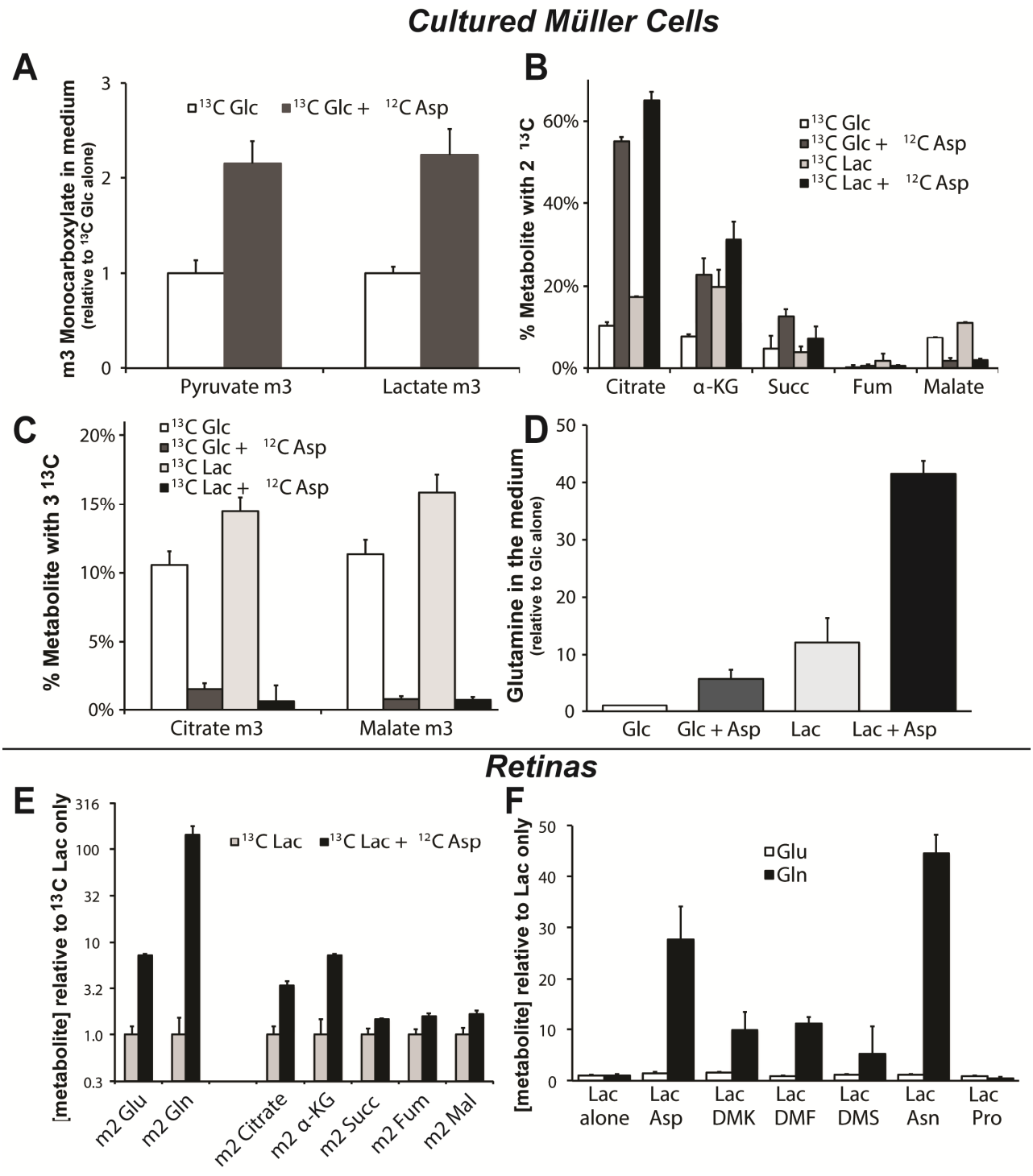

(A)Isolated Müller cells were incubated with 5 mM U-C^{13} Glucose with or without 5 mM unlabeled Aspartate for 1 hour. The medium was collected and analyzed by GC-MS. (B) Isolated Müller Cells were incubated with5 mM U-C^{13} Glucose or with U-C^{13} Lactate (5 mM) with vs. without 5 mM unlabeled Aspartate for 1 hour. The % of each metabolite in the m2 isotopomer is shown (n = 3). (C) Pyruvate carboxylase activity is a significant source of citrate and malate, but only in the absence of Aspartate (n = 3). m3 isotopomers of citrate and malate are made by carboxylation of Pyruvate. Total citrate and malate increased only 70% and 7% respectively when Aspartate was included. (D) Aspartate (5 mM) increases synthesis and release of Glutamine into the Müller Cell culture medium (n = 3). (E) Aspartate stimulates synthesis of Glutamine from U-C^{13} Lactate by Müller Cells in intact retinas. (note log scale on y-axis). (F) Aspartate and Asparagine are the most effective anaplerotic substrates for raising the concentration of Glutamine in retinas. Retinas were incubated with 5 mM lactate and 5 mM of additional substrate for 1.5 hours (n = 3). The effect on Glutamate is much smaller. In mouse retinas incubated with Lactate alone the Glutamate pool size is 130 x larger than the Glutamine pool size.

Müller Cells lack biochemical pathways needed to sustain glycolysis.

Neither C^{13} Glucose alone nor C^{13} Lactate alone are effective sources of carbon for mitochondrial intermediates (Fig. 9B,C). The limited ability of cultured Müller cells to incorporate C^{13} from Glucose or Lactate could mean they cannot make cytosolic NAD+ fast enough to sustain oxidation of these fuels. To sustain glycolysis a cell must re-oxidize NADH. LDH can regenerate NAD+ by converting Pyruvate to Lactate. However, Müller cells are pyruvate kinase-deficient so they cannot make enough pyruvate to support this. MAS activity would be an alternative way to regenerate NAD+ (31), but AGC1, a key component of the MAS, is absent from Müller cells in retinas (42) (Fig. 6). Consistent with this, microarray data revealed low AGC1 expression in MCs (0.031% of total transcripts in PRs vs. 0.0003% in MCs) (81)**.** The glycerol-3-phosphate shuttle (84) is unlikely to play a major role because transcripts encoding the two glycerol-3-phosphate dehydrogenases are low abundance in both PRs and MCs (each ~0.0006% of total transcripts)(81).

Figure 2.12 Analysis of the extent of de-differentiation of cultured Müller cells.

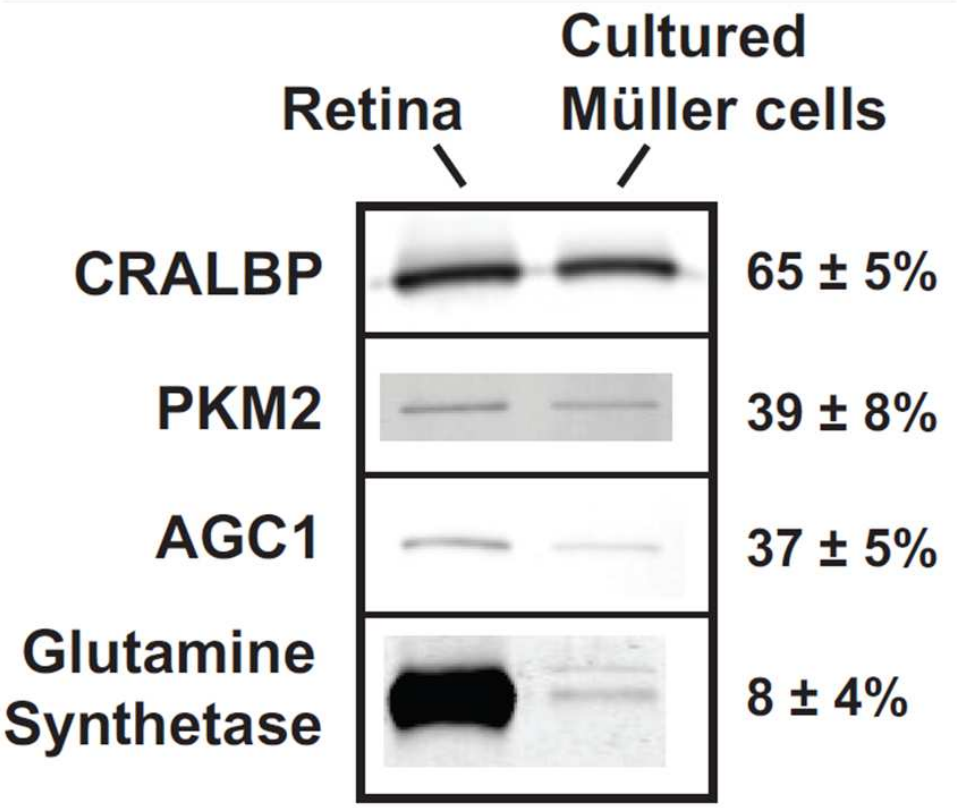

Immunoblot analysis showing expression of Müller cell markers in retina vs. in cultured Müller cells. 20 µg of protein from a retinal homogenate or 20 µg of protein from a cultured Müller cell homogenate were loaded. Blots were probed with antibodies to CRALBP, AGC1, PKM2 and Glutamine Synthetase.

Caveats associated with cultured MCs.

The experiments we described so far were done with Müller cells dissociated from p12 mouse retinas and cultured 10-14 days. Müller cells under these conditions partially de-differentiate(82) retaining some native characteristics, but lose others. We evaluated how much de-differentiation occurs in our cultured Müller cells. Müller cell-specific proteins, CRALBP and Glutamine Synthetase (GS), are present (Fig. 12), but only at 65±5% and 8 ±4% of levels in whole retina. AGC1 is present at 37±5% and PKM2 at 39±8% of whole retina levels (±SEM, n = 4). This finding confirms cultured

Müller cells partially de-differentiate. We also noted conversion of glucose into lactate and TCA intermediates by cultured Müller cells (Fig. 11A-C), which we would not expect based on IHC of intact retinas. Fig. 2 in this report shows PKM2 is undetectable in Müller cells within retinas and a previous analysis(42) and ours (**Fig. 6**) detected no AGC1 in Müller cells in intact retinas. Our findings with intact retinas and cultured Müller cells suggest a novel metabolic relationship in which Müller cells use lactate and aspartate made by photoreceptors. However, since cultured Müller cells differ from native Müller cells, we developed an independent strategy to analyze metabolic relationships between photoreceptors and Müller Cells in intact retinas.

Metabolic fate of C^{13} labeled Glutamine in intact retinas confirms a role for Aspartate in neuron/Müller cell symbiosis.

Photoreceptors are the primary site of glutamine catabolism and Müller cells are the primary site of glutamine synthesis, as supported by microarray data (81). Glutaminase (GLS) transcripts occur at ~8X higher frequency in photoreceptors than in Müller cells. In contrast, transcripts encoding Glutamine synthetase (GLUL) occur 50X more frequently in Müller cells than in photoreceptors. Based on these distributions and on the ability of aspartate and lactate to enhance glutamine synthesis we hypothesized the pathway in Figure13. Glutamine is imported into photoreceptors. Glutaminase converts it to glutamate, which is transaminated to α-ketoglutarate. A small fraction(64) of α-ketoglutarate is oxidized to succinate, malate and oxaloacetate, which then is transaminated to aspartate. Our model predicts that some of this aspartate exits the neuron to be imported into Müller cells. Once in the Müller cell cytosol, Aspartate is

transaminated to oxaloacetate, which then oxidizes cytosolic NADH. This is how aspartate helps maintain cytosolic NAD+ to support oxidation of glucose and lactate.

Malate from reduction of oxaloacetate in the Müller cell then enters mitochondria where NAD+ oxidizes it to oxaloacetate. Oxaloacetate is trapped in the Müller cell mitochondria because Müller cells lack AGC1, so it is used there to make citrate which then is oxidized to α-ketoglutarate and glutamate. Ultimately, in a Müller cell-specific reaction the glutamate is made into glutamine. The net result is that carbons from glutamine initially taken up by photoreceptors are used to resynthesize glutamine in Müller cells. Figure 13 tracks the flow of carbons in this model.

Figure 2.13: Glutamine flux through the retina.

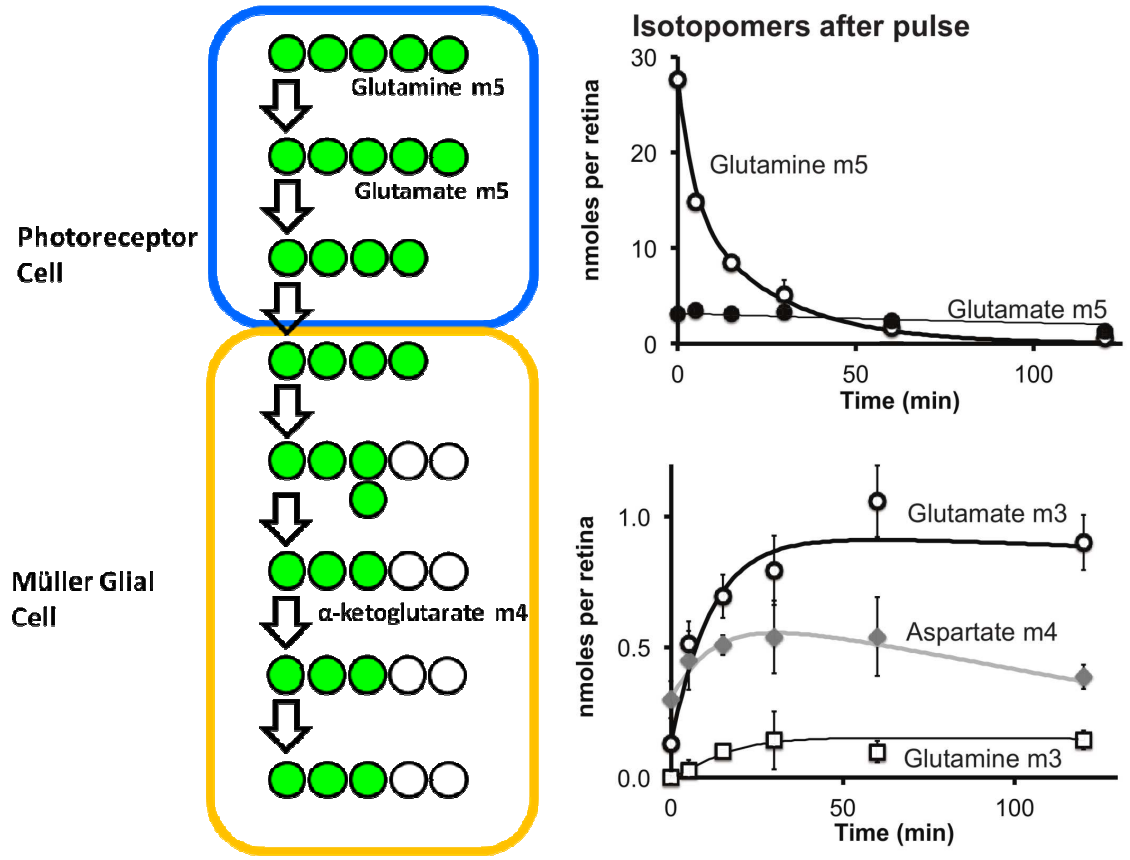

Pulse-chase analysis of U-C^{13} Glutamine in retina. (A) Schematic model for the role of Aspartate as a carrier of oxidizing power between retinal neurons and glia. Red circles represent the C^{13} carbons and black circles represent the C^{12} carbons. (B). C^{13} labeling of Aspartate, Glutamate and Glutamine from the pulse of U-C^{13} Glutamine. m5 Glutamine and Glutamate (shown in the top panel) are derived directly from the pulse of 5 mM U-C^{13} Glutamine. After 5 minutes the medium was changed into 5 mM unlabeled Lactate with no added Glutamine. Unlabeled Glutamine was not included in the chase because the intense signal from the added Glutamine would have obscured the isotopomer signals we intended to quantify. The retinas were subsequently harvested at the indicated times after the pulse. The bottom panel shows m4 Aspartate derived from oxidation of Glutamate via the TCA. m3 Glutamate is made by further oxidation via citrate and m3 Glutamine is made only in Müller cells by Glutamine Synthetase. (n = 6). This highlights the use of Aspartate as an intermediate in Muller glia Glutamine synthesis.

To test our hypothesis that aspartate transports oxidizing power and carbons from neurons to Müller cells in intact retinas, we utilized a pulse-chase protocol. Retinas were treated for 5 min with U-C^{13} Glutamine (m5) followed by incubation with 5 mM unlabeled Lactate. At various times retinas were harvested and metabolites extracted and analyzed by GC-MS. The upper panel of **Fig. 13B** shows that m5 Glutamine converts rapidly to m5 Glutamate. The lingering m5 Glutamate and m5 α -ketoglutarate are consistent with our previously reported finding that α-ketoglutarate in retinas is protected from oxidation in neurons(64). The lower panel of Fig. 13B shows how m4 Aspartate accumulates and then decays as m3 Glutamate and then m3 Glutamine accumulates. Conversion of m4 Aspartate into m3 Glutamine confirms that the subsequent reactions (see Fig. 13A) occur in Müller cells since only Müller cells express Glutamine Synthetase. Overall these results support the model in Figure 13A in which Aspartate from neurons supplies carbons and oxidizing power for synthesis of Glutamine by Müller cells.

Confirmation that Aspartate can be a surrogate for the missing MAS in Müller cells.

An alternative interpretation of our results could be that U-C^{13} glutamine is used directly by Müller cells where it is made directly into m3 glutamine. This would not require import of extracellular Aspartate into Müller glia. This alternative explanation is unlikely because the role of Müller cells is to synthesize Glutamine, not break it down. Nevertheless, to address this alternative explanation we performed the following control experiments that test whether or not glutamine synthesis in Müller cells depends on import of extracellular Aspartate.

Tests of Aspartate as a necessary component for Müller Glia Cell glutamine synthesis

A. (2S, 3S)-3-{3-[4-(trifluoromethyl)benzoylamino]benzyloxy]aspartate (TFB-TBOA) was added to retinas to inhibit Excitatory Amino Acid Transporter 1 (EAAT1), a transporter for Aspartate into Müller cells (85). Fig.14A shows it inhibits formation of m3 Glutamine from m5 Glutamine without affecting other metabolites.

B. Retinas were treated with Carbamoyl-phosphate synthetase 2, aspartate transcarbamylase, and dihydroorotase (CAD), a multi-enzyme complex that converts aspartate to N-carbamoyl aspartate(86), to deplete extracellular aspartate. Fig.14B shows that it inhibits m3 Glutamine formation without affecting other metabolites.

C. Glutamine in normal retinas and AGC1-/- retinas was compared. AGC1 is required for aspartate synthesized in neurons to escape from the matrix. Our model predicts AGC1 deficiency should limit synthesis of glutamine by Müller cells by limiting release of aspartate from neurons. Fig.14C shows that aspartate and Glutamine in AGC1-/- retinas are diminished compared to controls, consistent with our model. N-acetyl Asp (NAA) also is diminished in the absence of AGC1, consistent with a previous analysis of AGC1 deficiency in brain(87).

D. Our findings suggest AGC1 exclusion limits glutamine synthesis by preventing photoreceptors from exporting aspartate for import by Müller cells. We tested this by adding exogenous aspartate to AGC1-/- retinas. Fig.14D shows that aspartate restores glutamine synthesis in AGC1-/- retinas, consistent with our model.

E. Aminotransferases play key roles in both photoreceptors and Müller cells. We incubated retinas under conditions similar to those in Fig.13, but we also included 1 mM aminooxyacetate (AOA) to inhibit aminotransferase activities. Fig.14E shows AOA lowers aspartate and glutamine consistent with our model. These controls confirmed the importance of aspartate as a source of carbon for glutamine synthesis by Müller cells in intact retinas.

Figure 2.14 Inhibition of Aspartate transfer to Müller cells inhibits Glutamine synthesis in retina

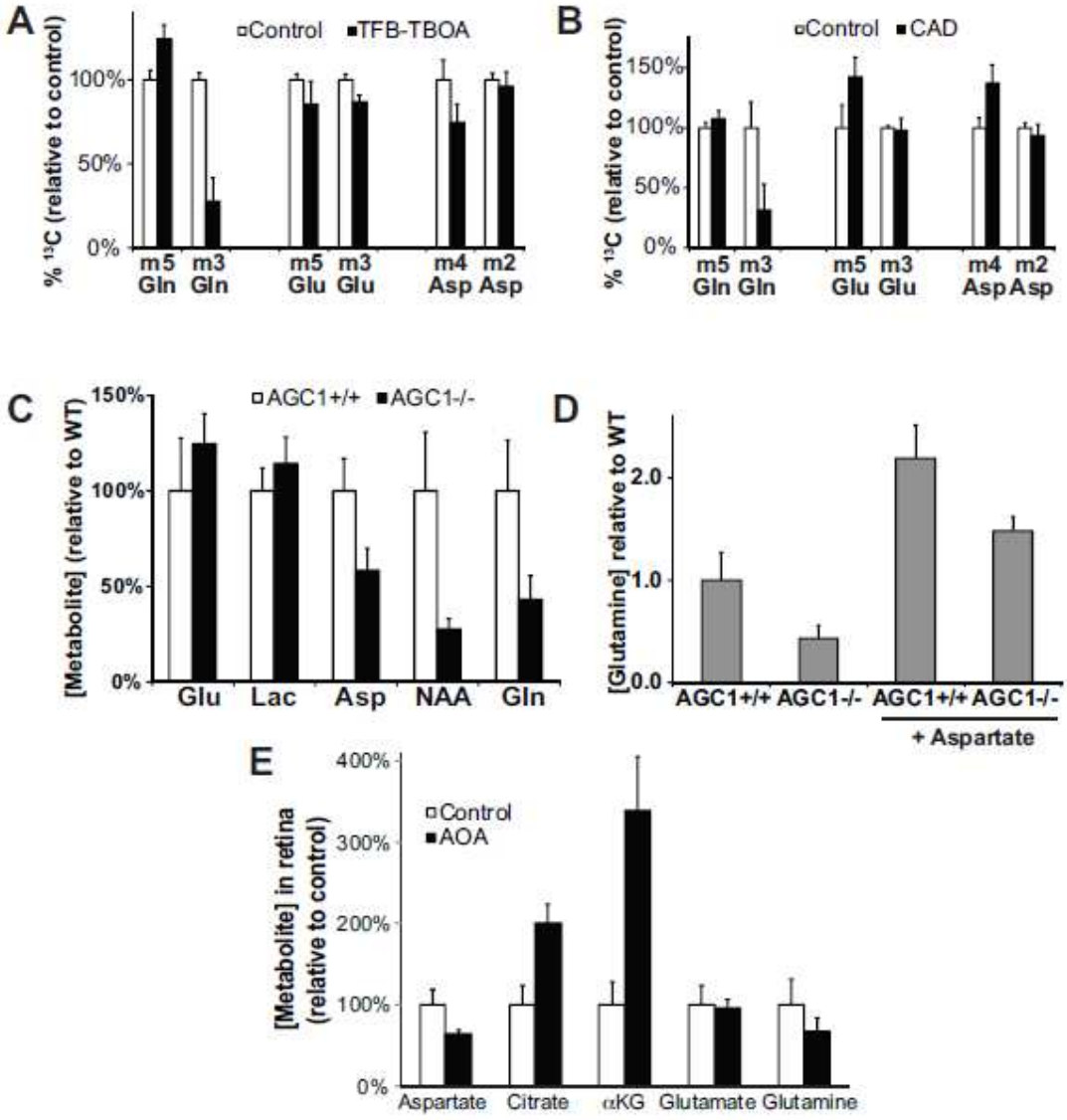

We conducted several experiment to test the use of aspartate as a necessary intermediate for glutamine synthesis. (A) Inhibition of EAAT1 by TFB-TBOA (10 µM). (B) Depletion of extracellular Asp by CAD. The medium contained CAD protein (6 µg/ml) and ATP (0.1 mM). (C) Aspartate, N-acetyl Asp (NAA) and Glutamine are diminished in AGC1-/- mouse retinas. (D) Aspartate boosts Glutamine levels in AGC1-defcient retinas (n = 4). (E) AOA, an aminotransferase inhibitor, inhibits formation of Aspartate and promotes formation of citrate, consistent with sequestering oxaloacetate in mitochondria so that it is more likely to be made into citrate. By preventing formation of Aspartate and by blocking aminotransferase activity in Müller cells AOA (1 mM) also causes accumulation of α-ketoglutarate and lowers glutamine (n = 3).

Discussion

Metabolic requirements in retina are different than in brain.

Retina and brain have different functions and structures that influence the nature of the interactions between their neurons and glia:

I

Glycolysis accounts for 25% of glucose metabolism in brain (61), but it accounts for 80-96% of it in retina (16,62,63). PKM2 is barely detectable in brain, but abundant in retina.

II

Brain astrocytes have direct access to nutrients and O_2 from vasculature, but some neurons do not. Those neurons rely on astrocytes for fuel(34,66). In retina, photoreceptors and Müller cells have direct and equal access to nutrients and O_2 from the Interphotoreceptor Matrix (IPM) that bathes the retina surface(23).

III

Neurons in brain fire intermittently, releasing glutamate primarily when they are stimulated. In darkness, photoreceptors are constantly depolarized so they release a continuous flow of glutamate at their terminals.

IV

Glutamate released from neuronal synapses in brain can diffuse from synapses to be recovered by astrocytes. Photoreceptor synapses are encapsulated structures with efficient EAAT5 transporters that recover glutamate before it can reach Müller cells (88). Brain slices, but not intact retinas, release glutamine into the culture medium(64).

Why do photoreceptors express so much PKM2?

PKM2 in a mouse retina is 25% as abundant as rhodopsin, the most prominent protein in photoreceptors. PKM2 is the isoform most suited for aerobic glycolysis in cancer cells(60,71), because its activity is poised for either positive or negative regulation. We have not found evidence that PKM2 is regulated by light, but there could be conditions we have not yet explored where its ability to be regulated imparts a selective advantage. PKM2 basal activity is lower than that of other isoforms(80), but it is so abundant in photoreceptors that retinas convert ~90% of the glucose they use to lactate.

Why do Müller cells have a PK deficiency?

The advantage to a Müller cell for exclusion of PK is that intermediates of glycolysis become available for anabolic activities. The disadvantage is that Müller cells become dependent on other cells to fuel their mitochondria. Müller cells may not be completely devoid of pyruvate kinase. Since previous studies of Müller cells treated with protease and mechanically dissociated from Guinea Pig retinas showed that they make lactate(7,89). Those studies found less lactate release from a complex of Müller cells and photoreceptors than from isolated Müller cells. They inferred a net flow of lactate from Müller cells to photoreceptors, but the analysis did not show it directly. The definitive conclusion from our studies is that Müller cells express much less PK that photoreceptors and therefore do not utilize glycolysis to its full extent. The role of pyruvate kinase exclusion most likely being for the cell to rely on exogenous lactate to fuel oxidative phosphorylation and allow glucose to be utilized by neighboring cells.

Why is AGC1 in neurons but not in glia?

AGC1 in neurons shuttles aspartate out of the matrix to oxidize NADH in the cytoplasm. A key function of Müller cells is to synthesize glutamine. AGC1-mediated efflux of aspartate from the matrix would divert oxaloacetate away from synthesis of α-ketoglutatarate, the precursor for glutamine. The advantage to a Müller cell of low AGC1 is that aspartate is not diverted from the path to glutamine.

Role of Lactate in the symbiotic relationship between Photoreceptors and Müller cells.

Our findings are consistent with the model in **Fig. 15** whereby Photoreceptors and Müller cells have direct access to the Interphotoreceptor Matrix that bathes the surface of the retina(23). Müller cells are PK deficient, so they cannot make much pyruvate directly from glucose. However, like cells in a tumor(90), Müller cells and photoreceptors express different amounts of PK. Photoreceptors express abundant PKM2, making them well-equipped to make lactate from glucose. Lactate can be released from photoreceptors via MCT1(91) and imported into Müller cells via MCT4(92).

Figure 2.15 Model for relationship between Photoreceptors and Müller cells.

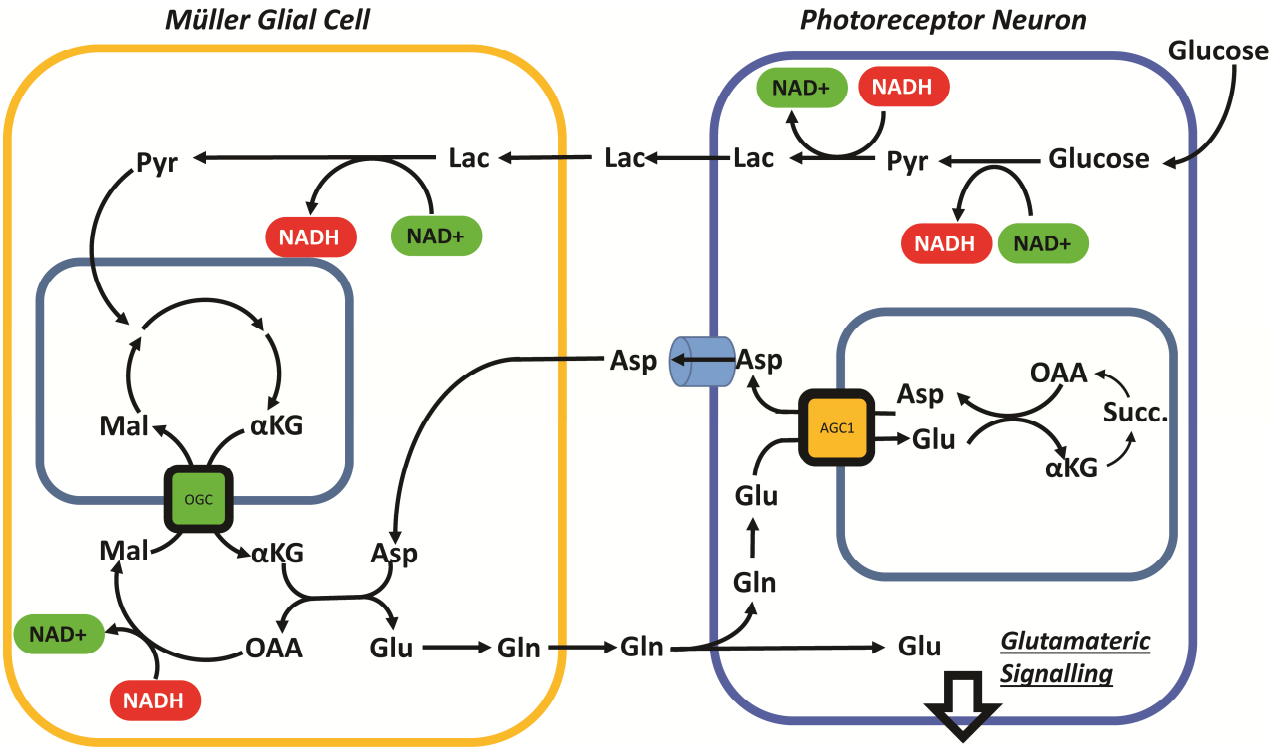

Müller cells are PK deficient so glycolytic intermediates can be used for anabolic activities. Müller cells are AGC1-deficient so that mitochondrial oxaloacetate in Müller cells is not diverted away from the pathway that leads to Glutamine synthesis. As a result of sustained glycolysis, photoreceptors produce lactate that Müller cells can oxidize to pyruvate to fuel their mitochondria. Photoreceptors also export aspartate that Müller cells can use to oxidize lactate. Nitrogen for the amino group of glutamine comes from aspartate and nitrogen for the amide group of glutamine comes from NH_4+ . "Lac": lactate; "Pyr": pyruvate; "OAA": oxaloacetate; "Mal": Malate; "α-KG": α-ketoglutarate; "IPM": Interphotoreceptor Matrix; "Glu": Glutamate; "Gln": Glutamine; "Succ": succinate. "OGC": Oxoglutarate Carrier; "AGC1": Aspartate/Glutamate carrier; "PKM2" M2 isoform of pyruvate kinase.

Role of Aspartate in the symbiotic relationship between Photoreceptors and Müller cells.

For Müller cells to oxidize the lactate they import from photoreceptors, they require an oxidant. Müller cells are PK deficient, so they cannot generate the pyruvate that LDH needs to oxidize NADH. Müller cells also are AGC1 deficient (Figure 2.8), so they also cannot use Malate Aspartate Shuttle activity to oxidize NADH. Exogenous Aspartate can provide the needed oxidizing power. As outlined in Fig.15, oxaloacetate derived from aspartate is a substrate that cytosolic malate dehydrogenase can use to oxidize NADH to NAD+. Malate from this reaction can enter Müller cell mitochondria via OGC(42) and be oxidized to oxaloacetate (Figure 2.15). The absence of AGC1 in Müller cell mitochondria prevents oxaloacetate from escaping. Instead, it is directed towards synthesis of citrate, isocitrate, α-ketoglutarate, and ultimately glutamine. Our findings reveal how lactate and aspartate have been selected as preferential substrates for Müller glia Glutamine Synthesis, due to exclusion of PK and AGC1 activities in Müller cells Figure 2.6 and 2.8). Aspartate promotes oxidation of NADH to support lactate consumption. Aspartate also provides NH_2 to convert α- ketoglutarate to glutamate(83) and both aspartate and lactate provide carbons to synthesize glutamine. (Figure 2.11D)

Conclusion

Beyond the unique metabolic network shared by the neurons and glia of the retina, questions remain regarding the extent of aerobic glycolysis in the retina. The next stage of this research would be to study what happens when PKM2 is knocked out specifically in photoreceptor cells. Using PKM2-Cre mouse crossed with Rhodopsin Self- Excising Cre (Rho-siCRE), we can study the effect of the unique expression of

PKM2 on photoreceptor cell function and degeneration. Further information can also be gleaned from experiments with cultured Müller glia cell lines which demonstrate that when Müller glia become reactive and proliferate, as in the case of photoreceptor degeneration, they begin to express PKM2. We wish to investigate this further by studying the expression of PKM2 in native Müller cells of retina degeneration models, such as RD1. This opens potential avenues for treating damage caused by retina gliosis in models of retina degeneration by using PKM2-specific activators, which would override damaging cell proliferation in the retina, thereby allowing for time and treatment of photoreceptor degeneration.

Our results demonstrate that there is a fundamentally intertwined metabolic relationship between photoreceptors and Müller glia cells that goes beyond previous models of these interactions in the brain. Our research has localized aerobic glycolysis to the photoreceptor cell rather than in the retina tissue as a whole, allowing us to begin to elucidate the role of this unusual form of metabolism. In addition, these observations suggest that the individual metabolic demands of a particular cell type may play a role in the cell's maintenance or degeneration. With advances made in studying the metabolic requirements of photoreceptor cells, we can begin to make sense of metabolic catastrophes that induce retina degeneration.

CHAPTER 3:

Culturing the isolated photoreceptor: Studies of Outer Segment Morphology and Live Cell imaging reveals a potential tension component necessary for outer-segment morphology.

Introduction:

In the course of our studies of retina metabolism, it has been a consistent challenge to identify which metabolic components are attributed to photoreceptors and which are a product of the retina as a whole. Attempts to cultivate isolated photoreceptors have failed to produce cells with their distinguishing morphology. The outer-segment process is a key component of the photoreceptor cell as it contains the machinery of the photo-transduction cascade and carries out the main function of the photoreceptor cell. While much has been learned of the degeneration and loss of outer-segments, little is known of what shapes the development and maintenance of this photon conduit. Building on knowledge of the membrane components and mechanisms regulating synthesis of photoreceptor outer-segments, we sought to determine how functionally intact photoreceptors may be cultured from primary cells so that we can begin to understand the demands of the photoreceptor out of the context of the retina.

Components of Outer Segment Discs

Understanding the metabolic components of the photoreceptor outer-segment provides clues as to which metabolic building blocks are necessary for synthesis of new discs. Turnover of fatty acids and glycerol in the retina have been shown to have rapid dynamics indicative of molecular replacement. Autoradiographic studies of palmitate(93) and glycerol(94) incorporated into the retina demonstrate that there is an initial

accumulation of these metabolites near the base of the outer segment, associated with the formation of a new outer segment disc. Once this new disc buds off and becomes the base of the outer-segment stack of discs, there is a gradual dispersing of the radiographic material, presumably due to the high rate of molecular replacement and the overall displacement of fatty acids between phospholipids in the disc membrane and throughout the discs of the outer-segment.

This process differs dramatically from that of membrane proteins associated with the outer segment, whereby newly formed Rhodopsin is associated with a single disc and remains with that disc until it is phagocytized and consumed by the retina pigment epithelium (95). Early studies of autoradiographic images tracking tritiated amino acids demonstrated the progression of newly formed outer-segment discs from the base of the outer-segment to the tip of the photoreceptor. These studies formed the basis of measuring disc renewal and revealed that establishment of overall outer-segment length is based on rapid formation of disc membranes during early development that levels off as the organism reaches adulthood(96)**.** As new discs are added to the base of the outer-segment, there is a steady accumulation of new discs synthesized with old discs shed at the apical tip. The entire outer segment is renewed over a span of 7-10 days.

The timing of disc shedding by photoreceptors and phagocytosis by the retinal pigment epithelium has suggested that there is a light dependent regulation of outer segment maintenance. Early efforts to study photoreceptor outer-segment synthesis by comparing mammalian and amphibian outer segment turnover revealed that while amphibians tend to synthesize new discs with heat or light as a stimulus (97)**,** mammals

respond to visual light as the stimulus to shed the apical rod outer segments (98) in a burst of outer-segment loss. In addition to this regulation by light stimulus, this process appears to be modulated by circadian factors in mammals, but not in amphibians (99).

If rats are kept on a 12:12 hour light cycle, during light onset, a burst of apical discs are shed followed by phagocytosis by the RPE(100).However, during conditions of constant light, shedding does not occur and outer segments elongate. A similar effect occurs during constant darkness, save that outer segment are shorter. What became clear was that if rats were kept in constant light conditions, a flash of darkness followed by light would initiate disc shedding. This suggests that not only does light/dark-adaptation plays a role in outer segment synthesis, but also the regulation of disc turnover, a necessary component for replenishing old outer segment discs.

The change in light and dark adaptation appears to initiate a signaling mechanism that is essential to outer-segment disc turnover. While initial light onset stimulates shedding of outer-segments tips, during conditions of constant light, outer-segments elongate. Under constant darkness, outer segments tend to shorten. It is through a cyclical pattern of dark adaptation followed by light adaptation that photoreceptors maintain their outer segment length by disc shedding and synthesis(101). This interaction between the photoreceptor and RPE is critical to turnover and synthesis as detachment of the RPE from the Photoreceptor outer segment prevents synthesis of new discs.

In addition to differences in their signaling properties, rods and cones differ in their method of disc synthesis. Whereas rod photoreceptors renew their outer segment discs and shed them at a relatively equal rate, cone photoreceptors retain their

formation and do not have the distinct disc compartmentalization like that associated with rod photoreceptors(29,102). As the goal of our work is to exam outer segment disc shedding, mice were used as an experimental model as the mouse retina is largely rod dominant, thereby allowing for a reliable system for studying outer segment retention.

Establishing Experimental Conditions

Current attempts to study functional photoreceptors in isolation rely on dissociation of primary cells from the retina. Previously it has been observed that isolated photoreceptors lose their outer segments within hours when dissociated from light adapted retinas (103). This would suggest that activation of photo-transduction or photo-toxicity during dissociation may influence outer segment retention. However to distinguish rounded photoreceptor cells from nearby neurons, we use a mouse strain expressing GFP under the Neural Retina Leucine Zipper (NRL) promoter (Nrl-GFP) (104), which express GFP in rod photoreceptors. This allowed us to use Fluorescent Activated Cell Sorting to obtain a pure population of photoreceptor cells.

Our experiment on the role of aerobic glycolysis in retina metabolism has revealed new aspects that distinguish the retina from traditional neuronal tissue models. This demonstrates that the two tissues are different in their metabolic interactions as well as metabolic demands. Several models of Müller glia cell lines have been developed, yet a cultured photoreceptor line that retains the outer segment morphology has been elusive. Current attempts to study effects on photoreceptor cell health in a high-throughput manner have used the w661 retinoblastoma cell line (105) to study a cultured photoreceptor cell system, due to the expression of photoreceptor specific

genes in this cell line. However, as these cells lack outer segment processes, there exist inherent metabolic differences that would be unique to the primary cell.

We sought to determine whether supplementation with metabolic substrates found in the intact retina could counter-act outer-segment degeneration in culture. This would provide a means of studying the substrates essential to development of the intact photoreceptor and which may be disrupted during retina degeneration or metabolic insult. Drawing from several studies on retina explants of mouse, rat, and xenopus, we examined components of the medium that would enhance maintenance of outer segments. This was accomplished by buffering the cell media towards acidic pH conditions and supplementing glycosylated substrates to mimic the IPM space. These advancements in cultivation of the isolated cell should facilitate future high-throughput studies of photoreceptor development and disease models in a purified *in vitro* system. In the course of our experiments, we noticed that degeneration of the outer-segment appeared to follow a coordinated path and may rely on cell to cell interactions to maintain outer segment morphology. With the assistance of Chip Asbury, we tested out the use of optical tweezers to apply force to isolated outer-segments. While typically a method of testing force and tension between individual proteins(106), this method has also been used in the force manipulation of individual cells(107). In the process, we found a potential tethering mechanism which may explain cell to cell interactions necessary for outer segment morphology, but also hinted at mechanical signaling mechanisms that may be in place to control outer-segment disc synthesis, a critical process to photoreceptor cell function and morphology.

Results:

Figure 3.1 Effect of Light Adaptation on Outer-segment morphology

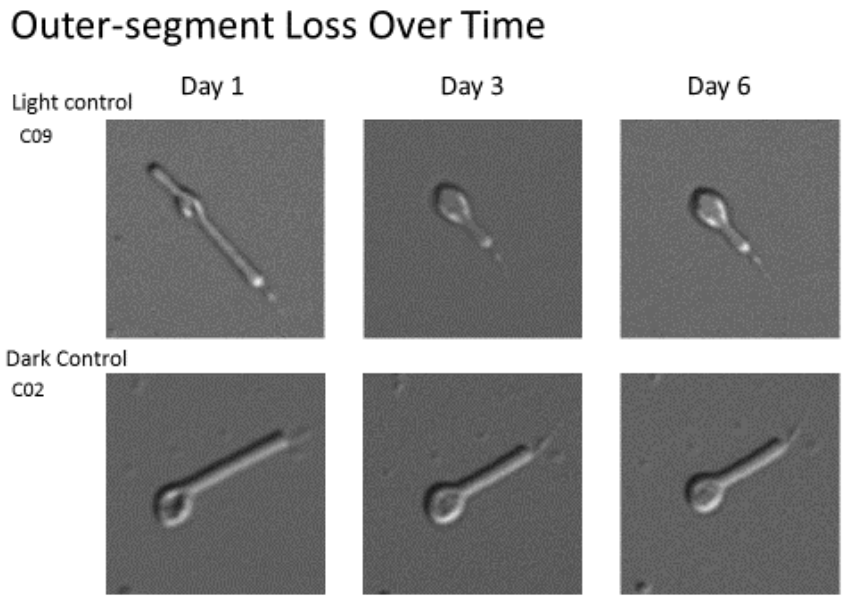

Retinas were isolated from mice that were either light or dark adapted and dissected under light or dark conditions. Retinas were dissociated and plated onto optical bottom 96-well plates and imaged over time. In general, light adapted outer-segments were observed to round-up over time, whereas outer segments from dark adapted retinas retained their morphology over a similar time span.

Figure 3.2 Outer-segment Circularity Ratios over time.

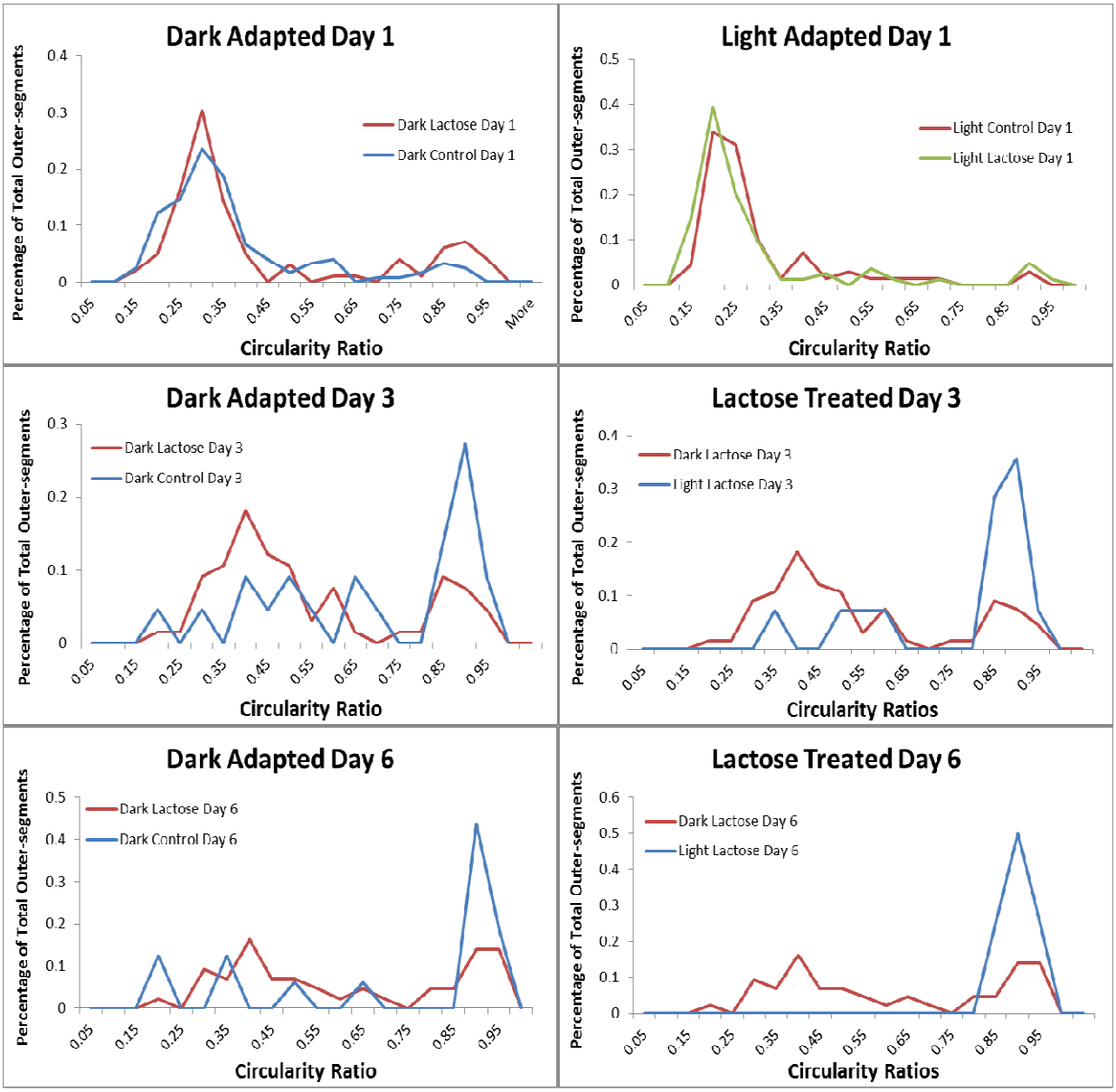

After initial plating the average circularity of GFP positive cells increases, as cells begin to round and lose their outer segments. Outer segments derived from dark adapted mouse retinas or incubated with Lactose retained their outer-segment length over a longer period of time. Circularity Ratios, defined by the length and radius of the overall shape allow for quantification of the overall morphology of the cell.

In a follow up to the work of previous experiments which revealed that light adaptation was detrimental to outer-segment retention in primary photoreceptor cells (103) we found that distinguishing photoreceptors from neighboring rounded cells was difficult. Utilizing the Nrl-GFP mouse line, we were able to distinguish photoreceptor cells that were initially rounded due to dissociation from those that retained their outer segments.

We compared light and dark adaptation effects on rounding of isolated outer segments. Our initial results revealed the same trend of outer-segment loss as observed by Derwent et. al(103) in the light adapted wild-type mouse model. This observation opens up the possibility of using fluorescent activated cell sorting (FACS) in future experiments to isolate photoreceptors from metabolites and growth factors of bystander cell types in typical dissociated retina preparations.

Buffering conditions and pH effects: HEPES vs. Bicarbonate Buffers.

Early studies of the IPM revealed a high concentration of lactic acid (23), a by-product of the high rate of glycolysis in photoreceptor cells. The extracellular pH of the photoreceptor has a significant impact on the overall redox state of the cell (64), and would be lower than that of bicarbonate-buffered media, typically kept in the range of pH 7.0. Conventional neuronal cell culture media rely on HEPES or bicarbonate buffers to maintain a neutral pH. Our initial foray into optimal DMEM conditions sought to establish the effect of various pH states and use of HEPES as a buffer of cell culture media. Our results indicate that use of HEPES improved the number of viable cells, allowing us to maintain lower pH levels, down to pH 5, over 6 days. The use of acidic conditions increased the number of viable cells in culture compared to more basic pH levels, such

as 7.5 or 8.0. While outer segment retention differs greatly between light and dark adapted cells, the light adapted state of the isolated photoreceptor in conjunction with HEPES buffering to significantly influence viability of the cell, nor did pH affect outer-segment retention.

Figure 3. pH of cell media influences Outer-segment GFP expression.

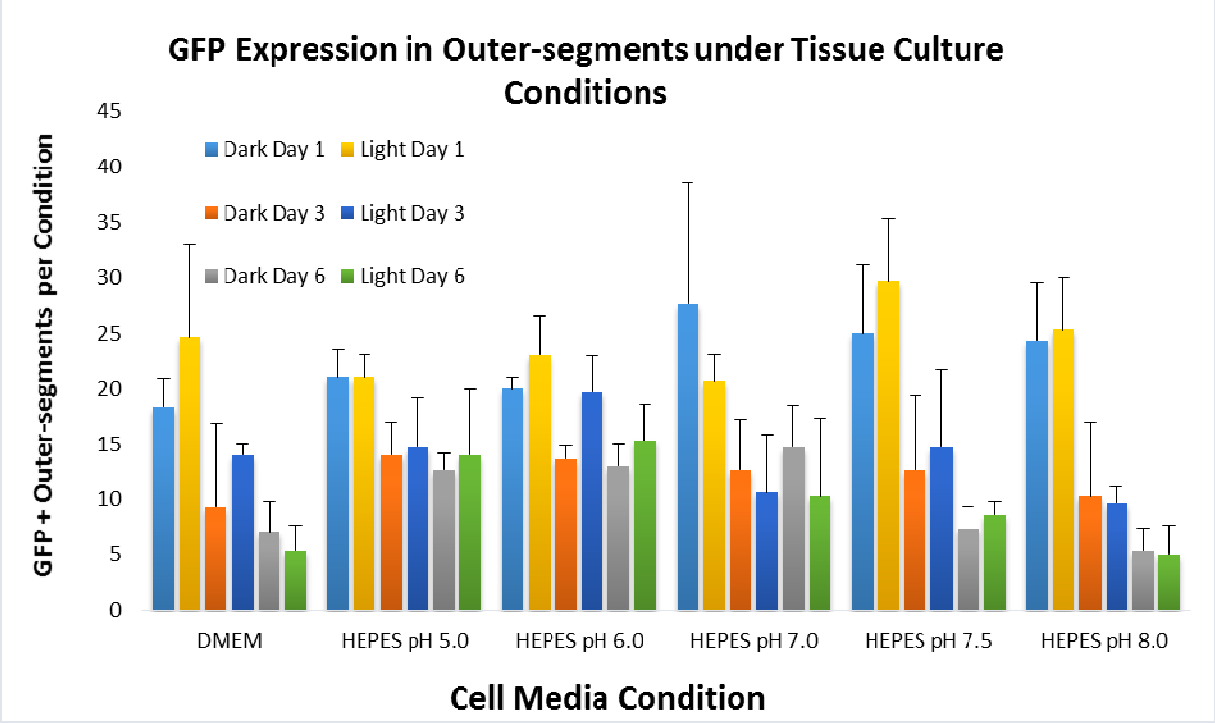

Outer segment GFP expression is not significantly altered by light or dark adaptation. However, addition of HEPES and buffering the DMEM to a lower pH significantly increases the number of GFP expressing outer segments per condition measured. This suggests that basic pH is detrimental to overall outer segment morphology.

Substitution of the Interphotoreceptor Matrix: Supplementation of Poly-saccharides

In addition to its relatively acidic environment, the IPM is highly concentrated in glycosylated proteins, which bridge the gap between the Retina Pigment Epithelium and the Photoreceptor and may be conducive to maintenance of outer segments. Studies of isolated retina explants from *Xenopus laevis* found that addition of β-lactose to retina explants aided in restoration of outer-segments(108,109). As such, binding of β-lactose to extracellular receptors may influence outer segment retention. The retention of outer segment was still influenced by light adaptation and there was little effect of β-lactose on overall cell viability.

Figure 3.4 Effect of Lactose on Outer Segment Retention

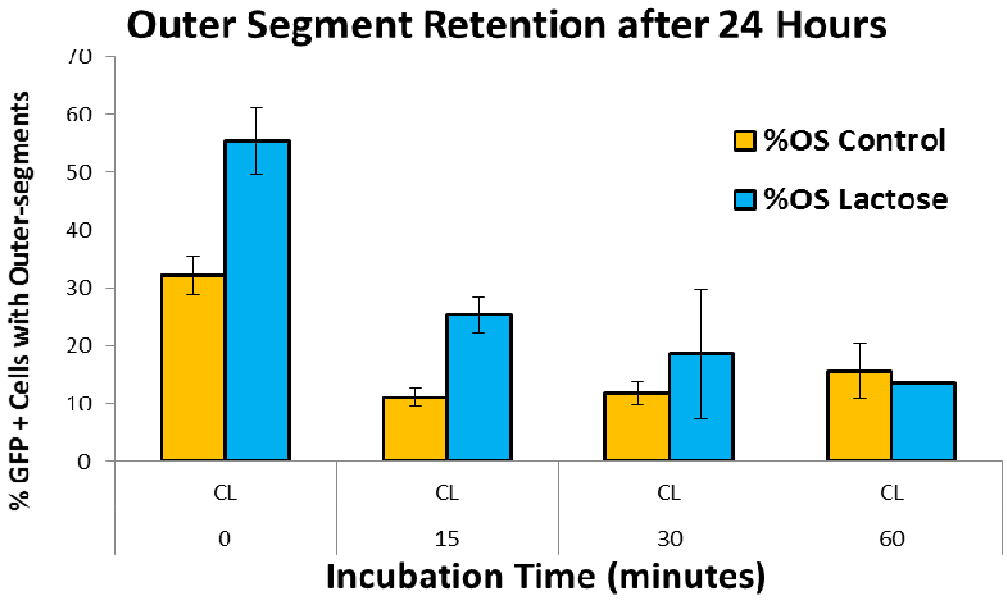

In experiments to determine the effect of culturing the retina prior to dissociation, it was found that while 10mM β-lactose dramatically improved outer segment retention of outer segments dissociated immediately after retina dissection, these effects were negated if the retina was incubated in culture media prior to dissociation of the retina or if the retina was obtained from light adapted animals.

FACS analysis of isolated adult photoreceptors.

Initial test of FACS sorted retina cells revealed loss of outer segments associated with mechanical dissociation. However, Nrl-GFP labeled photoreceptors would allow us to distinguish the effects we have seen with current media conditions between dissociated retina cell and that of isolated photoreceptors. Measuring outer segment retention in the isolated photoreceptor would allow us to distinguish the effect of β-Lactose supplementation as being photoreceptor cell specific, and not the result of the coordinated metabolism of the Photoreceptor and Müller glia, as suggested in previous studies of retina explants (110).

Figure 3.5 FACS Sorting: Isolating a Pure Population of Primary Photoreceptor Cells.

A) Isolation of Photoreceptor Cells **B) Fragments and Isolated Outer Segments**

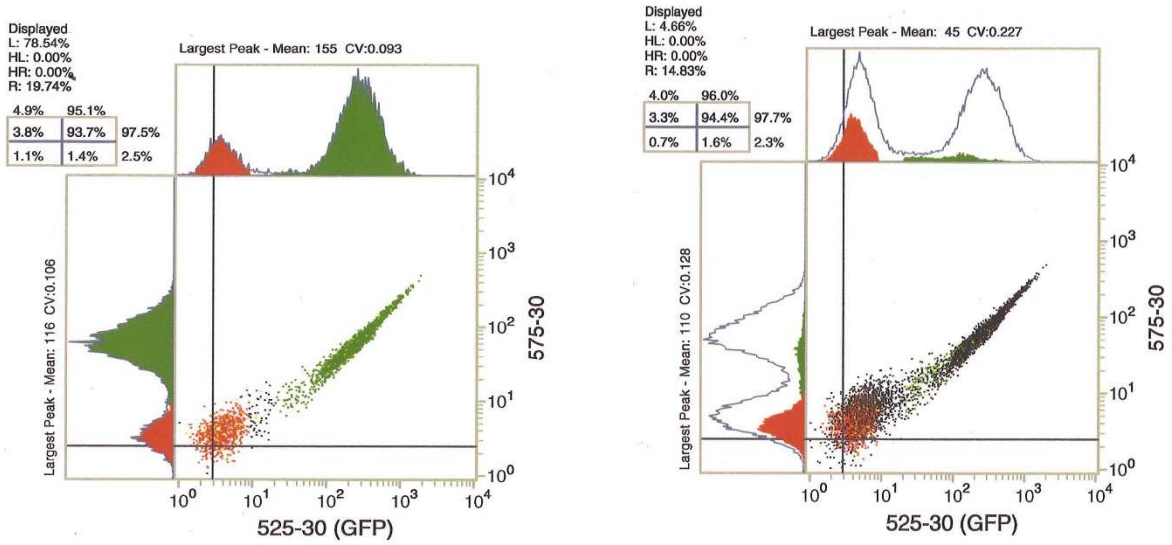

Preliminary FACS sorting of photoreceptor cells reveals that numerous cell types are present in a dissociated retina cell preparation. Measurement of GFP fluorescence reveals those cells that are photoreceptors, due to expression of Nrl-GFP (A) as seperation based on size demonstrates those population of cellular fragments that are broken off in the retina cell preparation (B). These experiments tested the feasibility of preparing a pure population of phtoreceptor cells from mouse retina tissue.

Optical Trap experiments reveal potential mechanical component to maintenance of outer-segment processes.

With the assistance of Chip Asbury's lab, we conducted preliminary experiments of the effects of force applied to isolated photoreceptor outer segments. In brief, we isolated dissociated photoreceptor cells and brought them to the Asbury lab, where they were added to cell media in a small chamber composed of a clear microscope slide and coverslip. An Optical trap laser was used to apply a force through a DIC objective, allowing for imaging of the isolated outer-segment in the vector of the optical trap laser, as it is perpendicular to the stage. Since outer-segments are not uniform for calibration, the exact force applied could not be measured, though it would be on the scale of piconewtons of force.

As the stage was moved, we were able to observe several outer-segments in our field of view. The optical trap could be turned on and off allowing us to trap individual outer-segment processes and move them by moving the x-y axis of the stage. In this way, several outer-segments were observed to move freely in the chamber with an optical trap force applied to them. However, in addition to un-attached outer-segments, several outer segment processes had the unique feature of adhering to the coverslip and providing resistance that would exceed the force of the optical trap. This attachment appeared to be mediated by an extension of the outer-segment resembling a tether, as in the case of Figure 3.6B. Our initial hypothesis is that this outer segment tether may join distal tips of photoreceptors to the RPE and provided a mechanical force necessary to signal the photoreceptor to continue outer-segment synthesis, which may explain the lack of disc synthesis following detachment of the retina from the RPE. Further

experiments will be necessary to understand the nature and structural components of this outer segment tether.

Figure 3.6 Optical Trap Experiment with Isolated Photoreceptor Outer Segments

A) **B)**

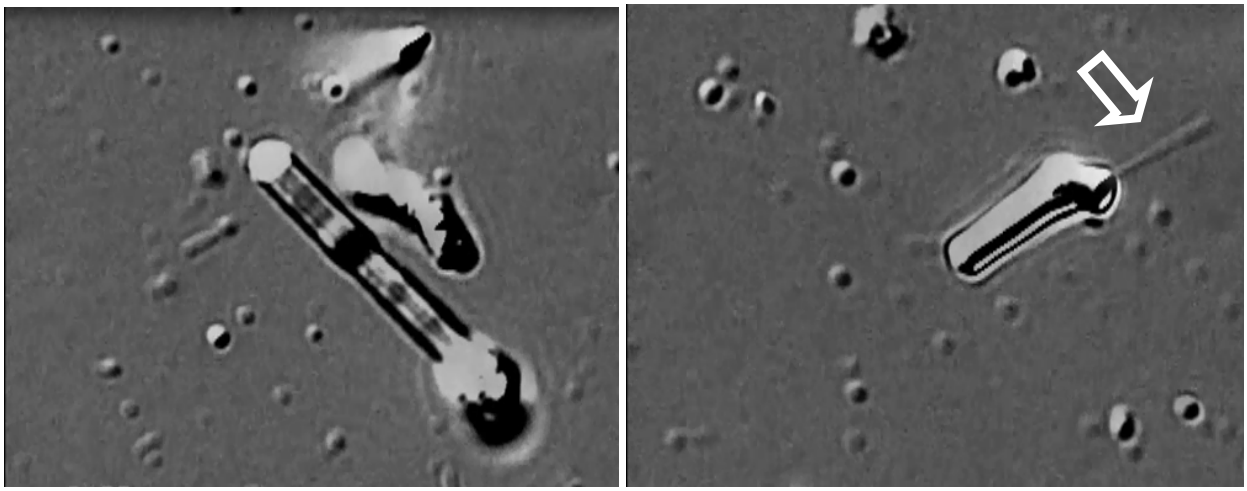

Optical trap imaging of isolated photoreceptor outer segment. A) an isolated outersegment which moves freely through solution, being pulled across the stage by the optical trap. B) a tethered outer segment which resists pulling by the optical trap, the tether stretching to, at times, the length of the outer segment. Tether indicated with white arrow in upper right hand corner of B.

Discussion:

The results of our findings demonstrate that the unique metabolic niche of the photoreceptor may be essential to maintenance of cell morphology *ex vivo*, due to the delicate nature of maintenance of cell identity. Establishment of buffered acidic conditions and receptor/trophic support allowed for isolation of outer segments exhibiting morphology heretofore unmet by previous methods. Of further interest is the result that while β-Lactose is capable of improving outer segment retention, the effect of light adaptation would appear to over-ride this effect. More importantly, in the context of overall outer segment identity, lower pH was shown to improve overall GFP expression

without improving outer segment retention, whereas lactose supplementation improved GFP expression and outer segment retention.

Conclusions and Future Directions:

The results of this study have examined the feasibility of studying the specific metabolic demands of the photoreceptor for both form and function. Making use of the Nrl-GFP mouse has made FACS a possibility, however there are still issues made with regard to photo-activation of photoreceptors using this method. One approach we are currently developing is the crossing of Nrl-GFP mouse into the Transducin knockout (Gnαt1-/-) background. As Transducin is necessary for initiation of the photo-transduction cascade, this would prevent the effects of typical light adaptation. More importantly, the Transducin knockout mouse retains morphologically intact outer-segments, making it possible to study outer-segment retention within our current system, while avoiding metabolic discrepancies associated with retina degeneration models. Furthermore, this would allow us to use FACS while circumventing the issues associated with light adaptation on retention of outer-segment morphology while studying the effect of phototoxicity from photo-transduction.

Beyond using genetic approaches of parsing the effects of light-adaptation on outer-segment formation and retention, there are further metabolic approaches that would improve our current techniques. From our research, lactose is an example of one poly-saccharide that has been used to studying outer-segment retention, however, it is not present in the retina and more physiological substrates could be used to mimic the IPM. Comparison of Lactose to Galactose would eliminate metabolic effects as the source of outer-segment retention. Addition of Maltose and Mannitol(111) would

separate metabolic supplementation from osmotic effects. This would allow us to distinguish receptor activation from metabolic and osmotic effects of these substrates.

Fatty Acids: The effect of DHA supplementation.

Across a variety of species, the fatty acid composition of the retina is comprised largely of poly-unsaturated fatty acids, with a significant amount of Docosahexaenoic Acid (DHA) present in the retina (112). The concentration of unsaturated fatty acids can be as high as 70% of the fatty acid composition in some species, primarily concentrated in photoreceptor outer segment discs. This suggests that optimal culturing of the photoreceptor may require a high localized concentration of poly-unsaturated fatty acids that is lacking in typical culture media conditions. Attempts to culture the photoreceptor as a neuron has overlooked this significant requirement for maintenance of photoreceptor morphology.

Growth Factor Influence on Outer Segment Retention: Neuronal Supplements

Cultivation of neurons has developed from use of conventional Fetal Bovine Serum towards more chemically defined media through the use of N2 or B27 Supplementation(113,114). In this system we can examine the effects of these supplements on outer segment retention and their effect on cellular metabolism.

Analysis of the mechanisms behind outer-segment retention.

Additional steps in the improvement of this project would be to follow up on studies in the zebrafish retina whereby genetically encoded fluorescent proteins under conditional heat-shock promoters could be used to visualize and detect outer segment growth(115)**.** These results would take this project beyond preservation of outer-

segments towards synthesis of new outer segment discs in an isolated photoreceptor cell *in vitro*. Using adeno associated virus (AAV) expressing an RFP-tagged Rhodopsin would allow us to track outer-segment synthesis in primary cultures. Combining this with our initial observations of metabolic building blocks necessary to maintain synthesis would allow us to utilize high-throughput techniques to find candidate metabolites or growth factors necessary for photoreceptor disc synthesis.

This project also has the capability to study events involved in outer-segment shedding previously only observed in freshly dissected retinas or retina explants(109). In previous studies of retina explants, exposure of phosphatidyl serine on the outer segment tip primed the outer segments for shedding and phagocytosis by the RPE, as observed with Red fluorescently labeled Annexin V (116). This effect was initiated by light exposure, but could be influenced by circadian rhythm. Teasing apart the effects of regulation on membrane synthesis or gene expression profiles could now be made in a purified photoreceptor system. By extension, this technique would allow us to approach fundamental research questions regarding this maintenance of outer-segments in the isolated photoreceptor, such as: What happens to the outer-segment without phagocytosis? Is this effect sustainable? If so, how? If not, why not? Dissociation of the RPE from the photoreceptor inhibits synthesis of outer-segments (117) and has been tied to expression of a specific gene expressed in the RPE (118), but the reasons for this inhibition whether of photoreceptor or RPE origin remain unclear.

These experiments pave the way for nutritional supplementation in 3-D cultures, such as the use of synthetic scaffolds (113) or cultivation of retina sheets (119), to test if isolated photoreceptor progenitor cells are capable of synthesizing new outer

segments. While orientation of the polarized cell as well as supplementation with essential growth factors may be a key part of outer segment maintenance our results indicate that it is a lack of necessary substrates which are preventing these cells from reaching their full potential. However, in light of our recent experiments with optical trap application of force to outer segments and the observation of a tether to the distal tips of outer segments, we cannot exclude that a mechanical tension may also be crucial for development of outer segment process. This opens up a further dimension of complexity including metabolic substrates, inter-cellular signaling processes, and potential inter-cellular mechanical signals that may all be necessary to signal this highly coordinated cellular process. Further research into what is required for disc synthesis *in vitro* would advance our knowledge in the study of photoreceptor development and retina degeneration.

Chapter IV: Mitochondrial Pyruvate Metabolism of the Retina and its impact on Photoreceptor Cell Survival in Culture.

Introduction

This chapter serves to summarize the results of several exploratory experiments that ultimately contributed to my study of retina metabolism, outside of my main focus of the role of glycolysis in retina function. They represent avenues of research reported in other papers to which I contributed. Additionally, these studies developed new techniques that will be used by the Hurley lab in future experiments. The overall subject matter is broken down into two themes:

- **Retina Degeneration linked to Pyruvate Metabolism: Effects of Phosphodiesterase 6B Inhibition with Zaprinast.**
- **Metabolic Effects of pro-survival compounds on retina Metabolism.**

As my advisor, James Hurley, has reminded me on numerous occasions, the path to what is ultimately published or what becomes the final hypothesis is not always a linear one. However, I will trace the development of these topics and how they contributed to the overall work. I hope you will enjoy it and learn from my experiences.

Results

Retina Degeneration linked to Pyruvate Metabolism: Effects of Phosphodiesterase 6B Inhibition with Zaprinast.

As established in the previous chapters, the bulk of our work has been to study the unique energy requirements of the photoreceptor cell and how this may contribute to photoreceptor cell degeneration. Early on in our studies of retina metabolism, we sought to analyze the effects of Light vs. Dark adaptation on retina survival to establish how the unique energy demands of light adaptation may influence photoreceptor cell survival. Of particular interest in the field of vision science is the different outcomes of mutations in various components in the photo-transduction cascade. For instance, defects in the gene Transducin (GNαT1) result in incomplete photo-transduction, but do not result in degeneration of photoreceptor cells(120) Conversely, mutations of Phosophodiesterase 6 (PDE6b)(121), a downstream component of the photo-transduction cascade results in early and rapid degeneration of photoreceptor cells. In both cases, the cells are essentially dark adapted, yet one mutation results in degeneration and the other does not. To investigate the effects of PDE mutants on retina metabolism, we made use of a known PDE6 inhibitor, Zaprinast, to chemically mimic the effects of PDE inhibition. (122)

Zaprinast is a known inhibitor of PDE6B activity, which was revealed by GC-MS analysis to disrupt pyruvate metabolism(41), but in what manner this occurred was unknown. To determine whether the effect was localized to mitochondrial metabolism rather than transport of mitochondrial substrates across the mitochondrial membrane, we tested the effects of Zaprinast on respiration of isolated brain mitochondria. Mitochondria were isolated from murine brain tissues, to serve as a surrogate for

photoreceptor mitochondria, and we analyzed the respiration of isolated mitochondria on a variety of mitochondrial substrates:

- Glutamate & Malate
- Pyruvate & Malate
- Succinate

These would help to parse whether an effect on mitochondrial metabolism would influence transport of substrates into the mitochondria or inhibit the activity of enzymes within the TCA cycle. The results (Figure 4.1 A & B) indicated that Zaprinast inhibits pyruvate and glutamate metabolism in the mitochondria, but that it has little effect on succinate-mediated respiration. This corroborated our initial clues from GC-MS analysis and introduced the idea that dysfunction of a particular mitochondrial pathway may lead to energy failures that ultimately result in photoreceptor degeneration. We compared the effects of Zaprinast to a known inhibitor of the Mitochondrial Pyruvate Carrier, UK5099, and found that it exhibited a similar effect on the retina metabolic profile as that of Zaprinast (Figure4.1 E & F) .(41) This suggested that the effects of Zaprinast, since they occurred at a concentration below that necessary for PDE6 inhibition, were primarily acting through disruption of pyruvate metabolism in the retina.

Figure 4.1 Zaprinast inhibits pyruvate-driven oxygen consumption

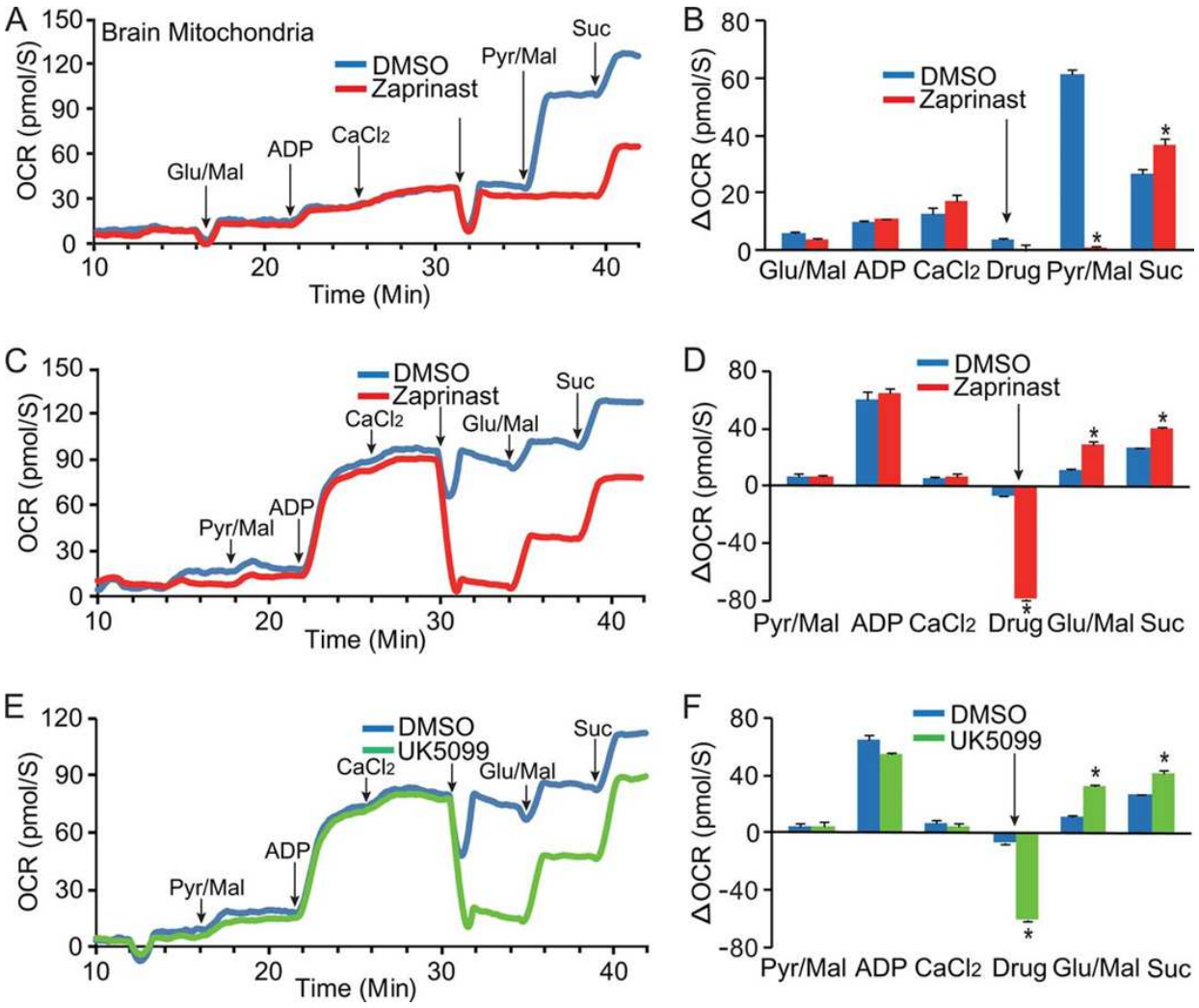

Zaprinast inhibits O_2 consumption in brain mitochondria when fueled by pyruvate but not when fueled by glutamate or succinate (*Suc*) in conditions starting with either glutamate/malate (*Glu/Mal*, *A* and *B*) or pyruvate/malate (*Pyr/Mal*, *C* and *D*). The large dip upon the addition of both Zaprinast (200 μM) and DMSO is an artifact caused by differences in O_2 solubility between water and DMSO. The substrate was added at the time point indicated by *arrows. B* and *D* are increments (ΔOCR) over the previous rate by subtracting OCR initiated by the substrate added before. *OCR*, oxygen consumption rate (*n* = 3). *E* and *F*, MPC inhibitor UK5099 inhibits pyruvate-driven oxygen consumption. Like Zaprinast, UK5099 at 10 nM inhibits oxygen consumption fueled by pyruvate but not glutamate and succinate. *E* is a representative trace from *F*, the normalized data (*n* = 3). * indicates *p* < 0.05 *versus* DMSO treated. *Drug* indicates the adding of DMSO, Zaprinast, or UK5099. * indicates *p*< 0.05 *versus* DMSO treated (*n* = 3). Figure from Du. Et. al. JBC 2013.

Calcium increases flux through Malate Aspartate Shuttle in Neuronal Mitochondria.

Due to the presence of this secondary effect of Zaprinast on the Mitochondrial Pyruvate Carrier, it remained uncertain as to what effect PDE6 mutations would have on mitochondrial metabolism directly. Attempts to test the effect of PDE inhibition with other compounds that would mimic the effect of PDE6 inhibition, such as 8-Br-cGMP or inhibitors of PKG or PKA, did not cause the same level of metabolic inhibition. Furthermore, GC-MS analysis of rd1 mouse retinas also failed to exhibit the metabolic changes observed with Zaprinast.(41) While the effects of Zaprinast could be explained by disruption of mitochondrial pyruvate metabolism, they did not explain the effect of light adaptation, or of PDE6 inhibition, if any, on mitochondrial function.

Previously, it had been observed that increasing cytosolic Ca^{2+} will increase the flux through the Aspartate Glutamate Carrier in neuronal mitochondria. As Ca^{2+} levels increase during dark adaptation, this raised the possibility that a similar mechanism could exist in photoreceptor cells. We tested the effect of Ca^{2+}on the metabolism of substrates pyruvate and malate vs. glutamate and malate. As observed in the literature, we saw that glutamate-mediated respiration was modulated by increasing levels of cytosolic Ca^{2+}(Figure 4.2). This suggests that metabolic substrates, such as pyruvate and glutamate, may be used differently depending on the energy demands of the cell, and in the case of the retina: light versus dark adaptation. Therefore, brain mitochondria may have a preference for glutamate over pyruvate during increased energy demand, which is associated with increased Ca^{2+}levels during synaptic signaling.

Figure 4.2: Mitochondria Respiration: Calcium effects on AGC

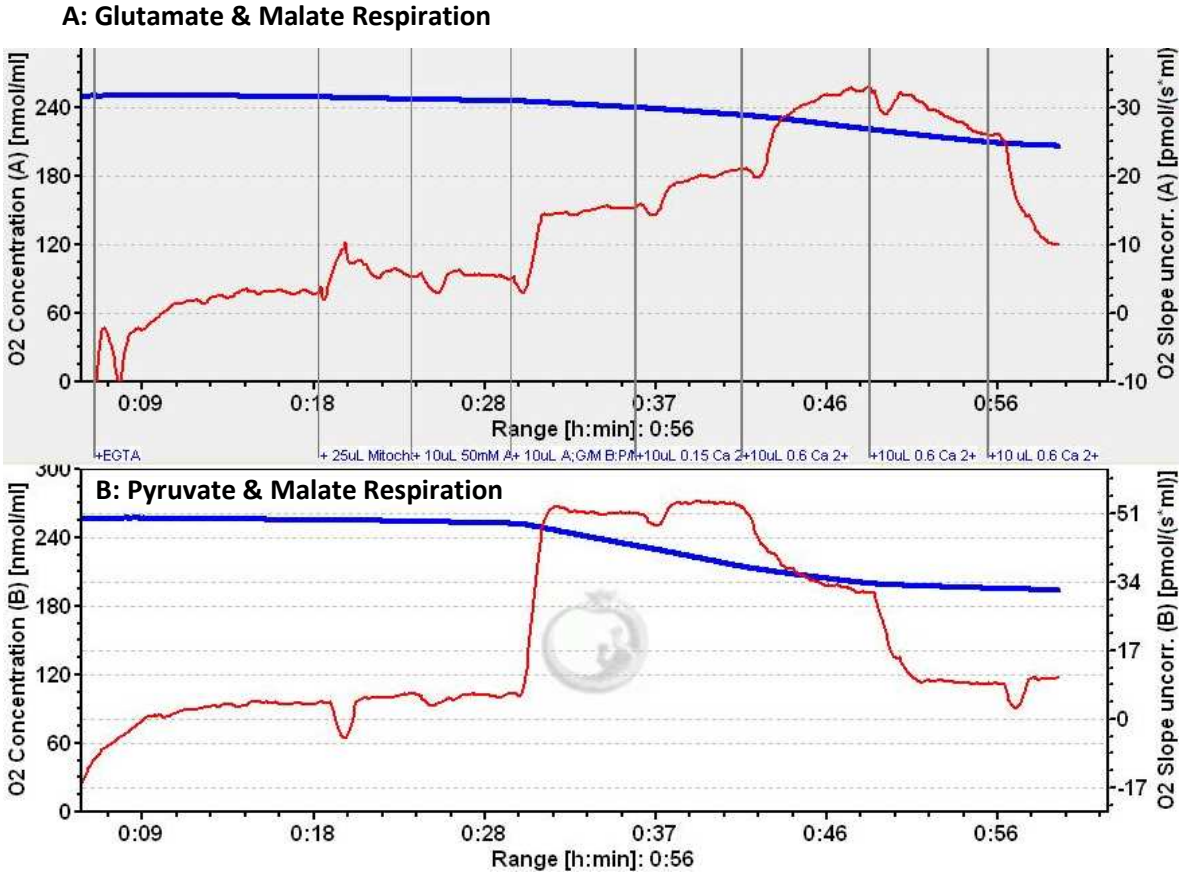

Mitochondria were isolated from Murine brain tissue and O_2 concentration of the media the incubation chamber, measured over time. Addition of ADP to Pyruvate/Malate substrate resulted in a dramatic increase in respiration, whereas Glutamate/ Malate respiration was almost half of the same rate of respiration. Addition of Ca^{2+}through 50nM increments resulted in a slow increase in glutamate/malate respiration (A), whereas pyruvate mediated respiration (B) remained relatively unchanged. Eventually, increasing Ca^{2+}concentrations result in a mitochondria permeability transition that depolarizes mitochondria and halts respiration. This experiment demonstrated the unique dependence of mitochondria on various substrates, but also that their preference for a particular substrate may be modified by cytosolic conditions, such as physiological changes in Ca^{2+}concentration.

To determine whether or not photoreceptor mitochondria respond in the same fashion as neuronal mitochondria, we isolated mitochondria from guinea pig retinas and proceeded with the same experimental conditions for studying Ca^{2+} regulation of AGC1. *(Due to the unique avascular nature of the guinea pig retina, mitochondria are localized*

largely to the photoreceptor layer(38)). Our experiment did not yield the same effect as observed with neuronal mitochondria, suggesting that Guinea Pig Retina mitochondria are not modulated by Ca^{2+}. However in comparison of pyruvate versus glutamate mediated respiration (Figure 4.3) it would appear that glutamate metabolism is favored above that of pyruvate in photoreceptor mitochondria.

Figure 4.3 Guinea Pig Retina Mitochondria prefer Glutamate as an aerobic substrate

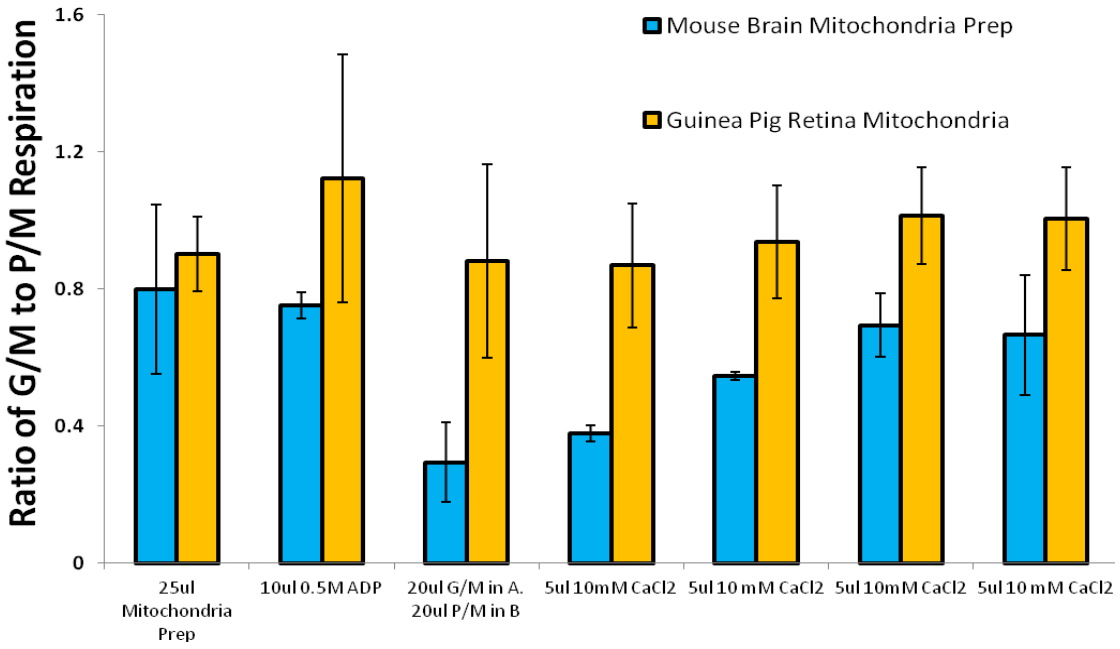

Our attempts to compare the overall metabolism of mouse brain versus Guinea Pig Retina mitochondria was used to identify basic metabolic differences between brain and photoreceptor cell mitochondria respectively. To this end, we compared differences in glutamate versus pyruvate metabolism. The Y-axis represents the ratio of glutamate to pyruvate metabolism. In the case of mouse brain mitochondria, represented in blue, as $Ca^{2+}$is added to the mitochondrial preparation, glutamate-mediated metabolism rises. However, in Guinea Pig Retina Mitochondria, the addition of Ca^{2+} to the mitochondria preparation had little effect on glutamate mediated respiration, but overall glutamate mediated respiration was equal to or exceeded that of pyruvate respiration, suggesting that guinea pig retina mitochondria rely more on glutamate than pyruvate to fuel their metabolic processes.

Ultimately, these observations reaffirmed that mitochondrial metabolism is essential to photoreceptor cell function and survival and differs from that of neuronal mitochondria. While the broader implications of pyruvate vs glutamate metabolism remained to be determined, these experiments introduced us to that idea of understanding what metabolic pathways are necessary for retina cell function and survival. As opposed to screening compounds to induce cell specific degeneration, we sought to screen for compounds that improved photoreceptor cell survival and assay their effect on retina metabolism.

Metabolic Effects of pro-survival compounds on Retina Metabolism.

In the era of high-throughput screens, it is not uncommon to test a library of chemical compounds on a particular cell line to test whether or not these compounds can improve overall cell health. In this way, many compounds have been discovered that alter cellular gene expression or overall metabolism towards cell survival(123). During our initial screen of the effects of metabolic inhibitors on isolated mitochondria, we began work in conjunction with the Reh Lab at the University Of Washington Department Of Biological Structure. Their experiments, led by Graduate Student Jule Gust and Post-Doctoral Researcher Deepak Lamba, demonstrated that dissociated adult photoreceptor cells could be transplanted and integrated into and adult retina to replace native photoreceptor. Thus, development of methods towards cultivation of adult photoreceptor cells *in vitro* could aid in treatment of photoreceptor degeneration. The goal of this approach was to measure the survival of isolated photoreceptor cells when supplemented with cell-survival compounds from the library of Sheng-Ding, currently at the Buck Institute. The result of their screen revealed two potential

compounds that improved cell survival. Our interest in retina metabolism led to a collaboration in which we analyzed the effect of these compounds on cell metabolism.

Figure 4.4: Measuring Photoreceptor Cell Death in Culture

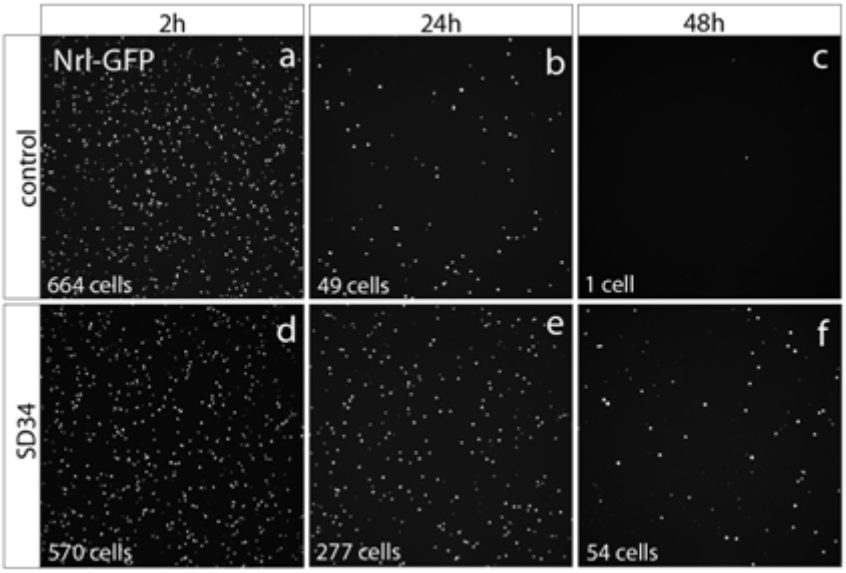

Retinal cells were dissociated from mice expressing GFP under the Nrl promoter and photoreceptor cell health was tracked by measuring the number of GFP-positive cells over time. Under control conditions, photoreceptors are lost within a span of 48 hours in culture. A library of compounds was applied to each condition, revealing compounds with the potential to improve cell survival, such as SD-34, which caused a dramatic improvement in the number of GFP-positive cells after 48 hours in culture.

Figure 4.5: Chemical Library Screen Reveals Pro-survival Compounds

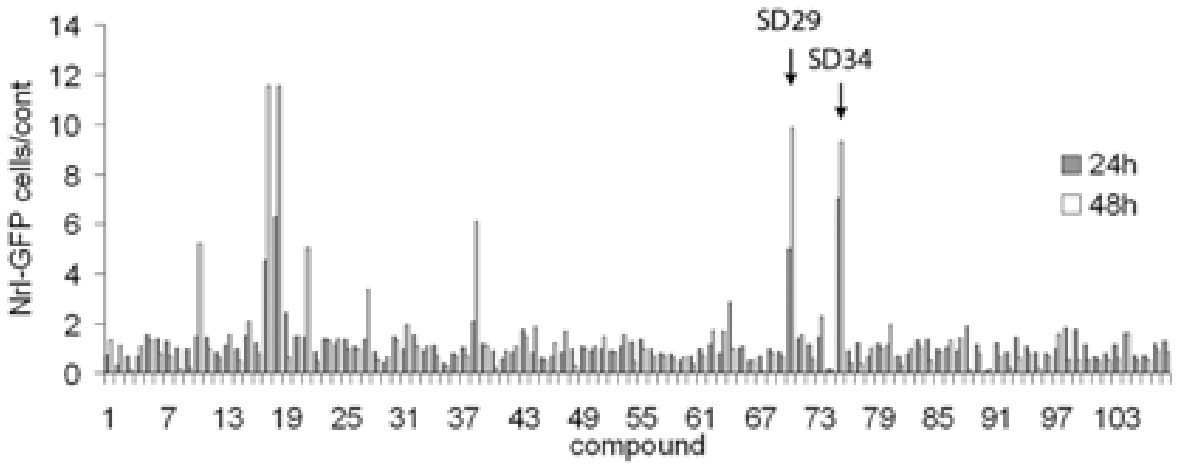

Comparison of a library of compounds and the number of GFP positive cells after 24 and 48 hours revealed several candidate compounds with the potential to improve photoreceptor cell survival in culture. The compound candidates of interest being SD-29 and SD-34.

Our results indicated that their candidate compounds: SD-29 and SD-34 both inhibited and uncoupled mitochondrial respiration, respectively. In the course of this work, we also identified other candidate compounds which improved cell survival in the cell culture model. In an attempt to understand the chemical nature of these compounds and their effect on retina metabolism, we tested structurally similar compounds and assayed their effect on improvement of cell survival and their effects on cellular metabolism. With this strategy, we might begin to see correlations between improved cell survival and effects on cell metabolism that are necessary for photoreceptor cell survival in culture.

Our initial experiments tested the effects of SD-29 and SD-34 on the respiration of isolated brain mitochondria, to determine whether these compounds inhibited or uncoupled oxidative phosphorylation of these substrates. Studies of isolated mitochondrial respiration revealed that SD-29 inhibits Complex I-mediated respiration.

Similar studies of SD-34 revealed that this compound uncouples mitochondrial respiration.

Figure 4.6: SD-29 Inhibits Mitochondrial Respiration

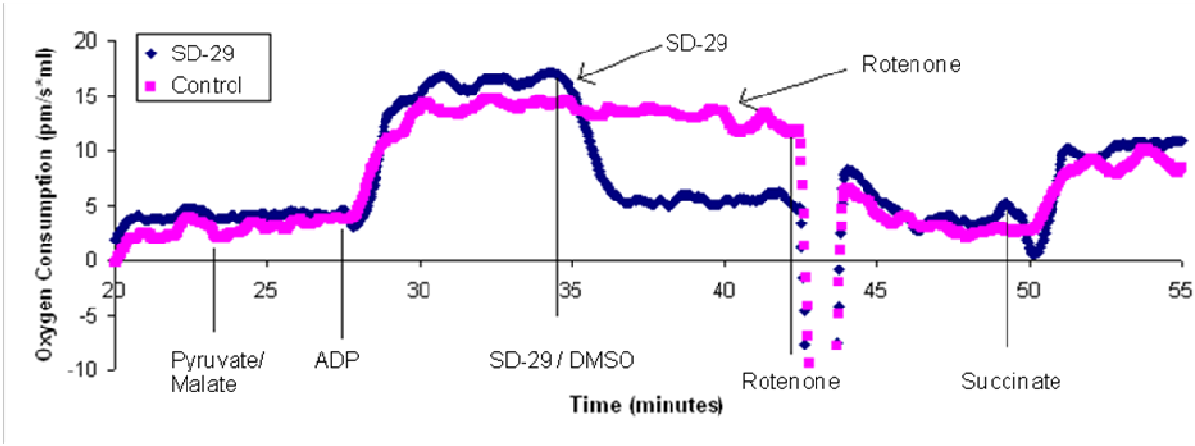

Oxygen consumption and metabolism of Pyruvate and Malate are initiated by addition of ADP. Addition of SD-29 caused an inhibition of oxygen consumption that was not observed with the carrier solvent DMSO. Addition of the known complex I inhibitor Rotenone resulted in a similar decrease in oxygen consumption as that observed with SD-29. Addition of Succinate, which bypassed Complex I by fueling Complex II, Succinate Dehydrogenase, rescued oxygen consumption. This implicates SD-29 as an inhibitor of mitochondrial Complex I respiration.

Figure 4.7: Chemical Structure of SD-29 and Chemical Analogue

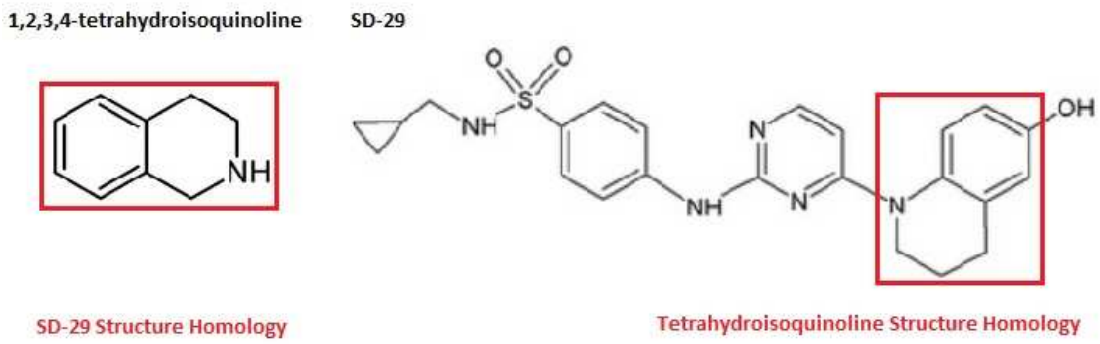

Compound SD-29 was tested against 1,2,3,4-tetrahydroisoquinoline, a known chemical precursor used in the synthesis of molecules such as SD-29.

Figure 4.8: SD-34 Uncouples Mitochondrial Respiration

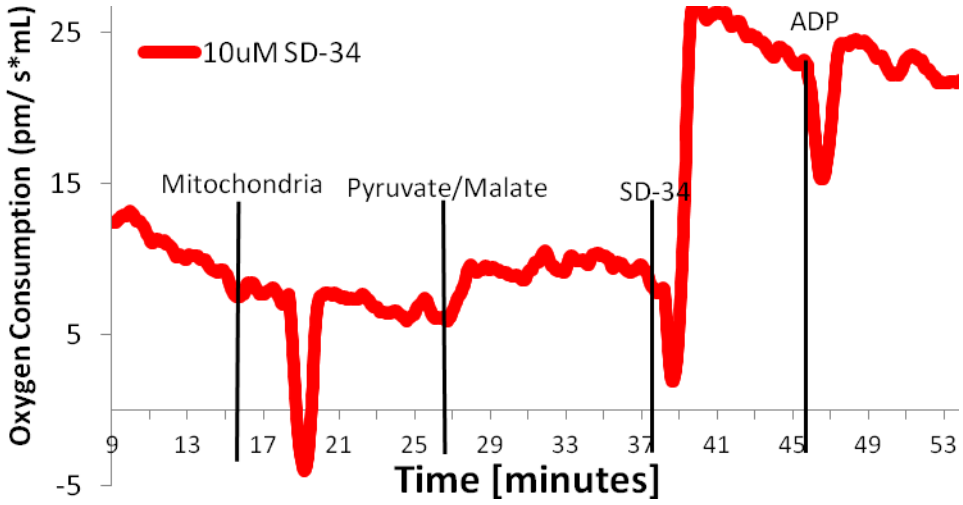

Oxidative Phosphorylation is initiated by addition of ADP in the presence of mitochondria substrates, such as pyruvate and malate. This is due to release of the mitochondrial membrane potential through complex IV or ATP synthase. In the absence of ADP, this potential is built up, but not released, resulting in an inhibition of mitochondrial oxygen consumption. Uncouplers, such as FCCP, act as ionophores, releasing the membrane potential, without producing ATP, thereby increased oxygen consumption without reliance on ADP, but also without ATP production. SD-34 exhibits qualities similar to most uncoupling compounds, due to the increase in oxygen consumption and consumption of pyruvate and malate without ADP present.

Figure 4.9: Chemical Structure of SD-34 and Uncoupler Analogue FCCP

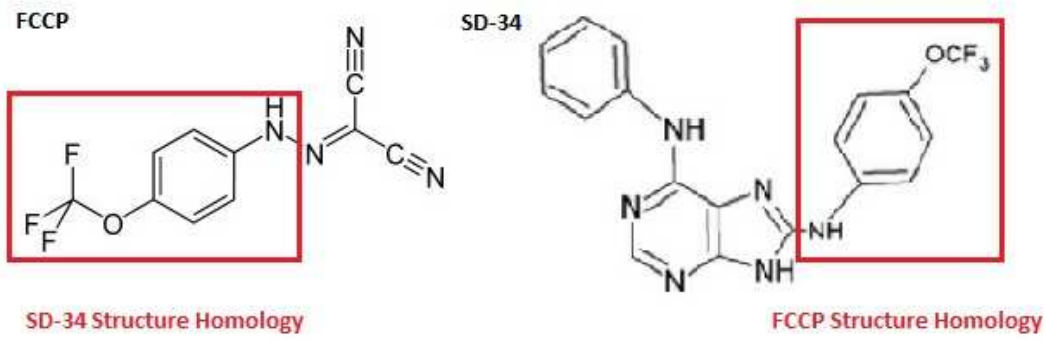

After an initial test was conducted on isolated brain mitochondria which demonstrated that SD-34 had the capability to uncouple mitochondrial respiration, we examined the structure of SD-34 and found that it had similar structural features to known mitochondrial uncoupler, FCCP.

Following these initial tests for effects on mitochondrial respiration, we sought to test the effects of inhibitors of Complex I, uncouplers of oxidative phosphorylation, and structurally similar chemicals to see if we could elicit improved survival in isolated photoreceptor cells in culture. Our initial tests demonstrated that the classic inhibitor of Complex I, Rotenone, and uncoupler Carbonyl cyanide-*4*-(trifluoromethoxy)phenylhydrazone **(**FCCP) did little to improve cell survival, whereas a compound with structural similarity to SD-29 , 1,2,3,4- tetrahydroisoquinoline (THIQ), dramatically improved the number of GFP positive cells in photoreceptor cell cultures.

Figure 4.10: Effects of Complex 1 Inhibition on Photoreceptor Cell Survival

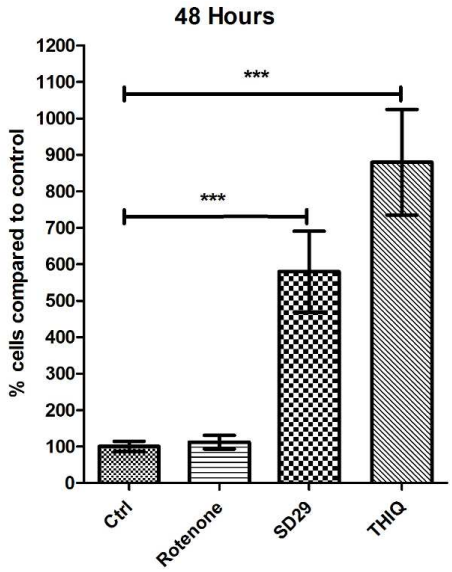

Our Initial studies of metabolism suggested that SD-29 would inhibit Complex I mediated mitochondrial respiration. However, test of the known inhibitor Rotenone did not elicit the same outcome on cell survival. We went on to test a structurally similar compound Tetrahydroisoquinoline (THIQ) and found that it did improve cell survival. This opened the possibility of characterizing the effects of THIQ on cellular metabolism.

In an attempt to distinguish the difference in these compounds from typical inhibitors of the Electron Transport Chain complexes, we analyzed the effect of these compounds on isolated components of the electron transport chain. SD-29 inhibits complex I and SD-34 has little effect on Complex II-mediated metabolism versus FCCP which is known to inhibit Complex II.

Figure 4.11: The Electron Transport Chain

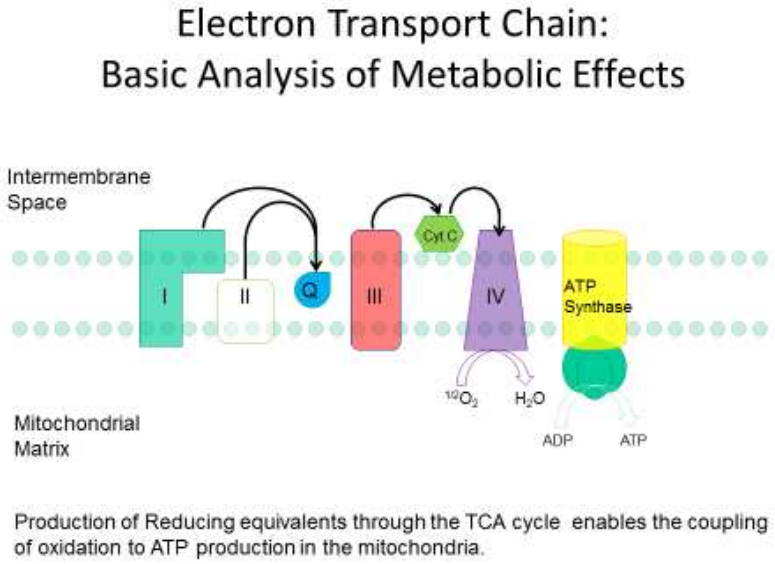

Figure 4.12: Layout of Assays for Electron Transport Chain Complex Activity

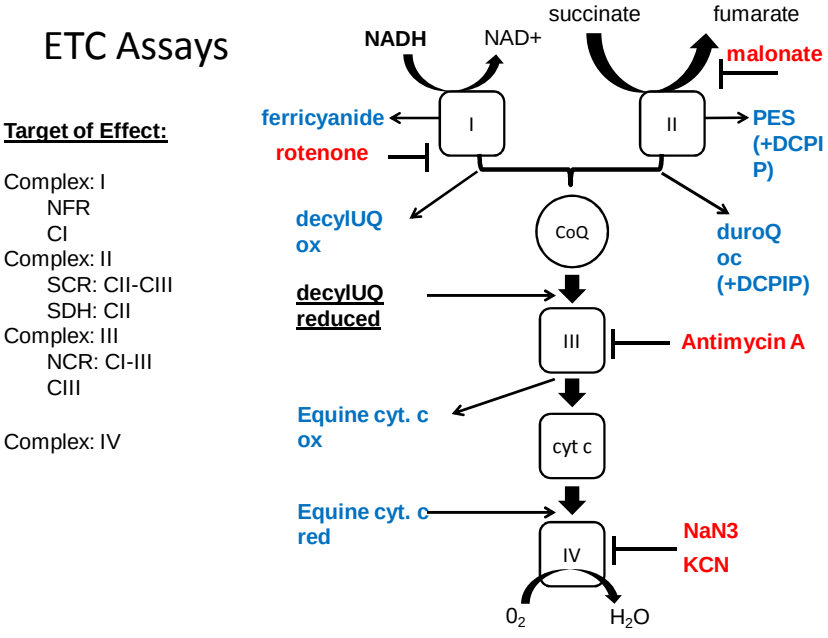

Several assays have been developed that allow us to determine overall activity of Electron Transport Chain Complexes in permeabilized mitochondria preparations. By adding substrates upstream of each individual step in the Electron transport chain, it is possible to test the overall activity of each complex.

Figure 4.13: ETC Assay Complex Tests of SD-29 and THIQ

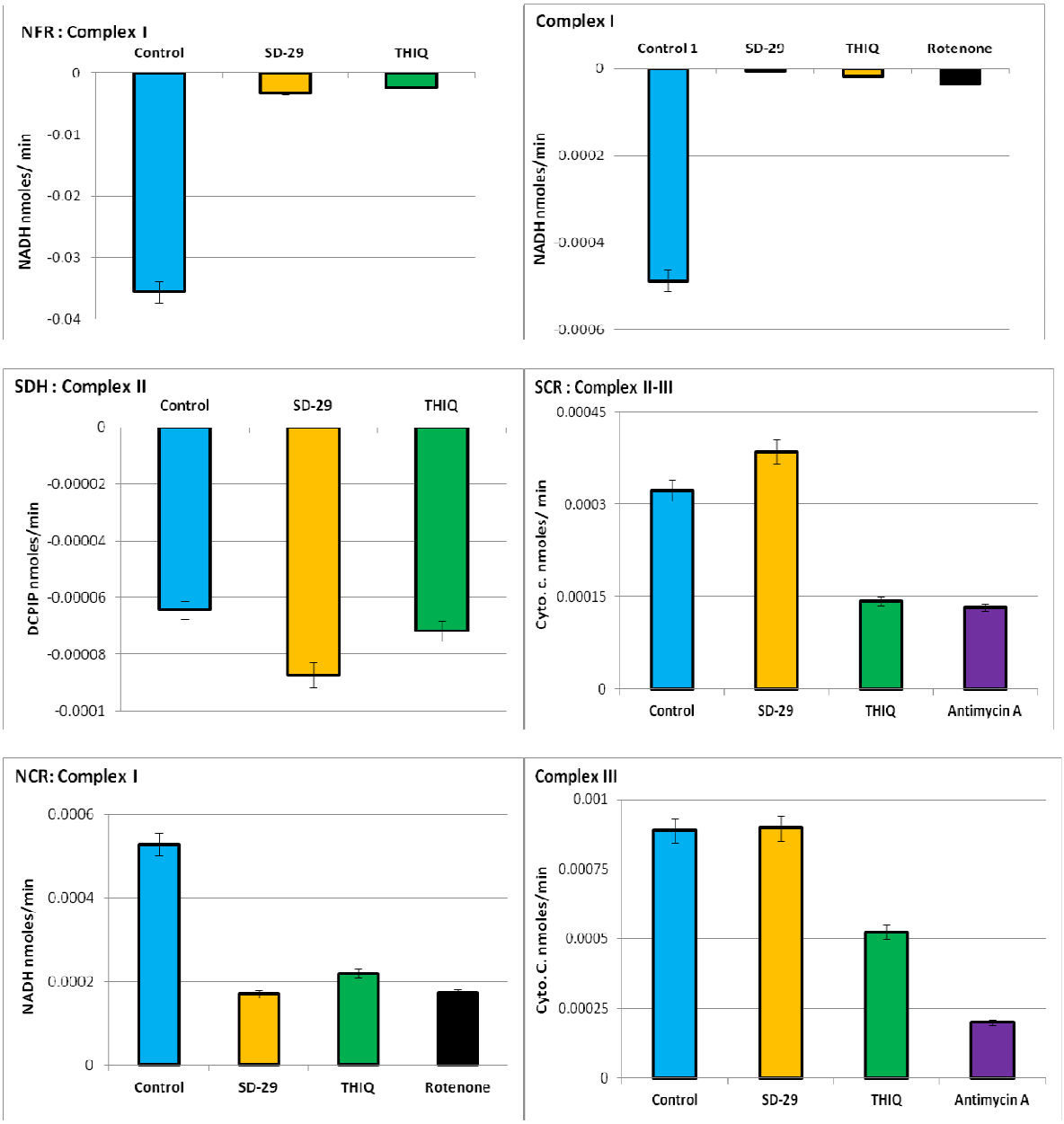

We surveyed the effects of SD-29 and THIQ on various complexes in the electron tranport chain. The results reconfirmed themitochondria respiration studies, in that SD-29 did inhibit Complex I, but that THIQ inhibited Complex III as well. This suggested that differences in these inhibitory capacities may explain the efficacy of these compounds on photoreceptor cell survival.

As complex I and III inhibition are linked to the generation of reactive oxygen species, we tested the effects of SD-29 and THIQ on mitochondrial reactive oxygen species (ROS) generation in isolated mitochondria using an Amplex Red-based assay(124).Attempts to ascertain the effects of inhibiting the Electron Transport Chain on ROS generation revealed that SD-29 tended to reduce ROS generated from oxidative phosphorylation of various metabolites (Figure 4.14), whereas candidate compound THIQ was shown to induce consistent ROS production in these assays. Conducting a separate experiment with THIQ vs. incubation with Catalase, demonstrated that THIQ was capable of generating hydrogen peroxide on its own. This unexpected result begged the question as to what role reactive oxygen species play in photoreceptor cell metabolism and overall cell survival. It is possible that application of THIQ provided a beneficial effect with production of ROS. Future experiments to determine this role on survival would be to test the effect of other peroxide generating compounds in this system or to study the effect on cell survival in mice over expressing catalase(125) to determine if prevention of ROS in the photoreceptor cell has an inhibitory effect on cell survival in culture.

Figure 4.14: SD-29 and THIQ exhibit differences in mitochondrial ROS production

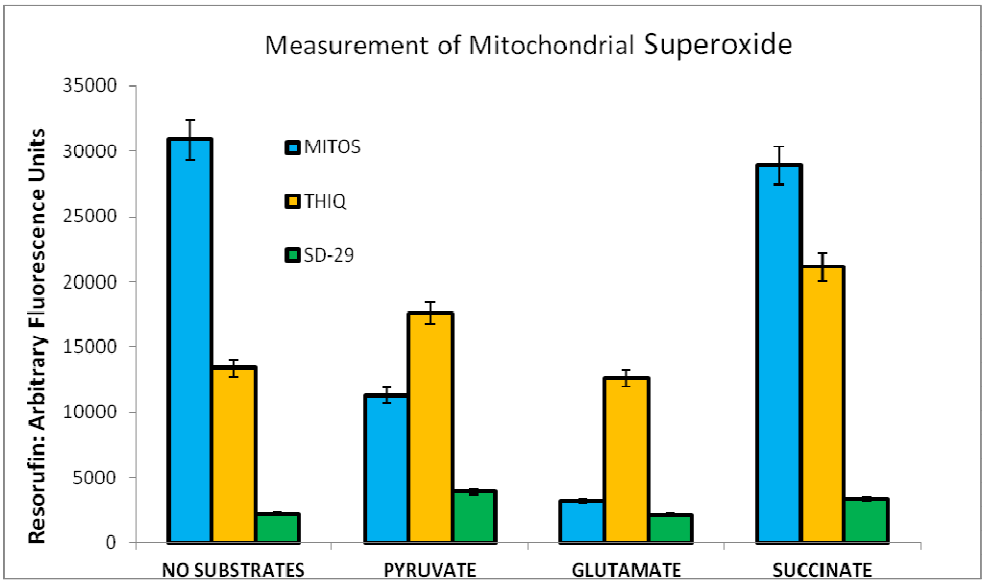

Isolated mouse brain mitochondria were incubated with in solution with either pyruvate, glutamate, succinate, or no substrates at all and ROS generation was measured with an Amplex Red-coupled assay. Mitochondria with pyruvate and malate appeared to generate little ROS compared to succinate or complete lack of substrates. Addition of SD-29 appeared to decrease overall ROS generation, whereas THIQ appeared to generate a consistent amount of ROS.

Figure 4.15: THIQ generates H_2O_2 in solution

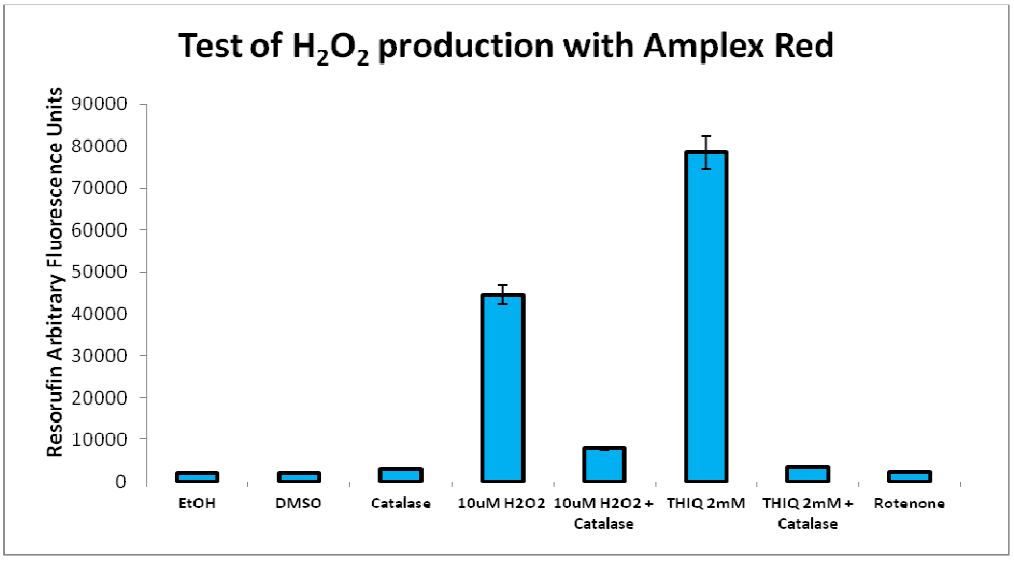

To ascertain whether the signal generated from THIQ was a product of THIQ itself, or on overall mitochondrial ROS generation, we incubated THIQ with Catalase and found that THIQ alone was sufficient to produce ROS in the Amplex Red ROS assay.

GC-MS analysis of SD-29 mediated metabolism in the presence of glucose vs. mitochondrial fuels revealed that these compounds do influence the incorporation of intermediates into the TCA cycle. In general, both SD-29 and THIQ decreased the amount of TCA cycle intermediates when relying solely on glucose. However, when incubated with a mixture of 10mM Pyruvate, 5mM Malate, 1mM Glutamine, and 1mM Leucine, where SD-29 showed a dramatic decrease in the amount of Succinate and Fumarate generated, THIQ was able to maintain levels similar to control conditions. This suggests that the effects on mitochondrial ETC complexes were reflected in redirecting glycolytic intermediates into oxidative phosphorylation and a redirection of TCA cycle intermediates towards Complex II-mediated respiration. While the implications of this redirection of metabolic flow remain uncertain, it has been observed in tissue culture cell models, that build-up of Succinate and Fumarate may influence signaling through HIF and provide a pro-survival mechanism.(126) Further experiments will be needed to determine whether modulation of HIF replicates these changes in cell survival or metabolic effects, and whether this is indeed the mechanism of action behind improvement in cell survival with treatment of THIQ.

Figure 4.16: Effects of SD-29 on Metabolites in the Retina

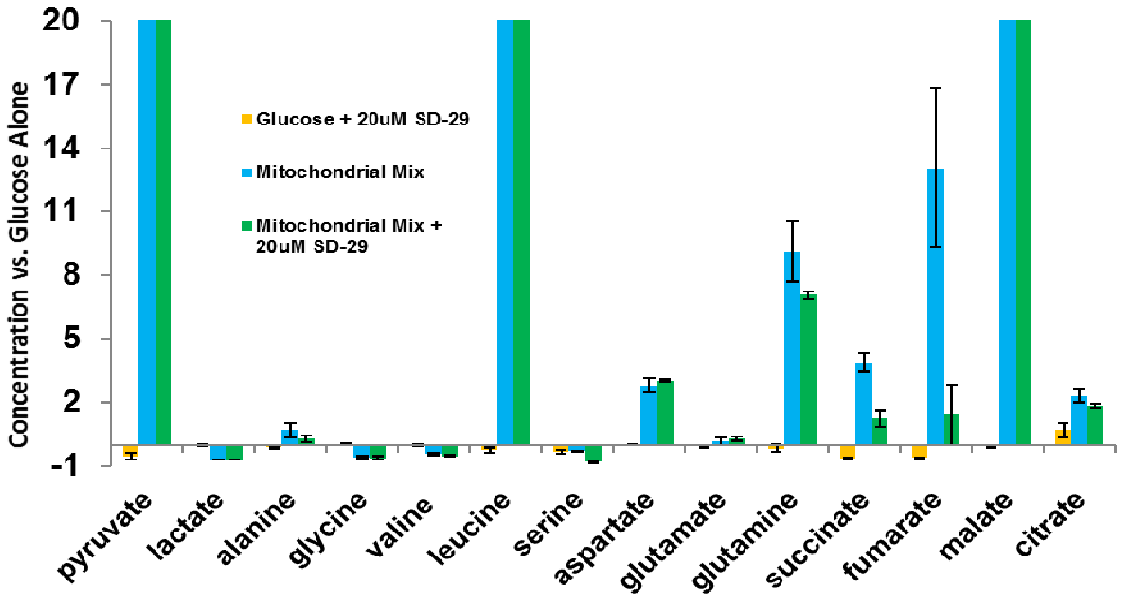

Figure 4.17 Effects of THIQ on Metabolites of the Retina

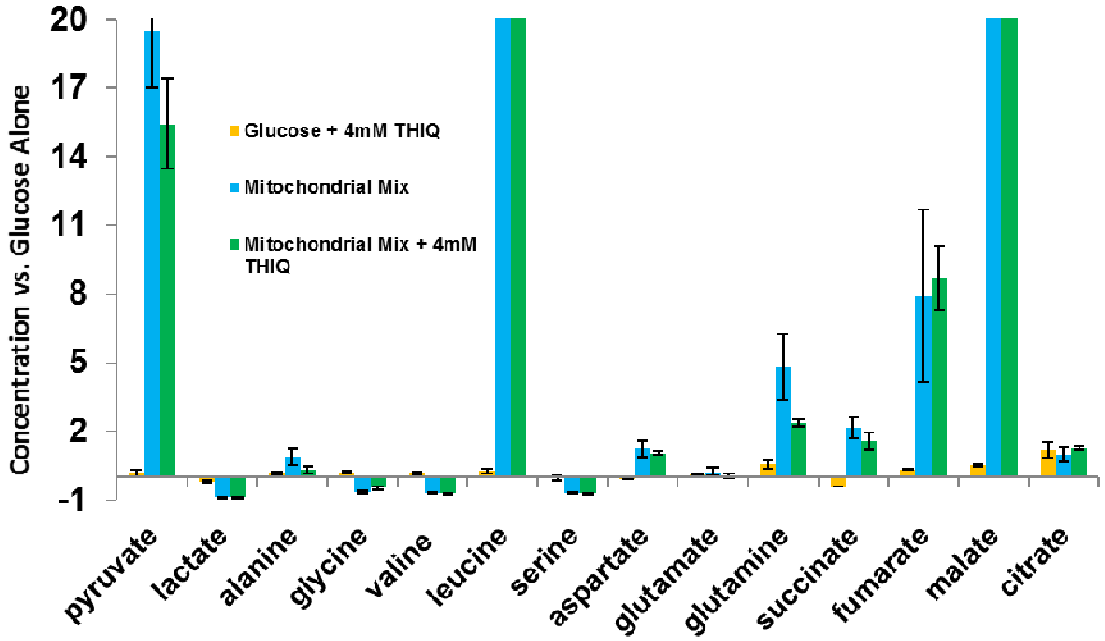

Retinas were incubated for 90 minutes in a solution of 5mM glucose or Mito-fuel mixture of 10mM Pyruvate, 5mM Malate, 1mM glutamine, and 1mM Leucine in the presence or absence of candidate compounds SD-29 or THIQ. While in both cases, overall glycolytic metabolite levels were dramatically decreased, in the case of THIQ, TCA cycle intermediates appear to be redirected towards Complex II intermediates such as Succinate and Fumarate. As Pyruvate, Leucine, and Malate were used in the mitochondrial mixture, their values could not be separated from background levels of supplied metabolites.

Discussion

In the course of examining the effects of pro-survival compounds on cellular metabolism, we found several potential mechanisms of action, which influence metabolic pathways. One candidate compound for photoreceptor cell survival, SD-29, was previously published to have effects on transcript levels of embryonic stem cells and it's mechanism of action linked to E-cadherin signaling.(123) However, can one ignore the potential metabolic side effects of these same candidate compounds? In the study of the effects of SD-29 on cellular reprogramming of embryonic stem-cells, no mention was made of the effects on metabolism. However, this introduces the intriguing idea that control of metabolism may have an important role in cell fate beyond survival, but that also includes cell differentiation. In the same way that some cells are heavily reliant on glycolysis or oxidative phosphorylation, inhibition or accentuation of distinct metabolic pathways may introduce new attributes to these same cell types.

Conclusions

The analysis of all off-target effects of a compound to be used in clinical settings is incredibly daunting. However, the analysis of the effects of compounds on overall metabolism is becoming easier. Technologies such as the XF-24 & 96 Seahorse apparatus allow us to make initial assessments of compounds on glycolysis and oxidative phosphorylation as well as fatty acid oxidation.(127) While I am certain that the use of animal models to determine a compound's mechanism of action on a systemic level will continue to be essential to the development of future chemical therapeutics, I am also confident that we are entering a new era in which metabolism is

recognized for its role in not only fueling cell survival, but that it is also a significant factor in cell function. The goal of this research was to investigate the effects of pro-survival compounds on metabolism of cells in the retina. In the process, we've established high-throughput methods of analyzing photoreceptor cell structure, survival, and perturbations on basal cell metabolism. The result is a comprehensive means of analyzing the effects of compounds on metabolic function, the understanding of which allows us to screen for new molecules that may be used to enhance survival of cells within the retina based on their unique metabolic requirements.

Chapter V: Materials and Methods

1. Care and Use of Animals.

All animal use was performed in accordance with ARVO statement on the "Use of Animals in ophthalmic and Vision Research" Protocols for animal use were approved by the Institutional Animal Care and Use Committee (IACUC) of the University of Washington and with procedures approved in the Directive 86/609/EEC of the European Union, and the Ethics Committee of the Universidad Autónoma de Madrid. WT C57Bl/6 mice were purchased from Jackson Laboratory (Bar Harbor, Maine) maintained in a vivarium of cyclic light with 100 LUX at maximal levels. 14 h on/ 10 h off.

Long Evans Rats were obtained from Charles River Laboratory and housed under similar conditions. Aralar/AGC1+/- mice were crossed to produce Aralar/AGC1-/- and Aralar/AGC1+/+ control littermates in Dr. Jorgina Sartrustegui's lab (Madrid, Spain). AIPL1, RD1, and GNAT1 deficient mice were from stocks maintained at the University of Washington. Experiments were carried out on mice of 3-6 weeks of age. Hartley strain Guinea Pigs were obtained from Charles River Laboratories.

2. Reagents.

Unless otherwise specified, all reagents were obtained from Sigma Aldrich. C^{13} isotopes: Uniformly C^{13} labeled glucose (U-C^{13} glucose), Palmitate (U-C^{16} Palmitic Acid and Palmitate) was obtained from Cambridge Isotope Laboratories, Inc. (Andover, MA). Unless specified, other ^{13}C tracers and reagents were from Sigma Aldrich. (2S, 3S)-3-{3-[4-(trifluoromethyl)benzoylamino]benzyloxy]aspartate (TFB-TBOA) was from Tocris Bioscience (Bristol, United Kingdom). Carbamoyl-phosphate synthetase 2, aspartate transcarbamylase, and dihydroorotase (CAD) recombinant protein was from Creative BioMart (Shirley, NY).

3. Protein concentration

After extracting metabolites, tissue pellets were dissolved in 200 µl of 0.1 M NaOH overnight at 37^{o}C. Protein concentration was determined by BCA assay kit (Thermo Fisher Scientific). We determined the absolute concentration of purified

PKM2 standards for calibration of immunoblots by amino acid analysis (AAA Service Lab, Damascus, OR).

4. Statistical analysis.

Data are expressed as mean ± SD. Significance of differences between means was determined by unpaired two-tailed t-tests or ANOVA with an appropriate post-hoc test. A p value < 0.05 was considered to be significant.

5. Maintenance of Tissue Culture Cell Lines

Cell Culture Retina Müller cells were isolated from postnatal day 12 (P12) retinas of C57BL/6 littermates(82). Retinas were dissected and dissociated in papain with 180 units/mL DNase (Worthington) and incubating at 37^{o}C for 10 min. Cells were gently pipetted 8-10 times and added to an equal volume of ovomucoid (Worthington). After centrifugation at 300 x g for 10 min, the cells were plated in neurobasal medium (Invitrogen) supplemented with 10% FBS, 1 mM L-glutamine , N2 (Invitrogen), 1% Penicillin–Streptomycin (Invitrogen), and EGF (100 ng/mL; R&D systems) at a density of two retinas per 35 mm dish at 37^{o}C in 5% CO_2. The media was changed every 2-3 days and the cells were passaged 1:2 to the 35 mm dishes.

HELA cell lines and rMC-1 cell lines were established cell lines obtained from the lab of Thomas A. Reh PhD. Cells lines were maintained in DMEM with 10% FBS, 1% Penicillin-Streptomycin, and 20mM Glucose unless otherwise specified. Cells were passaged every 3 days.

6. Retina tissue culture.

Mice were euthanized by cervical dislocation. Retinas were isolated and cultured as previously described.(128) Retina explants were incubated with 5 mM Glucose, or 5 mM other ^{13}C tracers in 37^{o}C, 5% CO_2 incubator.

7. Retina Dissection

Mice were euthanized with CO_2 gas followed by cervical dislocation under conditions specified in the experiment. Eyes were removed with tweezers and punctured with a 1mL 25g hypodermic needle to relieve pressure of the vitreous.

Eyes were hemisected along the scleral line with 10cm Spring Scissors (Fine Scientific Instruments) and retina removed with Dumont #5 forceps (Fine Scientific Instruments). Dissection was completed in HBSS buffer chilled on ice and stored in buffer prior to transfer to experimental conditions.

8. Preparation of Tissue Homogenates

For preparation of tissue homogenates, samples were snap-frozen in liquid nitrogen and stored @ -80℃. Samples composed of ty pically 1 mouse retina or 50 mg quantities of Brain, Liver, and Muscle tissue were homogenized into 200uL Retina Homogenization Buffer (50 mM Tris pH 7.4, 2 mM EGTA, and 1% NP-40) in a 1.5mL microfuge tube with a hand-held motorized pestle. Samples were spun @ 16,000 rpm for 15 minutes and supernatants stored at -80℃. Protein concentrations were measured using a Dc protein concentration assay from Bio-Rad with BSA used as a standard for protein concentration. Final concentrations used were 0.5ug/uL.

9. Serial Sectioning

To ascertain the distribution of pyruvate kinase within the retina, serial sections of rat retina were obtained as in Linton et. al. (77)**.** Rat retinas were dissected and placed on nitrocellulose membranes photoreceptor side down. These membranes were fixed to glass slides with super glue and frozen on dry ice. After overnight fixation, these retina sections were sectioned on a cryostat at 10um thickness and transferred to Retina Homogenization buffer. These sections were analyzed using a dot blots on PVDF to measure distribution of Rhodopsin and Synaptotagmin. Sections that had adequate separation or localization of these respective signals were used for Western Blot analysis and measurements of glycolytic enzyme activity.

10. SDS-PAGE Gels

For serial sections, 26-well 10-20% Linear Gradient Gels from Bio-Rad were used. With 12ul samples added per well and run @ 100V for 150 minutes @ room temperature.

For tissue homogenate western blots, 10% SDS-PAGE gels were cast and 5ug sample in 20ul buffer loaded per well. Gels were run @100 V for 120 minutes @ room temperature.

11. Glycolytic enzyme activities

- **Hexokinase** activity was measured as the change in absorbance at 340 nm in the presence of Glucose-6-Phosphate Dehydrogenase following addition of NADP+.
- **Phosphofructokinase (PFK)** Activity was measured using the 6-Phosphofructokinase Activity Assay Kit from Abcam #ab155898, measuring the change in absorbance @ 750nm as the change from Fructose 1,6,-Bisphosphate to glucose 6 phosphate.
- **Aldolase** was measured using Fructose 1,6-Bisphosphate and following reduction of NAD by 340nm using a GAPDH coupled reaction.
- **Triose Phosphate Isomerase (TPI)** activity was measured using an assay coupled with GAPDH and initiated with Glyceraldehyde-3-Phosphate and following oxidation of NADH @ 340nm.
- **Glyceraldehyde-3-Phosphate Dehydrogenase (GAPDH)** was measured using glyceraldehyde 3- phosphate following reduction of NAD by 340nm absorbance.
- **Enolase** was measured by following 340 nm absorbance from NADH using an enzyme coupled reaction with Pyruvate Kinase and Lactate Dehydrogenase.
- **Pyruvate Kinase** Activity was measured using an assay coupled with Lactate Dehydrogenase. Reagents were mixed together and background measured @ 340 nm for 10 minutes prior to addition of retina homogenate, whereby the decrease in 340 nm as NADH was oxidized was used to define pyruvate kinase activity.

12. Western Blots

Gels were transferred to PVDF membrane O/N @ 20V @ 4℃.

All Secondary antibodies were from LiCor and used at a 1:5000 dilution.

Membranes were analyzed using a LICOR system scanner.

13. Primary Antibodies

Antibodies were used for Western Blots and Immunohistochemistry at concentrations specified.

- PKM1 Antibody – Rabbit mAb - Cell Signalling #7067S
- PKM2 Antibody – Rabbit mAb - Cell Signalling #4053S
- PKLR Antibody – Rabbit – AbCam – #ab171744
- PKM2-Y105 – Rabbit mAb - Cell Signalling #3827S
- 4d2 Antibody – In house – Jing Huang – UW Department of Ophthalmology.
- GAPDH Antibody - Santa Cruz Biotechnology Inc. #sc-20357
- Enolase – Rabbit Ab - Santa Cruz Biotechnology Inc. #sc-15343
- CRALBP – In house – Jing Huang – UW Department of Ophthalmology
- AGC – Laura Contreras Satrústegui lab (129)
- OGC – Goat Polyclonal - Santa Cruz Biotechnology Inc. #sc-160804

  LICOR Goat anti-Rabbit 800 and LICOR Donkey anti-Goat 680 secondaries were used.

14. Immunohistochemistry

Mouse retinas were fixed in 4% paraformaldehyde solution for 20 minutes and cut into 20 micron sections using a cryostat. Prior to immunostaining, slides were allowed to air dry at room temperature for 15 minutes. Sections were hydrated with 1X PBS at room temperature for 5-10 minutes. Slides were blocked for 1 hour at room temperature in IHC Blocking Buffer.

IHC Blocking Buffer

In 1X PBS:

- 5% Normal Goat Serum,
- 1mg/mL BSA
- 0.3% Triton X-100

If Anti-goat Secondary antibodies were to be used:

In 1X PBS:

- 5% Donkey Serum
- 2mg/mL BSA
- 0.3% Triton X-100.

Sections were incubated with primary antibody diluted in blocking buffer @ 4℃ overnight. Slides were washed at room temperature with PBS, 3 washes with 10 minute incubations. Secondary antibodies were diluted in blocking buffer and incubated at room temperature in the dark followed by 3 x 5 minute washed with PBS. Nuclei were stained with 5uM Hoescht 33528 diluted in PBS was applied to the slides for 10 minutes at room temperature. This was followed by a final wash of PBS, 3 x 5 minutes. PBS was drawn off and slides mounted with Fluoromount G (Southern Biotech). Slides were allowed to dry overnight at room temperature and then sealed with nail polish. Once dried, slides were stored @ 4℃ until imaged. Primaries were used in 1:20, 1:20 0, and 1:2000 dilutions.Secondary antibodies were obtained from Invitrogen, Alexfluor 488, 568, and 594 used @ 1:200 dilutions.

15. Derivatization of metabolites for GC-MS

Each sample consisted of a single retina incubated in culture conditions. Retina were spun down and supernatant removed prior to snap-freezing in liquid nitrogen. Retina samples were homogenized in 100 µL of a 700 methanol-200 chloroform-50 water mixture and placed on dry ice. Retinal extracts were centrifuged at 18,000 rpm, and 80 µL of the supernatant was transferred into glass inserts. The extracts were dried under vacuum and derivatized with 70 µL freshly prepared methyl hydroxyl amine HCl in pyridine (20 mg/ml) and incubated at 37 ℃ for 90 minutes to stabilize ketone groups. Retinal extracts were further derivatized with 70 µL of N-tert-butyldimethylsilyl-N-methyltrifluoroacetamide (Sigma-Aldrich) at 70 ℃ for 30 minutes. The derivatized mixture was transferred to glass inserts to GC-MS vials and stored @ -80℃ until analyzed.

16. GC-MS Analysis of Metabolites

GC-MS was carried out using the Agilent 5973 MSD/6890 GC (Agilent Corp, Santa Clara, CA, USA). A Rtx-5MS (30 m × 0.25 mm × 0.5 µm film, Restek, Bellefonte, PA, USA) column was used for GC separation of metabolites. Ultra high purity helium was the gas carrier at a constant flow rate of 1 mL/min. Each sample had 1 µl injected in split-less mode by the Agilent 7683 autosampler. The temperature gradient began at 100 ℃ with a hold time of 4 minutes, and then increased at 5 ℃/min to 300 ℃ where it held for 5 minutes. The temperatures were set as follows: inlet 250 ℃, transfer line 280 ℃, ion source 230 ℃ and quadrupole 150 ℃. Mass spectra were collected from *m*/*z* 50 to 600 at 1.4 spectra/s after a 6.5-minute solvent delay. The peaks were analyzed using Agilent data analysis software. Metabolite peak identities were previously defined with standards and verified by mass after each experiment. Data are expressed as ion signal strength for each metabolite normalized to glucose samples. For isotope distribution, IsoCor software was used to determine C13 isotope incorporation (130,131) .

17. Preparation of Optical Plates for Imaging of Isolated Cells

96-well optical bottom plates were used for imaging of dissociated photoreceptors.

Obtained from

- Nunc (**1256670)** or
- Matricell Plates (**MGB096-1-2-LG-L)**

Plates were pre-treated with 0.1mg/mL Poly-D-Lysine overnight prior to retina dissociation. On the day of preparation, wells were washed with deionized water and replaced with cell culture media supplemented with additional test compounds and transferred to a CO_2 incubator. Upon addition of dissociated retina cells, plates were spun down for 5 min. at 2,000 rpm. Cells were transferred to the incubator and imaging proceeding thereafter.

18. Dissociation of Retina Cells and Isolated Photoreceptors

Following the methods of Zayas-Santiago et. al. (103)**,** retinas from NRL-GFP mice were dissected under conditions per experiment (for example, light adapted mice were dissected under light exposed conditions and dark adapted mice were dissected under dark adapted conditions). Dissected retinas (2) were spun down briefly spun-down in 1.5 mL falcon tubes using a table-top centrifuge. Media was drawn off and replaced with pre-warmed DMEM supplemented with 10mM Glucose. Retinas were mechanically dissociated by pipetting up and down 6 times. Cells were filtered through a 100micron filter.

- In Nunc plate 50uL of cells were added to 250 uL buffer
- In Matricell plates, 100uL of cells were added to 400uL buffer.

19. Culture Conditions

- Initial Experiments used DMEM, No Glucose, No Glutamine, No Phenol Red A14430-01 Invitrogen.
- pH adjusted media was made with DMEM – Basic Media Powder D5030-10XL Sigma Aldrich
- Media Composition.
    - 500mLs DMEM

- 5mLs N2
- 5mLs FBS
- 5mLs Pen-Strept.
- 2,5mLs 1M HEPES
- 0.6g NaHCO3

Stored in 37’C incubator with 5% CO_2

- Fetal Bovine Serum, Certified, Heat-Inactivated 10082-147
- B-27 Serum Free Supplement (50X)liquid 17504-044
- N-2 Supplement (100x) liquid 17502048

20. Imaging Isolated Photoreceptors

A Deltavision Widefield microscope was used with a 40X oil objective to visualize the GFP and DIC channels of individual culture wells on a 96-well optical bottom plate at 37’C. Softworx software was used to automate imaging of individual wells. 4 pictures were taken per well at days 1, 3, and 6 of plating.

21. Genotyping of Mouse Lines

GNαT1-/- and RD1-/- mice were kindly provided by the lab of Russ Van Gelder.

Primer Sequences:

GNαT1-/- mice

- KO Tra 1- 5'- GGGAACTTCCTGACTAGGGGAGG – 3'
- WT Tra 2- 5'- GCGGAGTCATTGAGCTGGTAT – 3'
- Tra 3- 5'- TATCCACCAGGACGGGTATTC – 3'

NRL-GFP mice

- F: 5'-GCACGACTTCTTCAGTCCGCCATGCC – 3'
- R: 5'-GCGGATCTTGAAGTCACCTTGATGCC – 3'

RD1-/- mice

- F: 5'- CATCCCACCTGAGCTCACAGAAAG – 3'
- R: 5'- GCCTACAACAGAGGAGCTTCTAGC – 3'

PKM2-Cre mice

- F: 5'-TAGGGCAGGACCAAAGGATTCCCT-3'
- R: 5'-CTGGCCCAGAGCCACTCACTCTTG-3'

22. Image J Analysis of Outer Segment Retention

Analysis of outer-segment retention and calculation of circularity ratios was limited to cells identified as photoreceptor cells due to expression of NRL-GFP. Making use of the image J circularity feature, we separated photoreceptors with pronounced outer segments to those without and separated them by circularity ratios from 0.1 (intact photoreceptor) to 1.0 (rounded cell). Data was transferred and analyzed with Microsoft Excel.

23. Isolation of Mouse Brain Mitochondria

Mice were euthanized by CO2 and brain tissue quickly removed and stored on ice in Mitochondria Isolation Buffer. 1 brain was homogenized with 12 strokes in in a 10-ml dounce homogenizer in 6 mls of mitochondrial isolation buffer.

Mitochondria Isolation Buffer

- 225 mM mannitol
- 75 mM sucrose
- 1 mM EGTA and
- 5 mM HEPES (pH 7.0)

Brain homogenate was divided between (4x) 1.5 mL centrifuge tubes. And centrifuged for 5 minutes @ 4,000 rpm @ 4'C. 700uL supernatant was transferred to a fresh tube and stored on ice. Volume was replaced with Mitochondria isolation buffer and pellet re-suspended prior to second centrifugation step. 700uL of supernatant was removed and added to 1st supernatant and pellet discarded. Combined supernatants were centrifuged once more and 1200uL supernatant was transferred to a new tube. The supernatant was centrifuged at 18,000 rpm for 15 minutes at 4 ℃.

Following centrifugation, supernatant was discarded and the combined pellets were re-suspended in 1 ml mitochondrial isolation buffer supplemented with 1 mg/ml fatty acid free bovine serum albumin. This was centrifuged again at 18,000 rpm for 15 minutes @ 4'C. Pellets were re-suspended in 400uL Mitochondria Isolation Buffer. Protein concentration was determined using a modified Bradford Assay from BioRad (Dc Protein Concentration assay) and mitochondria were resuspended to a concentration of 5ug/uL)

24. Measuring Mitochondrial Oxygen consumption

Mitochondrial respiration was measured in an Oroboros Oxygraph 2-K (Oroboros Instrument Corp.) utilizing a Clark electrode which measures oxygen consumption as the change in voltage with decreasing oxygen concentration within a fixed chamber. Methods were similar to those used in analysis of Ca^{2+}effects on Glutamate respiration(40).

Respiratory Assay Medium

- 120mM Mannitol
- 40mM MOPS pH 7.4
- 60 mM KCl
- 5 mM KH_2PO_4
- 5 mM $MgCl_2$

To start the experiment, 50 µl of mitochondria were injected into each chamber. Respiration was initiated by serial addition of pyruvate/malate and ADP. The final concentrations of substrates were 1.5 mM pyruvate, 0.5 mM malate and 0.25 mM ADP. After addition of each component a baseline was allowed to stabilize for 5 minutes, except after addition of ADP, and the data was recorded for 15 minutes. Data points were gathered every 20 seconds. Data shown are an average of the stable baseline. Mitochondria from each condition were tested in triplicate.

25. Measurement of Cellular Respiration.

To analyze cellular respiration, cells were plated onto Seahorse XF-24 plates allowing for measurement of cellular Oxygen Consumption Rate (OCR) and Extracellular Acidification Rate (ECAR) as readout for cellular glycolysis. Substrates and procedures were based on protocols given by Seahorse Bioscience Inc. (http://www.seahorsebio.com/learning/procedures.php) for Mito Stress Test, Glycolytic Stress Test, and Fatty Acid Oxidation, with conditions specified per experiment.

26. Electron Transport Chain Complex Assays (From lab of Philip Morgan(132))

NCR: NADH Cytochrome C. Reductase

(NCR: Complex I/III)

250.0 uL RXN

Reaction	MQH2O	GIMISH	Cyto. C.	KCN	Rotenone	Mitochondria	NADH
1	87.0 uL	142.5 uL	12.5 uL	2.5 uL	----------	0.5 uL	5.0 uL
2	87.0 uL	142.5 uL	12.5 uL	2.5 uL	2.5 uL	0.5 uL	5.0 uL

Read OD @ 550nm for 60 seconds

Measures the increase in OD due to reduction of Cytochrome C.

Calculation

Rate = nmole/min/mg wet wt.

Ex. Coef = 19.1

At E550nm change E/min Factor = 1000*60 / 19.1* mg protein

= 157000(2ug)

Result

Zero Order Rate Constant

HP System gives 1 read/ second. Therefore, need calculation factor of 60.

NFR: NADH Ferricyanide Reductase

(NFR: Complex I)

250.0 uL RXN

Reaction	MQH2O	GIMISH	NADH	NaN3	K3Fe(CN)6	Mitochondria
1	76.0 uL	142.5 uL	5.0 uL	5.0 uL	16.5 uL	5.0 uL
2	81.0 uL	142.5 uL	5.0 uL	5.0 uL	16.5 uL	----------

Read OD @ 340nm for 120 seconds

Measures the decrease in OD due the oxidation of NADH.

Calculation

Rate = nmole/min/mg wet wt.

Ex. Coef = 6.22

At E550nm change E/min Factor = 1000*60 / 6.22* mg protein

= -480000 (20ug)

Result

Zero Order Rate Constant

HP System gives 1 read/ second. Therefore, need calculation factor of 60.

0.01M EDTA

pH to 7.0 with 10.0 M KOH

Store @ 4.0'C. Expires after 3 Months.

5% BSA

5g/100mL MQH2O.

Store @ 4.0'C. Expires after 1 Month.

0.01M NADH

7.1mg NADH / 1mL H2O.

Prepare fresh each day.

0.1M Sodium Azide (NaN3)

65mg/ 10mL H2O

Store @ -60'C. Expires after 1 month.

10mM Potassium Ferricyanide (K3Fe(CN)6)

0.032g / 10mL H2O

Store @ -60'C. Expires after 1 month.

NADH Q Reductase

(Complex I)

250.0 uL RXN

Reaction	MQH2O	GIMISH	NADH	AA	Rotenone	DUQ	Mitochondria
1	91.25 uL	140.0 uL	5.0 uL	5.0 uL	----------	3.75 uL	5.0 uL
2	88.75 uL	140.0 uL	5.0 uL	5.0 uL	2.5 uL	3.75 uL	5.0 uL

Read OD @ 340nm for 120 seconds

Measures the decrease in OD due to the oxidation of NADH.

Calculation

Rate = nmole/min/mg wet wt.

Ex. Coef = 6.22

At E550nm change E/min Factor = 1000*60 / 6.22* mg protein

= -480000 (20ug)

Result

Zero Order Rate Constant

HP System gives 1 read/ second. Therefore, need calculation factor of 60.

0.1 M Potassium Phosphate monobasic (KPi)

pH to 7.4 with 1.0M KOH

Store @ 4.0'C. Expires after 3 Months.

5% BSA

5g/100mL MQH2O.

Store @ 4.0'C. Expires after 1 Month.

Asolectin

150mg/ 10mL MQH2O.

Store @ 4.0'C. Expires after 1 Month.

0.01M EDTA

pH to 7.0 with 10.0 M KOH

Store @ 4.0'C. Expires after 3 Months.

0.75mM Rotenone

3mg Rotenone /10mL 200pf EtOH.

Store @ 4.0'C. Expires after 1 Month

Antimycin A (AA)

1mg Antimycin A / 1mL 200 proof EtOH.

Avoid Exposure to light

Store @ 4.0'C. Expires after 1 Month.

50mM Decylubiquinone (DUQ)

0.048g Decylubiquinone / 3mL 200 proof EtOH.

Dilute 1:10 in 200 proof EtOH. Use 5mM for Assay.

Store @ -60'C. Expires in 3 months.

SCR: Succinate Cytochrome C. Reductase

(SCR: Complex II/III)

250.0 uL RXN

Reaction	MQH2O	GIMISH	Cyto. C.	KCN	AA	Mitochondria	Succinate
1	85.0 uL	142.5 uL	12.5 uL	2.5 uL	----------	2.5 uL	5.0 uL
2	82.5 uL	142.5 uL	12.5 uL	2.5 uL	2.5 uL	2.5 uL	5.0 uL

Read OD @ 550nm for 200 seconds

Measures the increase in OD due to reduction of Cytochrome C.

Calculation

Rate = nmole/min/mg wet wt.

Ex. Coef = 19.1

At E550nm change E/min Factor = 1000*60 / 19.1* mg protein

= 314000(10ug)

Result

Zero Order Rate Constant

HP System gives 1 read/ second. Therefore, need calculation factor of 60.

Antimycin A (AA)

1mg Antimycin A / 1mL 200 proof EtOH.

Avoid Exposure to light

Store @ 4.0'C. Expires after 1 Month.

1M Sodium Succinate (dibasic hexahydrate)

MW= 270.1 g/M

2.704g Sodium succinate / 10mL MQH2O

pH to 7.0 with 1M HCl.

Store @ -60'C. Expires after 3 Months.

0.1 M Potassium Phosphate monobasic (KPi)

pH to 7.4 with 1.0M KOH

Store @ 4.0'C. Expires after 3 Months.

3mM Cytochrome c.

MW= 12,270 g/M.

184mg Cyto. C. / 5mL MQH2O.

Store @ -60'C. Expires after 1 Month.

0.01M EDTA

MW = 372.24g/M.

372mg EDTA/ 100mL MQH2O.

pH to 7.0 with 10.0 M KOH

Store @ 4.0'C. Expires after 3 Months.

5% BSA

5g/100mL MQH2O.

Store @ 4.0'C. Expires after 1 Month.

0.15M Potassium Cyanide (KCN)

MW= 65.12 g/M

47.8 mg KCN /5mL MQH2O.

Store @ 4.0'C. Expires after 1 Month.

Asolectin

150mg/ 10mL MQH2O.

Store @ 4.0'C. Expires after 1 Month.

SDH: Succinate Dehydrogenase

(SDH:Complex II)

250.0 uL RXN

Reaction	MQH2O	GIMISH	Mitochondria	Succinate
1	90.0 uL	150.0 uL	5.0 uL	5.0 uL
2	95.0 uL	150.0 uL	----------	5.0 uL

Gimish **.

4.5mL of Tris/BSA

0.25mL of KCN

1mL of 10mM PES

0.6mL of 0.8mM (1/25 dilution of the stock) DCPIP

5.15mL of MQH2O.

Read OD @ 600nm for 600 seconds

Measures the decrease in OD due to reduction of DCPIP.

Calculation

Rate = nmole/min/mg wet wt.

Ex. Coef = 21.0

At E600nm change E/min Factor = 1000*60 / 21.0* mg protein

= -143000(20ug)

Result

Zero Order Rate Constant

HP System gives 1 read/ second. Therefore, need calculation factor of 60

REAGENTS

0.5M TRIZMA-HCl Bovine Serum Albumin (Tris-BSA)

3.632 g TRIZMA-HCl

0.6g BSA

In 50mL Milliq H2O

pH to 7.8 with KOH

Store @ 4'C, expires after 3 months, prepare as needed.

1M Sodium Succinate (dibasic hexahydrate)

MW= 270.1 g/M

2.704g Sodium succinate / 10mL MQH2O

pH to 7.0 with 1M HCl.

Store @ -60'C. Expires after 3 Months.

0.01M Phenazine Ethosulphate (PES)

MW = 334.39

33 mg PES / 10mL MQH2O

Avoid exposure to light.

Store @ 60'C, expires after 1 month, prepare as needed.

0.15M Potassium Cyanide (KCN)

MW = 65.12

48.7 mg KCN / 5mL MQH2O

Store @ 4'C, expires after 1 month, prepare as needed.

20mM 2.6 Dichlorophenol-indophenol (DCPIP)

MW= 290.1

58.02 mg DCPIP / 10mL MQH2O

Avoid exposure to Light

OR

Stir excess DCPIP into MQH2O

Millipore Filter

Measure absorbacen @ 600nm wavelength.

Store @ -60'C, expires after 6 months, prepare as needed.

(Make this. Spec @ 600nm 980uL H2O + 20uL Stock. OD x 100 = mM DCPIP Stock. Dilute to 20mM)

Standardization of DCPIP

Sample: DCPIP Stock Solution

1.0mL – 1.0M KPi buffer, pH 7.0

0.1mL – DCPIP stock solution

Final colume of 100mL with MQh2O

Store @ -20'C.

Read E 660nm

Blank – 0.1 M KPi buffer, pH 7.0

DCPIP sample

Calculation Factor: sample O.D. x 100 = mM stock DCPIP.

Complex II

250.0 uL RXN

Reaction	GIMISH	DCPIP	MQH2O	Mito.	Malonate	DQ/DMSO	Succinate
1	138.75 uL	7.5 uL	98.75 uL	7.5 uL	----------	----------	5.0 uL
2	138.75 uL	7.5 uL	93.75 uL	7.5 uL	5.0 uL	----------	5.0 uL
3	138.75 uL	7.5 uL	96.25 uL	7.5 uL	----------	2.5 uL	5.0 uL
4	138.75 uL	7.5 uL	91.25 uL	7.5 uL	5.0 uL	2.5 uL	5.0 uL

Gimish **.

20 mL 0.1 M KPi

0.8mL 5% BSA

0.8mL NaN3

0.2mL MQH2O

0.4mL 0.1 M EDTA

Read OD @ 600nm for 600 seconds

Measures the decrease in OD due to reduction of DCPIP.

Rate = (3-1) – (4-2)

Calculation

Rate = nmole/min/mg wet wt.

Ex. Coef = 21.0

At E600nm change E/min Factor = 1000*60 / 21.0* mg protein

= -286000(20ug)

Result

Zero Order Rate Constant

HP System gives 1 read/ second. Therefore, need calculation factor of 60.

REAGENTS

50mM Thenoyltrifluoroacetone (TTFA)

MW = 222.18

0.111g TTFA / 10mL Absolute EtOH.

Store @ -60'C, expires after 1 month, prepare as needed.

50mM Duroquinone (DQ)

MW = 164.2

0.062g DQ / 10mL Dimethyl Sulfoxide (DMSO)

Store @ -60'C, expires after 1 month, prepare as needed.

20mM 2.6 Dichlorophenol-indophenol (DCPIP)

MW= 290.1

58.02 mg DCPIP / 10mL MQH2O

Avoid exposure to Light

OR

Stir excess DCPIP into MQH2O

Millipore Filter

Measure absorbacen @ 600nm wavelength.

Store @ -60'C, expires after 6 months, prepare as needed.

(Make this. Spec @ 600nm 980uL H2O + 20uL Stock. OD x 100 = mM DCPIP Stock. Dilute to 20mM)

Standardization of DCPIP

Sample: DCPIP Stock Solution

1.0mL – 1.0M KPi buffer, pH 7.0

0.1mL – DCPIP stock solution

Final colume of 100mL with MQh2O

Store @ -20'C.

Read E 660nm

Blank – 0.1 M KPi buffer, pH 7.0

DCPIP sample

Calculation Factor: sample O.D. x 100 = mM stock DCPIP.

0.1M Sodium Azide (NaN3)

65mg/ 10mL H2O

Store @ -60'C. Expires after 1 month.

0.1M EDTA

MW = 372.24

2.92 g EDTA

Add to 100mL of MQH2O

pH to 7.0 with 10.0 M KOH

Store @ 4.0'C. Expires after 3 Months.

0.1 M Potassium Phosphate monobasic (KPi)

pH to 7.4 with 1.0M KOH

Store @ 4.0'C. Expires after 3 Months.

5% BSA

5g/100mL MQH2O.

Store @ 4.0'C. Expires after 1 Month.

1M Sodium Succinate (dibasic hexahydrate)

MW= 270.1 g/M

2.704g Sodium succinate / 10mL MQH2O

pH to 7.0 with 1M HCl.

Store @ -60'C. Expires after 3 Months.

Decylubiquinol Cytochrome c. Reductase

(ETC 1', Complex III)

250.0 uL RXN

Reaction	MQH2O	GIMISH	KCN	Cyt. C.	AA	Mito	Red decylUQ
1	108.0 uL	132.5 uL	2.5 uL	5.0 uL	----------	0.5 uL	1.5 uL
2	105.5 uL	132.5 uL	2.5 uL	5.0 uL	2.5 uL	0.5 uL	1.5 uL

Gimish **.

10mL 0.1M KPi

0.5mL 5% BSA

0.1mL 0.01 M EDTA

Read OD @ 550nm for 90 seconds

Measures the increase in OD due to the reduction of Cytochrome c.

Calculation

Rate = nmole/min/mg wet wt.

Ex. Coef = 19.1

At E550nm change E/min Factor = 1000*60 / 19.1* mg protein

= -1570000 (2ug)

Result

Zero Order Rate Constant

HP System gives 1 read/ second. Therefore, need calculation factor of 60.

Note:

Background always high. Run background every time (everything except mitochondria)

0.1 M Potassium Phosphate monobasic (KPi)

pH to 7.4 with 1.0M KOH

Store @ 4.0'C. Expires after 3 Months.

5% BSA

5g/100mL MQH2O.

Store @ 4.0'C. Expires after 1 Month.

3mM Cytochrome c.

MW= 12,270 g/M.

184mg Cyto. C. / 5mL MQH2O.

Store @ -60'C. Expires after 1 Month.

0.1M Sodium Azide (NaN3)

65mg/ 10mL H2O

Store @ -60'C. Expires after 1 month.

0.01M EDTA

MW = 372.24g/M.

372mg EDTA/ 100mL MQH2O.

pH to 7.0 with 10.0 M KOH

Store @ 4.0'C. Expires after 3 Months.

Antimycin A (AA)

1mg Antimycin A / 1mL 200 proof EtOH.

Avoid Exposure to light

Store @ 4.0'C. Expires after 1 Month.

10mM Decylubiquinol (DHUQ)

Follow the Attached protocol for preparation of DHUQ from Decylubiquinone.

NCR: NADH Cytochrome C. Oxidase

(ETC 1': Complex IV)

250.0 uL RXN

Reaction	MQH2O	0.1M KPi	1.5% Asolectin	KCN	Mito	Red cyt. C.
1	87.0 uL	142.5 uL	12.5 uL	2.5 uL	----------	0.5 uL
2	87.0 uL	142.5 uL	12.5 uL	2.5 uL	2.5 uL	0.5 uL

Read OD @ 550nm with the background correction at 540nm for 900 seconds.

Measures the increase in OD due to reduction of Cytochrome C.

Calculation

Rate = AU/min/mg protein

Factor 60/mg protein

Factor 1000 X 60/ 19.1 x mg protein = 1570000 (2 ug)

Result

Zero Order Rate Constant

HP System gives 1 read/ second. Therefore, need calculation factor of 60.

GIMISH

CI: NFR, NCR, and SCR

10mL 0.1M KPi (0.1M K2HPO4, 0.1M KH2PO4)

0.8mL 5.0% BSA

0.2mL 1.5% Asolectin

0.2mL 0.01M EDTA

CII

20mL 0.1M KPi

0.8mL 5% BSA

0.8mL NaN3

0.2mM MQH2O

0.4mL 0.1M EDTA

CIII

10mL 0.1M KPi

0.5mL %BSA

0.1mL 0.01M EDTA

0.1 M Potassium Phosphate monobasic (KPi)

pH to 7.4 with 1.0M KOH

Store @ 4.0'C. Expires after 3 Months.

5% BSA

5g/100mL MQH2O.

Store @ 4.0'C. Expires after 1 Month.

Asolectin

150mg/ 10mL MQH2O.

Store @ 4.0'C. Expires after 1 Month.

0.01M EDTA

MW = 372.24g/M.

372mg EDTA/ 100mL MQH2O.

pH to 7.0 with 10.0 M KOH

Store @ 4.0'C. Expires after 3 Months.

27. Amplex Red ROS Assay

Reagents

Amplex Red (A) 80uM (final conc.) 10M Stock

RXN Buffer:

125mM KCl

10mM HEPES

5mM MgCl2

2mM K2HPO4 pH 7.4

H_2O_2 Standard (20mM)

22.7uL 3.0% H_2O_2 in 977uL 1X Reaction Buffer

Horseradish Peroxidase (HRP)

(2uL/RXN) = (0.02U/mL)

Superoxide Dismutase (SOD)

(2uL/RXN) = (0.05U/mL)

STOCKS:

A: 10mM in DMSO

HRP: 1U/uL in H2O

SOD 5U/uL in H2O

General Procedure:

+ 100uL RXN Buffer

+ 2uL HRP

+ 2uL SOD

+ 2uL Amplex Red

+ 1uL Compound of Interest

Read Ex. 545nm.

Em. 590nm.

Read 1 read/min for 20 min.

Bibliography:

1. Burns ME, Arshavsky VY. Beyond counting photons: trials and trends in vertebrate visual transduction. Neuron [Internet]. 2005 Nov 3 [cited 2014 Jun 16];48(3):387–401. Available from: http://www.ncbi.nlm.nih.gov/pubmed/16269358

2. Papermaster DS, Dreyer WJ. Rhodopsin Content in the Outer Segment Membranes. 13(11):2438–44.

3. Stenkamp RE, Teller DC, Palczewski K. Crystal structure of rhodopsin: a G-protein-coupled receptor. Chembiochem [Internet]. 2002 Oct 4;3(10):963–7. Available from: http://www.ncbi.nlm.nih.gov/pubmed/12362360

4. Dowling JE. The Retina: An Approachable Part of the Brain. Belknap Press; 2012.

5. Murakami, M. Shimoda, Y. Nakatani, K. Miyachi, E. Watanabe S. GABA-mediated negative feedback from horizontal cells to cones in carp retina. Japan J Physiol [Internet]. 1982;32(6):911–26. Available from: http://www.ncbi.nlm.nih.gov/pubmed/7169699

6. Giaume C, Kirchhoff F, Matute C, Reichenbach a, Verkhratsky a. Glia: the fulcrum of brain diseases. Cell Death Differ [Internet]. 2007 Jul [cited 2014 Jul 20];14(7):1324–35. Available from: http://www.ncbi.nlm.nih.gov/pubmed/17431421

7. Poitry-Yamate CL, Poitry S, Tsacopoulos M. Lactate released by Müller glial cells is metabolized by photoreceptors from mammalian retina. J Neurosci [Internet]. 1995 Jul;15(7 Pt 2):5179–91. Available from: http://www.ncbi.nlm.nih.gov/pubmed/7623144

8. Pugh EN, Lamb TD. Amplification and kinetics of the activation steps in phototransduction. Biochim Biophys Acta [Internet]. 1993 Mar 1;1141(2-3):111–49. Available from: http://www.ncbi.nlm.nih.gov/pubmed/8382952

9. Fung BK, Hurley JB, Stryer L. Flow of information in the light-triggered cyclic nucleotide cascade of vision. Proc Natl Acad Sci U S A [Internet]. 1981 Jan;78(1):152–6. Available from: http://www.pubmedcentral.nih.gov/articlerender.fcgi?artid=319009&tool=pmcentrez&rendertype=abstract

10. Chem JB, Devlin J. Isolation and characterization of cGMP phosphodiesterase from bovine rod outer Isolation Bovine and Characterization Rod Outer Segments * of cGMP Phosphodiesterase from. 1979;

11. Koch KW, Kaupp UB. Cyclic GMP directly regulates a cation conductance in membranes of bovine rods by a cooperative mechanism. J Biol Chem [Internet]. 1985 Jun 10;260(11):6788–800. Available from: http://www.ncbi.nlm.nih.gov/pubmed/2581960

12. Sterling P, Matthews G. Structure and function of ribbon synapses. Trends Neurosci [Internet]. 2005 Jan [cited 2014 Jun 10];28(1):20–9. Available from: http://www.ncbi.nlm.nih.gov/pubmed/15626493

13. Mendez a, Burns ME, Sokal I, Dizhoor a M, Baehr W, Palczewski K, et al. Role of guanylate cyclase-activating proteins (GCAPs) in setting the flash sensitivity of rod photoreceptors. Proc Natl Acad Sci U S A [Internet]. 2001 Aug 14;98(17):9948–53.

Available from: http://www.pubmedcentral.nih.gov/articlerender.fcgi?artid=55558&tool=pmcentrez&rendertype=abstract

14. Chen J, Makino CL, Peachey NS, Baylor DA, Simon MI. Mechanisms of Rhodopsin Inactivation in Vivo as Revealed. 2000;267(January 1995).

15. Bader BYCR, Bertrand D, Schwartzt EA. CURRENTS STUDIED IN SOLITARY ROD INNER SEGMENTS FROM. 1982;253–84.

16. Ames a, Li YY, Heher EC, Kimble CR. Energy metabolism of rabbit retina as related to function: high cost of Na+ transport. J Neurosci [Internet]. 1992 Mar;12(3):840–53. Available from: http://www.ncbi.nlm.nih.gov/pubmed/1312136

17. Okawa H, Sampath AP, Laughlin SB, Fain GL. ATP consumption by mammalian rod photoreceptors in darkness and in light. Curr Biol [Internet]. Elsevier Ltd; 2008 Dec 23 [cited 2013 Dec 14];18(24):1917–21. Available from: http://www.pubmedcentral.nih.gov/articlerender.fcgi?artid=2615811&tool=pmcentrez&rendertype=abstract

18. Linsenmeier R a. Effects of light and darkness on oxygen distribution and consumption in the cat retina. J Gen Physiol [Internet]. 1986 Oct;88(4):521–42. Available from: http://www.pubmedcentral.nih.gov/articlerender.fcgi?artid=2228847&tool=pmcentrez&rendertype=abstract

19. Fleisch,V.

20. Winkler BS, Starnes C a, Twardy BS, Brault D, Taylor RC. Nuclear magnetic resonance and biochemical measurements of glucose utilization in the cone-dominant ground squirrel retina. Invest Ophthalmol Vis Sci [Internet]. 2008 Oct [cited 2014 Jul 7];49(10):4613–9. Available from: http://www.ncbi.nlm.nih.gov/pubmed/18566456

21. Bui B V. The Contribution of Glycolytic and Oxidative Pathways to Retinal Photoreceptor Function. Invest Ophthalmol Vis Sci [Internet]. 2003 Jun 1 [cited 2014 Jul 22];44(6):2708–15. Available from: http://www.iovs.org/cgi/doi/10.1167/iovs.02-1054

22. Cohen,L.H. 1959.pdf.

23. Adler AJ, Southwick RE. Distribution of Glucose and Lactate in the. 1992;02114.

24. Warburg BYO, Wind F. I . Killing-Off of Tumor Cells in Vitro . 1927;

25. Heiden MG Vander, Cantley LC, Thompson CB, Mammalian P, Exhibit C, Metabolism A. Understanding the Warburg Effect□: Cell Proliferation. 2009;324(May):1029–33.

26. Vander Heiden MG, Locasale JW, Swanson KD, Sharfi H, Heffron GJ, Amador-Noguez D, et al. Evidence for an alternative glycolytic pathway in rapidly proliferating cells. Science [Internet]. 2010 Sep 17 [cited 2013 Nov 7];329(5998):1492–9. Available from: http://www.pubmedcentral.nih.gov/articlerender.fcgi?artid=3030121&tool=pmcentrez&rendertype=abstract

27. Hamanaka RB, Chandel NS. Cell biology. Warburg effect and redox balance. Science [Internet]. 2011 Dec 2 [cited 2013 Nov 16];334(6060):1219–20. Available from: http://www.ncbi.nlm.nih.gov/pubmed/22144609

28. Young RW. Friedenwald Lecture Visual cells and the concept of renewal. :700–25.

29. Young RW. The renewal of rod and cone outer segments in the rhesus monkey. J Cell Biol [Internet]. 1971 May 1;49(2):303–18. Available from: http://www.pubmedcentral.nih.gov/articlerender.fcgi?artid=2108322&tool=pmcentrez&rendertype=abstract

30. Young RW, Bok D. Participation of the retinal pigment epithelium in the rod outer segment renewal process. J Cell Biol [Internet]. 1969 Aug;42(2):392–403. Available from: http://www.pubmedcentral.nih.gov/articlerender.fcgi?artid=2107669&tool=pmcentrez&rendertype=abstract

31. Ishikawa T. On the stability of DNA in photoreceptor cells of the rat retina. Cell Tissue Res [Internet]. 1986;243(2):445–8. Available from: http://www.ncbi.nlm.nih.gov/pubmed/3948242

32. Winkler BS. An hypothesis to account for the renewal of outer segments in rod and cone photoreceptor cells: renewal as a surrogate antioxidant. Invest Ophthalmol Vis Sci [Internet]. 2008 Aug [cited 2014 Jul 7];49(8):3259–61. Available from: http://www.ncbi.nlm.nih.gov/pubmed/18660422

33. Brooks G a. Cell-cell and intracellular lactate shuttles. J Physiol [Internet]. 2009 Dec 1 [cited 2014 Oct 18];587(Pt 23):5591–600. Available from: http://www.pubmedcentral.nih.gov/articlerender.fcgi?artid=2805372&tool=pmcentrez&rendertype=abstract

34. Pellerin L, Magistretti PJ. Sweet sixteen for ANLS. J Cereb Blood Flow Metab [Internet]. Nature Publishing Group; 2012 Jul [cited 2014 Jul 13];32(7):1152–66. Available from: http://www.pubmedcentral.nih.gov/articlerender.fcgi?artid=3390819&tool=pmcentrez&rendertype=abstract

35. Genc S, Kurnaz I a, Ozilgen M. Astrocyte-neuron lactate shuttle may boost more ATP supply to the neuron under hypoxic conditions--in silico study supported by in vitro expression data. BMC Syst Biol [Internet]. BioMed Central Ltd; 2011 Jan [cited 2013 Dec 13];5(1):162. Available from: http://www.pubmedcentral.nih.gov/articlerender.fcgi?artid=3202240&tool=pmcentrez&rendertype=abstract

36. Rajala A, Gupta VK, Anderson RE, Rajala RVS. Light activation of the insulin receptor regulates mitochondrial hexokinase. A possible mechanism of retinal neuroprotection. Mitochondrion [Internet]. Elsevier B.V. and Mitochondria Research Society. All rights reserved.; 2013 Nov [cited 2013 Dec 17];13(6):566–76. Available from: http://www.ncbi.nlm.nih.gov/pubmed/23993956

37. John S, Weiss JN, Ribalet B. Subcellular localization of hexokinases I and II directs the metabolic fate of glucose. PLoS One [Internet]. 2011 Jan [cited 2013 Dec 12];6(3):e17674. Available from:

http://www.pubmedcentral.nih.gov/articlerender.fcgi?artid=3052386&tool=pmcentrez&rendertype=abstract

38. Stone J, van Driel D, Valter K, Rees S, Provis J. The locations of mitochondria in mammalian photoreceptors: relation to retinal vasculature. Brain Res [Internet]. 2008 Jan 16 [cited 2013 Dec 14];1189:58–69. Available from: http://www.ncbi.nlm.nih.gov/pubmed/18048005

39. Kim J, Lee E, Chang BS, Oh CS, Mun G-H, Chung YH, et al. The presence of megamitochondria in the ellipsoid of photoreceptor inner segment of the zebrafish retina. Anat Histol Embryol [Internet]. 2005 Dec [cited 2014 Jul 22];34(6):339–42. Available from: http://www.ncbi.nlm.nih.gov/pubmed/16288603

40. Gellerich FN, Gizatullina Z, Arandarcikaite O, Jerzembek D, Vielhaber S, Seppet E, et al. Extramitochondrial Ca2+ in the nanomolar range regulates glutamate-dependent oxidative phosphorylation on demand. PLoS One [Internet]. 2009 Jan [cited 2013 Dec 13];4(12):e8181. Available from: http://www.pubmedcentral.nih.gov/articlerender.fcgi?artid=2784944&tool=pmcentrez&rendertype=abstract

41. Du J, Cleghorn WM, Contreras L, Lindsay K, Rountree AM, Chertov AO, et al. Inhibition of mitochondrial pyruvate transport by Zaprinast causes massive accumulation of aspartate at the expense of glutamate in the retina. J Biol Chem [Internet]. 2013 Nov 1 [cited 2013 Nov 8]; Available from: http://www.ncbi.nlm.nih.gov/pubmed/24187136

42. Xu Y, Ola MS, Berkich D a, Gardner TW, Barber a J, Palmieri F, et al. Energy sources for glutamate neurotransmission in the retina: absence of the aspartate/glutamate carrier produces reliance on glycolysis in glia. J Neurochem [Internet]. 2007 Apr [cited 2014 Jul 18];101(1):120–31. Available from: http://www.ncbi.nlm.nih.gov/pubmed/17394462

43. Huster D, Hjelle OP, Haug FM, Nagelhus E a, Reichelt W, Ottersen OP. Subcellular compartmentation of glutathione and glutathione precursors. A high resolution immunogold analysis of the outer retina of guinea pig. Anat Embryol (Berl) [Internet]. 1998 Oct;198(4):277–87. Available from: http://www.ncbi.nlm.nih.gov/pubmed/9764542

44. Adler L, Chen C, Koutalos Y. Mitochondria contribute to NADPH generation in mouse rod photoreceptors. J Biol Chem [Internet]. 2014 Jan 17 [cited 2014 Jun 26];289(3):1519–28. Available from: http://www.ncbi.nlm.nih.gov/pubmed/24297174

45. Pow D V, Crook DK. Immunocytochemical evidence for the presence of high levels of reduced glutathione in radial glial cells and horizontal cells in the rabbit retina. Neurosci Lett [Internet]. 1995 Jun 23;193(1):25–8. Available from: http://www.ncbi.nlm.nih.gov/pubmed/7566658

46. Marc RE, Cameron D. A molecular phenotype atlas of the zebrafish retina. J Neurocytol [Internet]. 2001 Jul;30(7):593–654. Available from: http://www.ncbi.nlm.nih.gov/pubmed/12118163

47. Schütte M, Werner P. Redistribution of glutathione in the ischemic rat retina. Neurosci Lett [Internet]. 1998 Apr 17;246(1):53–6. Available from: http://www.ncbi.nlm.nih.gov/pubmed/9622206

48. Stephen P Daiger. RetNet: Retina Information Network [Internet]. Available from: https://sph.uth.edu/Retnet/

49. Chen CK, Burns ME, Spencer M, Niemi G a, Chen J, Hurley JB, et al. Abnormal photoresponses and light-induced apoptosis in rods lacking rhodopsin kinase. Proc Natl Acad Sci U S A [Internet]. 1999 Mar 30;96(7):3718–22. Available from: http://www.pubmedcentral.nih.gov/articlerender.fcgi?artid=22360&tool=pmcentrez&rendertype=abstract

50. Yamamoto, S. Sippel, K.C. Berson, E.L., Dryja TP. Defects in rhodopsin kinase gene in the Oguchi form of stationary night blindness. Nat Genet [Internet]. 1997;15(2):175–8. Available from: http://www.ncbi.nlm.nih.gov/pubmed/9020843

51. Ramamurthy V, Niemi G a, Reh T a, Hurley JB. Leber congenital amaurosis linked to AIPL1: a mouse model reveals destabilization of cGMP phosphodiesterase. Proc Natl Acad Sci U S A [Internet]. 2004 Sep 21;101(38):13897–902. Available from: http://www.pubmedcentral.nih.gov/articlerender.fcgi?artid=518850&tool=pmcentrez&rendertype=abstract

52. Kelsell RE, Gregory-Evans K, Payne a M, Perrault I, Kaplan J, Yang RB, et al. Mutations in the retinal guanylate cyclase (RETGC-1) gene in dominant cone-rod dystrophy. Hum Mol Genet [Internet]. 1998 Jul;7(7):1179–84. Available from: http://www.ncbi.nlm.nih.gov/pubmed/9618177

53. Kersten HM, Roxburgh RH, Danesh-Meyer H V. Ophthalmic manifestations of inherited neurodegenerative disorders. Nat Rev Neurol [Internet]. Nature Publishing Group; 2014 Jun [cited 2014 Jul 11];10(6):349–62. Available from: http://www.ncbi.nlm.nih.gov/pubmed/24840976

54. Carelli V, La Morgia C, Valentino ML, Barboni P, Ross-Cisneros FN, Sadun A a. Retinal ganglion cell neurodegeneration in mitochondrial inherited disorders. Biochim Biophys Acta [Internet]. Elsevier B.V.; 2009 May [cited 2014 Jul 11];1787(5):518–28. Available from: http://www.ncbi.nlm.nih.gov/pubmed/19268652

55. Maurer CM, Schönthaler HB, Mueller KP, Neuhauss SCF. Distinct retinal deficits in a zebrafish pyruvate dehydrogenase-deficient mutant. J Neurosci [Internet]. 2010 Sep 8 [cited 2014 Jul 11];30(36):11962–72. Available from: http://www.ncbi.nlm.nih.gov/pubmed/20826660

56. Hartong DT, Dange M, McGee TL, Berson EL, Dryja TP, Colman RF. Insights from retinitis pigmentosa into the roles of isocitrate dehydrogenases in the Krebs cycle. Nat Genet [Internet]. 2008 Oct [cited 2013 Dec 14];40(10):1230–4. Available from: http://www.pubmedcentral.nih.gov/articlerender.fcgi?artid=2596605&tool=pmcentrez&rendertype=abstract

57. Umino Y, Everhart D, Solessio E, Cusato K, Pan JC, Nguyen TH, et al. Hypoglycemia leads to age-related loss of vision. Proc Natl Acad Sci U S A [Internet]. 2006 Dec 19;103(51):19541–5. Available from: http://www.pubmedcentral.nih.gov/articlerender.fcgi?artid=1697832&tool=pmcentrez&rendertype=abstract

58. Zarnowski T, Tulidowicz-Bielak M, Kosior-Jarecka E, Zarnowska I, A Turski W, Gasior M. A ketogenic diet may offer neuroprotection in glaucoma and mitochondrial diseases of the optic nerve. Med hypothesis, Discov Innov Ophthalmol [Internet]. 2012 Jan;1(3):45–9. Available from: http://www.pubmedcentral.nih.gov/articlerender.fcgi?artid=3939735&tool=pmcentrez&rendertype=abstract

59. Gatenby R a, Gillies RJ. Why do cancers have high aerobic glycolysis? Nat Rev Cancer [Internet]. 2004 Nov [cited 2014 Jul 9];4(11):891–9. Available from: http://www.ncbi.nlm.nih.gov/pubmed/15516961

60. Lunt SY, Vander Heiden MG. Aerobic glycolysis: meeting the metabolic requirements of cell proliferation. Annu Rev Cell Dev Biol [Internet]. 2011 Jan [cited 2014 Jul 10];27:441–64. Available from: http://www.ncbi.nlm.nih.gov/pubmed/21985671

61. Goyal MS, Hawrylycz M, Miller J a, Snyder AZ, Raichle ME. Aerobic glycolysis in the human brain is associated with development and neotenous gene expression. Cell Metab [Internet]. Elsevier Inc.; 2014 Jan 7 [cited 2014 Aug 4];19(1):49–57. Available from: http://www.ncbi.nlm.nih.gov/pubmed/24411938

62. Wang L, Kondo M, Bill a. Glucose metabolism in cat outer retina. Effects of light and hyperoxia. Invest Ophthalmol Vis Sci [Internet]. 1997 Jan;38(1):48–55. Available from: http://www.ncbi.nlm.nih.gov/pubmed/9008629

63. Winkler BS. Glycolytic and oxidative metabolism in relation to retinal function. J Gen Physiol [Internet]. 1981 Jun;77(6):667–92. Available from: http://www.pubmedcentral.nih.gov/articlerender.fcgi?artid=2215447&tool=pmcentrez&rendertype=abstract

64. Du J, Cleghorn W, Contreras L, Linton JD, Chan GC-K, Chertov AO, et al. Cytosolic reducing power preserves glutamate in retina. Proc Natl Acad Sci U S A [Internet]. 2013 Nov 12 [cited 2014 Jun 26];110(46):18501–6. Available from: http://www.pubmedcentral.nih.gov/articlerender.fcgi?artid=3831988&tool=pmcentrez&rendertype=abstract

65. Barres B a. The mystery and magic of glia: a perspective on their roles in health and disease. Neuron [Internet]. Elsevier Inc.; 2008 Nov 6 [cited 2014 Jul 16];60(3):430–40. Available from: http://www.ncbi.nlm.nih.gov/pubmed/18995817

66. Bélanger M, Allaman I, Magistretti PJ. Brain energy metabolism: focus on astrocyte-neuron metabolic cooperation. Cell Metab [Internet]. 2011 Dec 7 [cited 2013 Nov 8];14(6):724–38. Available from: http://www.ncbi.nlm.nih.gov/pubmed/22152301

67. Bouzier-Sore A-K, Pellerin L. Unraveling the complex metabolic nature of astrocytes. Front Cell Neurosci [Internet]. 2013 Jan [cited 2014 Jul 22];7(October):179. Available from: http://www.pubmedcentral.nih.gov/articlerender.fcgi?artid=3795301&tool=pmcentrez&rendertype=abstract

68. Shen W, Fruttiger M, Zhu L, Chung SH, Barnett NL, Kirk JK, et al. Conditional Müllercell ablation causes independent neuronal and vascular pathologies in a novel transgenic

model. J Neurosci [Internet]. 2012 Nov 7 [cited 2014 Aug 12];32(45):15715–27. Available from: http://www.pubmedcentral.nih.gov/articlerender.fcgi?artid=4014009&tool=pmcentrez&rendertype=abstract

69. Christofk HR, Vander Heiden MG, Harris MH, Ramanathan A, Gerszten RE, Wei R, et al. The M2 splice isoform of pyruvate kinase is important for cancer metabolism and tumour growth. Nature [Internet]. 2008 Mar 13 [cited 2014 Jul 9];452(7184):230–3. Available from: http://www.ncbi.nlm.nih.gov/pubmed/18337823

70. Mazurek S, Boschek CB, Hugo F, Eigenbrodt E. Pyruvate kinase type M2 and its role in tumor growth and spreading. Semin Cancer Biol [Internet]. 2005 Aug [cited 2014 Aug 4];15(4):300–8. Available from: http://www.ncbi.nlm.nih.gov/pubmed/15908230

71. Chaneton B, Gottlieb E. Rocking cell metabolism: revised functions of the key glycolytic regulator PKM2 in cancer. Trends Biochem Sci [Internet]. Elsevier Ltd; 2012 Aug [cited 2014 Aug 4];37(8):309–16. Available from: http://www.ncbi.nlm.nih.gov/pubmed/22626471

72. Locasale JW, Grassian AR, Melman T, Lyssiotis C a, Mattaini KR, Bass AJ, et al. Phosphoglycerate dehydrogenase diverts glycolytic flux and contributes to oncogenesis. Nat Genet [Internet]. Nature Publishing Group; 2011 Sep [cited 2014 Jul 21];43(9):869–74. Available from: http://www.pubmedcentral.nih.gov/articlerender.fcgi?artid=3677549&tool=pmcentrez&rendertype=abstract

73. Sarthy VP, Brodjian SJ, Dutt K, Kennedy BN, French RP, Crabb JW. Establishment and characterization of a retinal Müller cell line. Invest Ophthalmol Vis Sci [Internet]. 1998 Jan;39(1):212–6. Available from: http://www.ncbi.nlm.nih.gov/pubmed/21535230

74. Reidel B, Thompson JW, Farsiu S, Moseley MA, Skiba NP, Arshavsky VY. Proteomic profiling of a layered tissue reveals unique glycolytic specializations of photoreceptor cells. Mol Cell Proteomics [Internet]. 2011 Mar [cited 2013 Nov 12];10(3):M110.002469. Available from: http://www.pubmedcentral.nih.gov/articlerender.fcgi?artid=3047149&tool=pmcentrez&rendertype=abstract

75. Leskov IB, Klenchin V a, Handy JW, Whitlock GG, Govardovskii VI, Bownds MD, et al. The gain of rod phototransduction: reconciliation of biochemical and electrophysiological measurements. Neuron [Internet]. 2000 Sep;27(3):525–37. Available from: http://www.ncbi.nlm.nih.gov/pubmed/11055435

76. Lyubarsky AL, Daniele LL, Pugh EN. From candelas to photoisomerizations in the mouse eye by rhodopsin bleaching in situ and the light-rearing dependence of the major components of the mouse ERG. Vision Res [Internet]. 2004 Dec [cited 2014 Jul 22];44(28):3235–51. Available from: http://www.ncbi.nlm.nih.gov/pubmed/15535992

77. Linton JD, Holzhausen LC, Babai N, Song H, Miyagishima KJ, Stearns GW, et al. Flow of energy in the outer retina in darkness and in light. Proc Natl Acad Sci U S A [Internet]. 2010 May 11 [cited 2014 Jun 23];107(19):8599–604. Available from:

http://www.pubmedcentral.nih.gov/articlerender.fcgi?artid=2889335&tool=pmcentrez&rendertype=abstract

78. Sokolov M, Lyubarsky AL, Strissel KJ, Savchenko AB, Govardovskii VI, Pugh EN, et al. Massive Light-Driven Translocation of Transducin between the Two Major Compartments of Rod Cells□: A Novel Mechanism of Light Adaptation. 2002;33:95–106.

79. Hitosugi T, Kang S, Vander Heiden MG, Chung T-W, Elf S, Lythgoe K, et al. Tyrosine phosphorylation inhibits PKM2 to promote the Warburg effect and tumor growth. Sci Signal [Internet]. 2009 Jan [cited 2013 Dec 17];2(97):ra73. Available from: http://www.pubmedcentral.nih.gov/articlerender.fcgi?artid=2812789&tool=pmcentrez&rendertype=abstract

80. Ye J, Mancuso A, Tong X, Ward PS, Fan J, Rabinowitz JD. Pyruvate kinase M2 promotes de novo serine synthesis to sustain mTORC1 activity and cell proliferation. 2012;2–7.

81. Roesch K, Jadhav AP, Trimarchi JM, Stadler MB, Roska B, Sun BB, et al. The transcriptome of retinal Müller glial cells. J Comp Neurol [Internet]. 2008 Jul 10 [cited 2014 Jul 29];509(2):225–38. Available from: http://www.pubmedcentral.nih.gov/articlerender.fcgi?artid=2665263&tool=pmcentrez&rendertype=abstract

82. Ueki Y, Karl MO, Sudar S, Pollak J, Taylor RJ, Loeffler K, et al. P53 is required for the developmental restriction in Müller glial proliferation in mouse retina. Glia [Internet]. 2012 Oct [cited 2014 Jun 26];60(10):1579–89. Available from: http://www.pubmedcentral.nih.gov/articlerender.fcgi?artid=3422417&tool=pmcentrez&rendertype=abstract

83. Pardo B, Rodrigues TB, Contreras L, Garzón M, Llorente-Folch I, Kobayashi K, et al. Brain glutamine synthesis requires neuronal-born aspartate as amino donor for glial glutamate formation. J Cereb Blood Flow Metab [Internet]. 2011 Jan [cited 2013 Dec 13];31(1):90–101. Available from: http://www.pubmedcentral.nih.gov/articlerender.fcgi?artid=3049464&tool=pmcentrez&rendertype=abstract

84. McKenna MC, Waagepetersen HS, Schousboe A, Sonnewald U. Neuronal and astrocytic shuttle mechanisms for cytosolic-mitochondrial transfer of reducing equivalents: current evidence and pharmacological tools. Biochem Pharmacol [Internet]. 2006 Mar 14 [cited 2014 Jul 31];71(4):399–407. Available from: http://www.ncbi.nlm.nih.gov/pubmed/16368075

85. Shimamoto K, Brun BLE, Yasuda-kamatani Y, Sakaitani M, Shigeri Y. A Potent Blocker of Excitatory Amino Acid Transporters. 1998;201:195–201.

86. Davidson, J.N. Chen, K.C., Jamison, R.S., Musmanno, L.A. Kern CB. The evolutionary history of the first three enzymes of pyrimidine biosynthesis. Bioessays [Internet]. 1993;15(3):157–64. Available from: http://www.ncbi.nlm.nih.gov/pubmed/8098212

87. Jalil MA, Begum L, Contreras L, Pardo B, Iijima M, Li MX, et al. Reduced N-acetylaspartate levels in mice lacking aralar, a brain- and muscle-type mitochondrial

aspartate-glutamate carrier. J Biol Chem [Internet]. 2005 Sep 2 [cited 2014 Aug 12];280(35):31333–9. Available from: http://www.ncbi.nlm.nih.gov/pubmed/15987682

88. Hasegawa J, Obara T, Tanaka K, Tachibana M. High-density presynaptic transporters are required for glutamate removal from the first visual synapse. Neuron [Internet]. 2006 Apr 6 [cited 2014 Aug 5];50(1):63–74. Available from: http://www.ncbi.nlm.nih.gov/pubmed/16600856

89. Poitry-Yamate, C.L. Tsacopoulos M. Glucose Metabolism in freshly isolated Muller Glial cell from a mammalian retina. J Comp Neurol. J. Comp Neurol.; 1992;320(2):257–66.

90. Israelsen WJ, Dayton TL, Davidson SM, Fiske BP, Hosios AM, Bellinger G, et al. PKM2 isoform-specific deletion reveals a differential requirement for pyruvate kinase in tumor cells. Cell [Internet]. Elsevier Inc.; 2013 Oct 10 [cited 2013 Dec 14];155(2):397–409. Available from: http://www.ncbi.nlm.nih.gov/pubmed/24120138

91. Philp NJ. Loss of MCT1, MCT3, and MCT4 Expression in the Retinal Pigment Epithelium and Neural Retina of the 5A11/Basigin-Null Mouse. Invest Ophthalmol Vis Sci [Internet]. 2003 Mar 1 [cited 2014 Aug 4];44(3):1305–11. Available from: http://www.iovs.org/cgi/doi/10.1167/iovs.02-0552

92. Adijanto J, Philp NJ. The SLC16A family of monocarboxylate transporters (MCTs)--physiology and function in cellular metabolism, pH homeostasis, and fluid transport. [Internet]. Current topics in membranes. Elsevier; 2012 [cited 2014 Aug 13]. Available from: http://www.ncbi.nlm.nih.gov/pubmed/23177990

93. Bibb C, Young RW. Renewal of fatty acids in the membranes of visual cell outer segments. J Cell Biol [Internet]. 1974 May;61(2):327–43. Available from: http://www.pubmedcentral.nih.gov/articlerender.fcgi?artid=2109290&tool=pmcentrez&rendertype=abstract

94. Bibb C, Young RW. Renewal of glycerol in the visual cells and pigment epithelium of the frog retina. J Cell Biol [Internet]. 1974 Aug;62(2):378–89. Available from: http://www.pubmedcentral.nih.gov/articlerender.fcgi?artid=2109391&tool=pmcentrez&rendertype=abstract

95. Voi I, Anderson RE, Kelleher PA, Maude MB, Maida TM. Neurochemistry. 1980;29–42.

96. LaVail MM. Kinetics of rod outer segment renewal in the developing mouse retina. J Cell Biol [Internet]. 1973 Sep;58(3):650–61. Available from: http://www.pubmedcentral.nih.gov/articlerender.fcgi?artid=2109077&tool=pmcentrez&rendertype=abstract

97. Basinger SF, Hollyfield JG. No Title. 1980;I:81–92.

98. Hollyfield JOEG, Rayborn ME. ROD OUTER SEGMENTS ELONGATE IN CONSTANT LIGHT□: DARKNESS IS REQUIRED. 1977;

99. LaVail MM. Rod outer segment disc shedding in relation to cyclic lighting. Exp Eye Res [Internet]. 1976 Aug;23(2):277–80. Available from: http://www.ncbi.nlm.nih.gov/pubmed/987920

100. Rod Outer Segment Disk Shedding in Rat Retina : Relationship to Cyclic Lighting Author (s): Matthew M . LaVail Published by : American Association for the Advancement of Science Stable URL : http://www.jstor.org/stable/1743230 . 2013;194(4269):1071–4.

101. Besharse JC, Hollyfield JG. Articles Turnover of mouse photoreceptor outer segments in constant light and darkness. 1979;

102. Kinney MS, Fisher SK. The Photoreceptors and Pigment Epithelium of the Larval Xenopus Retina: Morphogenesis and Outer Segment Renewal. Proc R Soc B Biol Sci [Internet]. 1978 May 5 [cited 2014 Jul 7];201(1143):149–67. Available from: http://rspb.royalsocietypublishing.org/cgi/doi/10.1098/rspb.1978.0037

103. Zayas-Santiago A, Kang Derwent JJ. Preservation of intact adult rat photoreceptors in vitro: study of dissociation techniques and the effect of light. Mol Vis [Internet]. 2009 Jan;15(December 2008):1–9. Available from: http://www.pubmedcentral.nih.gov/articlerender.fcgi?artid=2614449&tool=pmcentrez&rendertype=abstract

104. Akimoto M, Cheng H, Zhu D, Brzezinski J a, Khanna R, Filippova E, et al. Targeting of GFP to newborn rods by Nrl promoter and temporal expression profiling of flow-sorted photoreceptors. Proc Natl Acad Sci U S A [Internet]. 2006 Mar 7;103(10):3890–5. Available from: http://www.pubmedcentral.nih.gov/articlerender.fcgi?artid=1383502&tool=pmcentrez&rendertype=abstract

105. Tan E. Expression of Cone-Photoreceptor-Specific Antigens in a Cell line Derived from Retinal Tumors in Transgenic Mice. Invest Ophthalmol Vis Sci. 2004;45(3):764–8.

106. Johnathan W. Driver, Andrew F. Powers, Krishna K. Sarangapani, Sue Biggins CLA. Measuring Kinetochore-Microtubule Interaction In Vitro. Methods in Enzymology. Elsevier; 2014. p. 321–37.

107. Tanaka Y, Wakida S-I. Controlled 3D rotation of biological cells using optical multiple-force clamps. Biomed Opt Express [Internet]. 2014 Jul 1 [cited 2014 Dec 2];5(7):2341–8. Available from: http://www.pubmedcentral.nih.gov/articlerender.fcgi?artid=4102368&tool=pmcentrez&rendertype=abstract

108. Jablonski MM, Iannaccone A. Lactose supports Müller cell protein expression patterns in the ab- sence of the retinal pigment epithelium. 2001;(September 2000):27–35.

109. Wang X, Iannaccone A, Jablonski MM. Permissive glycan support of photoreceptor outer segment assembly occurs via a non-metabolic mechanism. Mol Vis [Internet]. 2003 Dec 16;9(December):701–9. Available from: http://www.ncbi.nlm.nih.gov/pubmed/14685143

110. Wang X, Iannaccone A, Jablonski MM. NIH Public Access. 2006;1–6.

111. Bortner CD, Scoltock AB, Sifre MI, Cidlowski J a. Osmotic stress resistance imparts acquired anti-apoptotic mechanisms in lymphocytes. J Biol Chem [Internet]. 2012 Feb 24 [cited 2014 Jul 18];287(9):6284–95. Available from: http://www.pubmedcentral.nih.gov/articlerender.fcgi?artid=3307331&tool=pmcentrez&rendertype=abstract

112. James B. Hurley, Andrei O. Chertov, Ken Lindsay, Michelle Giamarco, Whitney Cleghorn, Jianhai Du and SB. Energy Metabolism in the Vertebrate Retina. Vertebrate Photoreceptors. 2014. p. 91–137.

113. McUsic AC, Lamba D a, Reh T a. Guiding the morphogenesis of dissociated newborn mouse retinal cells and hES cell-derived retinal cells by soft lithography-patterned microchannel PLGA scaffolds. Biomaterials [Internet]. Elsevier Ltd; 2012 Feb [cited 2014 Jul 12];33(5):1396–405. Available from: http://www.pubmedcentral.nih.gov/articlerender.fcgi?artid=3249403&tool=pmcentrez&rendertype=abstract

114. Brunner D, Frank J, Appl H, Schöffl H, Pfaller W, Gstraunthaler G. Serum-free cell culture: the serum-free media interactive online database. ALTEX [Internet]. 2010 Jan;27(1):53–62. Available from: http://www.ncbi.nlm.nih.gov/pubmed/20390239

115. Willoughby JJ, Jensen AM. Generation of a genetically encoded marker of rod photoreceptor outer segment growth and renewal. Biol Open [Internet]. 2012 Jan 15 [cited 2013 Nov 23];1(1):30–6. Available from: http://www.pubmedcentral.nih.gov/articlerender.fcgi?artid=3507166&tool=pmcentrez&rendertype=abstract

116. Ruggiero L, Connor MP, Chen J, Langen R, Finnemann SC. Diurnal, localized exposure of phosphatidylserine by rod outer segment tips in wild-type but not Itgb5-/- or Mfge8-/- mouse retina. Proc Natl Acad Sci U S A [Internet]. 2012 May 22 [cited 2013 Nov 20];109(21):8145–8. Available from: http://www.pubmedcentral.nih.gov/articlerender.fcgi?artid=3361434&tool=pmcentrez&rendertype=abstract

117. Xenopus A, Resolution A. Prevention of Rod Disk Shedding by Detochment From the Retinol Pigment Epithelium. 1987;184–7.

118. D'Cruz PM, Yasumura D, Weir J, Matthes MT, Abderrahim H, LaVail MM, et al. Mutation of the receptor tyrosine kinase gene Mertk in the retinal dystrophic RCS rat. Hum Mol Genet [Internet]. 2000 Mar 1;9(4):645–51. Available from: http://www.ncbi.nlm.nih.gov/pubmed/10699188

119. Assawachananont J, Mandai M, Okamoto S, Yamada C, Eiraku M, Yonemura S, et al. Transplantation of Embryonic and Induced Pluripotent Stem Cell-Derived 3D Retinal Sheets into Retinal Degenerative Mice. Stem cell reports [Internet]. The Authors; 2014 May 6 [cited 2014 Jul 16];2(5):662–74. Available from: http://www.pubmedcentral.nih.gov/articlerender.fcgi?artid=4050483&tool=pmcentrez&rendertype=abstract

120. Calvert PD, Krasnoperova N V, Lyubarsky a L, Isayama T, Nicoló M, Kosaras B, et al. Phototransduction in transgenic mice after targeted deletion of the rod transducin alpha -subunit. Proc Natl Acad Sci U S A [Internet]. 2000 Dec 5;97(25):13913–8. Available from: http://www.pubmedcentral.nih.gov/articlerender.fcgi?artid=17675&tool=pmcentrez&rendertype=abstract

121. Pawlyk BS, Li T, Scimeca MS, Sandberg M a, Berson EL. Absence of photoreceptor rescue with D-cis-diltiazem in the rd mouse. Invest Ophthalmol Vis Sci [Internet]. 2002 Jun;43(6):1912–5. Available from: http://www.ncbi.nlm.nih.gov/pubmed/12036998

122. Zhang X, Feng Q, Cote RH. Efficacy and selectivity of phosphodiesterase-targeted drugs in inhibiting photoreceptor phosphodiesterase (PDE6) in retinal photoreceptors. Invest Ophthalmol Vis Sci [Internet]. 2005 Sep [cited 2014 Jul 7];46(9):3060–6. Available from: http://www.pubmedcentral.nih.gov/articlerender.fcgi?artid=1343468&tool=pmcentrez&rendertype=abstract

123. Xu Y, Zhu X, Hahm HS, Wei W, Hao E, Hayek A, et al. Revealing a core signaling regulatory mechanism for pluripotent stem cell survival and self-renewal by small molecules. Proc Natl Acad Sci U S A [Internet]. 2010 May 4 [cited 2014 Dec 1];107(18):8129–34. Available from: http://www.pubmedcentral.nih.gov/articlerender.fcgi?artid=2889586&tool=pmcentrez&rendertype=abstract

124. Chen Q, Vazquez EJ, Moghaddas S, Hoppel CL, Lesnefsky EJ. Production of reactive oxygen species by mitochondria: central role of complex III. J Biol Chem [Internet]. 2003 Sep 19 [cited 2014 Jul 18];278(38):36027–31. Available from: http://www.ncbi.nlm.nih.gov/pubmed/12840017

125. Schriner SE, Linford NJ, Martin GM, Treuting P, Ogburn CE, Emond M, et al. Extension of Murine Life Span by Overexpression of Catalase Targeted to Mitochondria. 2005;308(June):1909–12.

126. Koivunen P, Hirsilä M, Remes AM, Hassinen IE, Kivirikko KI, Myllyharju J. Inhibition of hypoxia-inducible factor (HIF) hydroxylases by citric acid cycle intermediates: possible links between cell metabolism and stabilization of HIF. J Biol Chem [Internet]. 2007 Feb 16 [cited 2013 Nov 10];282(7):4524–32. Available from: http://www.ncbi.nlm.nih.gov/pubmed/17182618

127. Gohil VM, Sheth S a, Nilsson R, Wojtovich AP, Lee JH, Perocchi F, et al. Nutrient-sensitized screening for drugs that shift energy metabolism from mitochondrial respiration to glycolysis. Nat Biotechnol [Internet]. Nature Publishing Group; 2010 Mar [cited 2013 Dec 13];28(3):249–55. Available from: http://www.pubmedcentral.nih.gov/articlerender.fcgi?artid=3135002&tool=pmcentrez&rendertype=abstract

128. Chertov AO, Holzhausen L, Kuok IT, Couron D, Parker E, Linton JD, et al. Roles of glucose in photoreceptor survival. J Biol Chem [Internet]. 2011 Oct 7 [cited 2013 Nov 23];286(40):34700–11. Available from: http://www.pubmedcentral.nih.gov/articlerender.fcgi?artid=3186402&tool=pmcentrez&rendertype=abstract

129. Del Arco a., Satrustegui J. Molecular Cloning of Aralar, a New Member of the Mitochondrial Carrier Superfamily That Binds Calcium and Is Present in Human Muscle and Brain. J Biol Chem [Internet]. 1998 Sep 4 [cited 2014 Aug 4];273(36):23327–34. Available from: http://www.jbc.org/cgi/doi/10.1074/jbc.273.36.23327

130. Millard P, Letisse F, Sokol S, Portais J-C. IsoCor: correcting MS data in isotope labeling experiments. Bioinformatics [Internet]. 2012 May 1 [cited 2014 Oct 11];28(9):1294–6. Available from: http://www.ncbi.nlm.nih.gov/pubmed/22419781

131. Van Winden W a, Wittmann C, Heinzle E, Heijnen JJ. Correcting mass isotopomer distributions for naturally occurring isotopes. Biotechnol Bioeng [Internet]. 2002 Nov 20 [cited 2014 Sep 26];80(4):477–9. Available from: http://www.ncbi.nlm.nih.gov/pubmed/12325156

132. Suthammarak W, Somerlot BH, Opheim E, Sedensky M, Morgan PG. Novel interactions between mitochondrial superoxide dismutases and the electron transport chain. Aging Cell [Internet]. 2013 Dec [cited 2014 Dec 1];12(6):1132–40. Available from: http://www.pubmedcentral.nih.gov/articlerender.fcgi?artid=3838459&tool=pmcentrez&rendertype=abstract